



Cardiff  
Catalysis Institute  
Sefydliad Catalysis  
Caerdydd



International Flavors & Fragrances

# **The Aerobic, Partial Oxidation of THPMI for the Production of Cashmeran**

Joseph Macginley

Thesis submitted in accordance with the requirement of Cardiff  
University for the degree of Doctor of Philosophy

Cardiff University

November 2021

# Acknowledgments

Firstly, I would like to thank the Centre for Doctoral Training in Catalysis for offering me the opportunity to undertake this project and for providing funding. I would also like to thank Professor Graham Hutchings for his experienced academic supervision throughout the project and Dr Samuel Pattisson for his supervision both academically and experimentally. I would also like to thank Dr Mark Douthwaite, Dr Rebecca Engel and Matthew Conway for their contributions to the project. And finally, Dr David Morgan, Dr Thomas Morgan, and Dr Simon Waller for assistance with XPS, SEM and ICP-MS respectively.

I need to thank also International Flavors and Fragrances for their funding of the project. Dr Carlos Lopez Cruz proved to be an insightful and friendly industrial supervisor and the rest of the team on site in Benicaló, Spain, including Jordi Pastor Folch, were extremely kind and welcoming during my visit.

The whole team at the Cardiff Catalysis Institute made me feel very welcome from the very first day in 2016 to the very last day in 2020. My fellow PhD students made my time at Cardiff extremely enjoyable both in and out of work. I would like to give a special mention to Owen Rogers, Parag Shah, DM, Nia Richards, Matt Conway, Annie Cooper, and Alexandra Barnes; to name only a few.

My final thanks have to be to my family for raising me to become capable of completing a PhD and most of all to my wonderful girlfriend, Bethany Hartevelde, for supporting me throughout.

# Abstract

The industrial production of Cashmeran is of vital importance to the fragrance industry. This is due to Cashmeran being the only molecule with a floral-fruity musky odour with conifer woody aspects, that also has a low odour threshold.

The current process to produce Cashmeran is an aerobic, partial oxidation of the bicyclic alkene, tetrahydropentamethyl indane (THPMI); this process is currently limited by low selectivity at high conversion. This thesis explores the effect the current industrial catalyst, Co-bis(2-ethylhexanoate), has on this reaction. Although without any catalyst the oxidation occurs rapidly, inclusion of Co-bis(2-ethylhexanoate) improves overall selectivity to the desired products (Cashmeran and Cashmeran-alcohol), increases the Cashmeran to Cashmeran-alcohol ratio, and slightly increases the rate of reaction. The catalyst suppresses build-up of the primary oxidation product, tetrahydropentamethyl indane hydroperoxide (THPMI-HP), which is likely the cause of increased selectivity as undesired radical reaction routes are suppressed. The catalyst also causes reaction quenching, which is related to the temperature of reaction and strongly to the loading of catalyst in the reaction. This quenching phenomenon is likely a result of free cobalt ions causing radical termination reactions, drastically slowing down the rate of THPMI oxidation.

Alternative catalysts were tested including supported cobalt oxide on aminated silica ( $\text{CoO}/\text{SiO}_2$ ), cobalt (II, III) oxide ( $\text{Co}_3\text{O}_4$ ), Molybdenum blue and various acid catalysts. The cobalt-based catalysts demonstrate catalytic activity to convert THPMI into THPMI-HP, but not for the decomposition of THPMI-HP into the desired products. Molybdenum blue, glutaric acid, and Amberlyst-15 suppress conversion and selectivity significantly. Small amounts of cobalt leaching occurs when using heterogeneous cobalt catalysts which was shown to have minimal impact on the reaction. It was also demonstrated that ppm levels of Co-bis(2-ethylhexanoate) are capable of initiating oxidation of THPMI into THPMI-HP, although do not facilitate THPMI-HP decomposition into the desired products.

This work has demonstrated the complex, radical-mediated nature of the oxidation of THPMI into Cashmeran and the subtle yet vital effect Co-bis(2-ethylhexanoate) has on the reaction. Although no superior alternative catalyst has been demonstrated, this work builds the foundation for further research into this reaction and how to control selectivity and so improve yield of Cashmeran.

# Table of Contents

1	Introduction .....	1
1.1	Thesis Aims.....	1
1.2	Brief History of Fragrance Chemistry.....	1
1.3	Cashmeran .....	2
1.3.1	Use of Cashmeran .....	2
1.3.2	Cashmeran Production.....	3
1.4	Oxidation.....	5
1.4.1	Heterolytic Oxygen Activation .....	7
1.4.2	Homolytic Oxygen Activation.....	7
1.5	Homogeneous Cobalt-Catalysed Oxidation Reactions .....	8
1.6	Quenching of Oxidation Reactions .....	10
1.7	Heterogeneous Catalysts for Oxidation of Alkenes .....	12
1.7.1	Considering Reaction Conditions .....	12
1.7.2	Gold Catalysts for Oxidation .....	13
1.7.3	Copper and Other Catalysts for Oxidation.....	14
1.7.4	Summary of Heterogeneous Catalysts for Oxidation .....	16
1.8	Summary .....	16
1.9	References .....	17
2	Experimental Section .....	25
2.1	Introduction .....	25
2.2	Oxidation of THPMI.....	25
2.3	Preparation of Heterogeneous Catalysts.....	26
2.3.1	Preparation of CoO/SiO <sub>2</sub> .....	26
2.3.2	Preparation of Co <sub>3</sub> O <sub>4</sub> .....	27
2.3.3	Preparation of Molybdenum Blue .....	27
2.4	Analysis of Reaction Products by Gas-Chromatography.....	27

2.4.1	Theory .....	27
2.4.2	Experimental .....	30
2.5	Gas Chromatography Mass Spectrometry (GC-MS) .....	33
2.5.1	Theory .....	33
2.5.2	Experimental .....	34
2.6	Thermogravimetric Analysis (TGA) .....	34
2.6.1	Theory .....	34
2.6.2	Experimental .....	34
2.7	Microwave Plasma Atomic Emission Spectroscopy (MP-AES).....	35
2.7.1	Theory .....	35
2.7.2	Experimental .....	35
2.8	X-ray Photoelectron Spectroscopy (XPS) .....	36
2.8.1	Theory .....	36
2.8.2	Experimental .....	36
2.9	Powder X-ray Diffraction (XRD).....	37
2.9.1	Theory .....	37
2.9.2	Experimental .....	39
2.10	Scanning Electron Microscopy (SEM)/Energy Dispersive X-ray Spectroscopy (EDX)..	39
2.10.1	SEM Theory .....	39
2.10.2	EDX Theory.....	40
2.10.3	SEM/EDX Experimental .....	41
2.11	Infra-red Spectroscopy (IR) .....	41
2.11.1	Theory .....	41
2.11.2	Experimental .....	42
2.12	Brunauer-Emmett-Teller Surface Area Analysis (BET) .....	42
2.12.1	Theory .....	42
2.12.2	Experimental .....	44
2.13	References .....	45
3	The Effect of Co-bis(2-ethylhexanoate) on the Aerobic Oxidation of THPMI.....	47

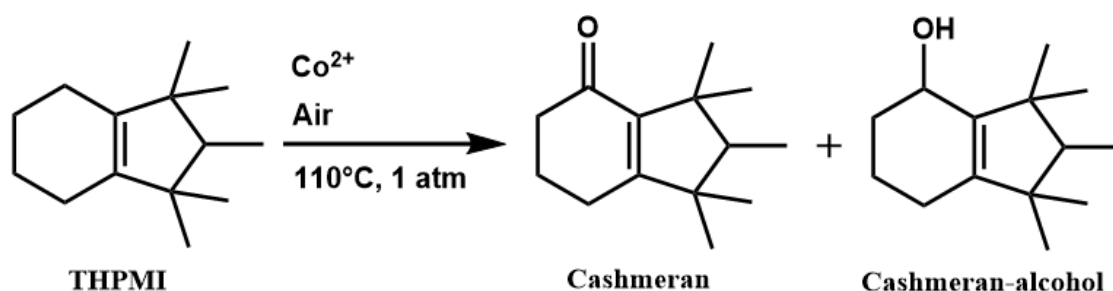
3.1	Introduction .....	47
3.2	Development of Reaction Conditions .....	49
3.3	Characterisation of Undesired Products.....	51
3.4	Aerobic Oxidation of THPMI at Industry Temperature.....	52
3.4.1	Undesired Products.....	57
3.4.2	Mass Balance.....	59
3.5	Effect of Varying Temperature.....	60
3.5.1	Blank Reaction.....	60
3.5.2	Reactions with Co-bis(2-ethylhexanoate).....	65
3.6	Effect of Varying Co-bis(2-ethylhexanoate) Loading .....	69
3.7	Effect of Radical Scavengers .....	71
3.8	Separating Ligand Effects from Metal Effects in Co-bis(2-ethylhexanoate) .....	75
3.9	Conclusions .....	78
3.10	References .....	80
4	Investigating Alternative Catalysts for the Oxidation of THPMI .....	84
4.1	Introduction .....	84
4.2	Acid Catalysts .....	85
4.3	CoO/SiO <sub>2</sub> as a Catalyst for THPMI Oxidation .....	90
4.3.1	Characterisation of CoO/SiO <sub>2</sub> .....	90
4.3.2	Catalytic Testing of CoO/SiO <sub>2</sub> .....	97
4.4	Co <sub>3</sub> O <sub>4</sub> as a Catalyst for THPMI Oxidation .....	100
4.4.1	Thermogravimetric Analysis (TGA) of Cobalt Carbonate .....	101
4.4.2	Characterisation of Co <sub>3</sub> O <sub>4</sub> .....	101
4.4.3	Catalyst Testing of Co <sub>3</sub> O <sub>4</sub> .....	105
4.5	Cobalt Leaching.....	109
4.6	Molybdenum Blue as a Catalyst for THPMI Oxidation.....	112
4.6.1	Characterisation of Molybdenum Blue .....	113
4.6.2	Catalytic Testing of Molybdenum Blue .....	118
4.7	Conclusions .....	119

4.8	References .....	121
5	Conclusions & Future Work .....	124
5.1	Conclusions .....	124
5.1.1	The Effect of Co-bis(2-ethylhexanoate) on the Oxidation of THPMI .....	124
5.1.2	Investigating Alternative Catalysts for the Oxidation of THPMI .....	126
5.2	Future Work .....	127
5.3	References .....	129

# 1 Introduction

## 1.1 Thesis Aims

The aim of this thesis is to study the industrial aerobic oxidation of 4,5,6,7-tetrahydro-1,1,2,3,3-pentamethylindane (THPMI) into 1,2,3,5,6,7-hexahydro-1,1,2,3,3-pentamethyl-4H-inden-4-one (Cashmeran) and 1,2,3,5,6,7-hexahydro-1,1,2,3,3-pentamethyl-4H-inden-4-ol (Cashmeran-alcohol) (Scheme 1.1). The goal is to gain further understanding of the current process and investigate new catalysts that can be employed to improve selectivity to the desired products. Chapter 3 studies the current reaction conditions by investigating the effect of the current catalyst, Co-bis(2-ethylhexanoate), or Co-bis(2-EH) for brevity, on the reaction along with the effect of temperature, mass transfer and radical scavengers. The chapter also presents studies of some of the side products produced in the reaction. Chapter 4 provides a study into alternative catalysts for the oxidation of THPMI including both heterogeneous and homogeneous catalysts with a detailed characterisation of the heterogeneous catalysts and an investigation into leaching effects.

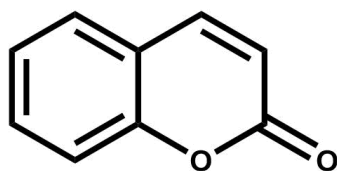


**Scheme 1.1** Oxidation of THPMI into Cashmeran and Cashmeran-alcohol.

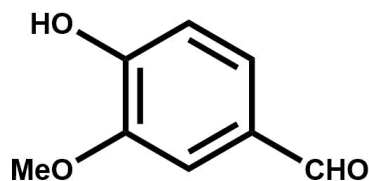
## 1.2 Brief History of Fragrance Chemistry

The extraction and use of fragrances from both plants and animals is ubiquitous across human civilisations. This historic use of fragrances was advanced in the 19<sup>th</sup> century when synthetic fragrant chemicals began to appear in the chemical literature and on the market.<sup>1</sup> Two of the first industrially produced fragrant chemicals were Coumarin (**1**), first synthesised in 1868 by William Henry Perkin,<sup>2</sup> and Vanillin (**2**) first industrially produced in Germany in 1876 (Figure

1.1).<sup>3</sup> Both of these fragrances are naturally occurring, with Coumarin first being extracted from tonka beans<sup>4</sup> and vanillin being extracted from vanilla beans, with accounts of Spanish conquistadors being served chocolate and vanilla flavoured drinks by the Aztec people in 1520.<sup>5</sup> Producing fragrant chemicals synthetically is far more cost effective than their extraction from natural sources and so the chemical fragrance production has grown into a behemoth industry with many multinational companies including International Flavours and Fragrances (IFF), Givaudan, Danisco and Symrise. Each of these companies have market capitalisations in the tens of billions of dollars at the time of writing. As an example to demonstrate the size of the industry, the annual global demand for vanillin was approximately 18 600 tons in 2016, which is expected to grow by 6 % by 2025.<sup>6</sup> To add to this, only 1 % of global vanillin production is satisfied by the natural source, the beans of *Vanilla planifolia*.<sup>7</sup> This demonstrates that even a very small improvement in the efficiency in the chemical production of vanillin and other large scale fragrant molecules will lead to significant economic savings for producers.



1 (1868)



2 (1876)

Figure 1.1. Chemical structures of Coumarin 1 and Vanillin 2.

## 1.3 Cashmeran

### 1.3.1 Use of Cashmeran

Cashmeran (**3**) (Figure 1.2) is a fragrant molecule described as having a floral-fruity musky odour with conifer woody aspects.<sup>8</sup> The molecule was first discovered by John Hall of International Flavours and Fragrances in 1973 when a significant gap in the market for a cheap molecule of a persistent musk woody odour was presented.<sup>9</sup> The odour of Cashmeran is extremely desirable in the fragrance industry, yet almost no other odorants exist that match its profile.<sup>10</sup> One of the few odorants to show similar properties to Cashmeran is a *tert*-butyl substituted 5,5-dimethylcyclopentenyl butanone (**4**) (Figure 1.2), however this molecule has a musk more similar to moxalone and importantly has a much higher odour threshold (25 ng L<sup>-1</sup> air) compared to Cashmeran (0.89 ng L<sup>-1</sup> air).<sup>11</sup> The uniqueness, quality, and cost of Cashmeran means that it has become popular as an ingredient in many fragrances including “Dans Tes Bras” (Frederic Mali, 2008) and “Duro” (Nasomatto, 2007) as a 25 % composition of each, and is also

an ingredient of “Only the Brave Extreme” (Diesel, 2016), amongst many other commercial fragrant products.<sup>12</sup> Cashmeran is also used as a precursor to other fragrant molecules such as Operanide (**5**)<sup>13</sup> (Figure 1.3) which is used at 3 % in “Y Eau de Parfum” (Yves Saint Laurent, 2018).<sup>12</sup> If even a small efficiency increase can be achieved in the industrial production of Cashmeran this would mean significant savings for the producers, IFF, and would mean more Cashmeran is available to companies who use it in fragrant formulations.

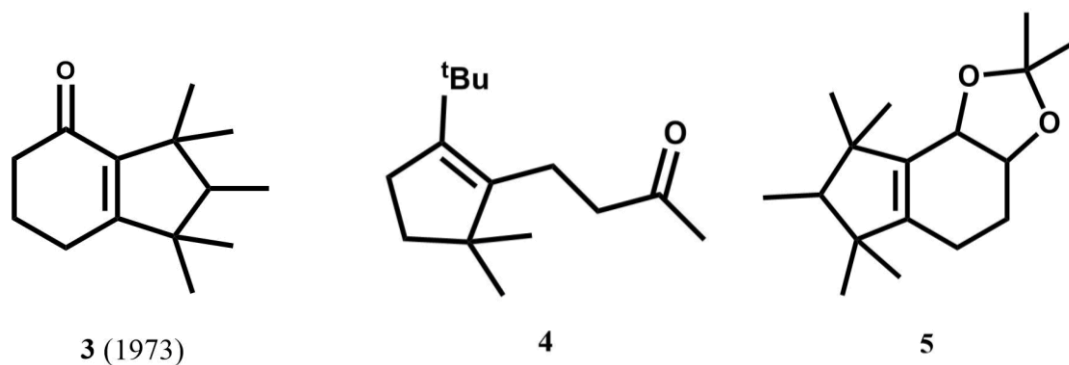
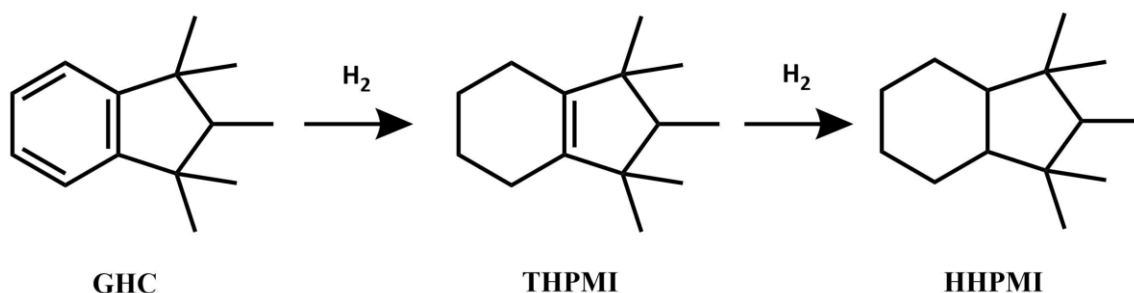


**Figure 1.2.** Chemical structure of Cashmeran (**3**), the Cashmeran-like fragrant molecule (**4**) and Operanide (**5**).

### 1.3.2 Cashmeran Production

The original patent for the production of Cashmeran in 1974 describes a procedure with THPMI as the starting material, an oxidant of O<sub>2</sub> either in the form of air or as a pure gas, either being introduced at atmospheric pressure through bubbling or at an increased pressure of up to 138 bar. A metal-organic catalyst is employed that is made up of at least one metal with an atomic number between 24 – 30 (either nickel, cobalt, copper, or manganese) and an aliphatic or carboxylic acid including acetate, propionate or naphthenate. Cobalt or copper acetate and cobalt naphthenate are the preferred catalysts for the oxidation. The loading of the catalyst is between 1 – 20 % of the starting material. The reaction can be run between 50 – 150 °C, but usually between 80 – 100 °C, and for between 5 – 75 hours, but usually between 10 – 50 hours. After completion of the reaction, aqueous iron sulfate is added to decompose any peroxides or hydroperoxides present and the products are extracted by distillation.<sup>14</sup> A patent published in 2011 covers an updated production method for Cashmeran, although it is very similar to the 1974 patent. A metal organic or metal salt catalyst is still mandated, however it is specified to have between 4 – 30 carbon atoms, the metal is still either nickel, cobalt, copper or manganese and cobalt/copper acetate or cobalt naphthenate are still preferred. It is now specified that the catalyst can be in its pure form or as part of a mixture with paraffinic compounds such as mineral spirits. The properties of the oxidant are maintained from the 1974 patent, however the range of pressures that can be applied has been narrowed to up to 100 bar and usually up to 20 bar.

The range of temperatures has been expanded to between 25 – 200 °C with an ideal range of between 80 – 160 °C. Certain products or reactants including water can now be added to or removed from the reaction deliberately to affect the equilibrium. The patent now also states that free-radical initiators can be added, and a range of solvents can be used. The major difference in the newer patent is the inclusion of gold catalysts with a weight loading of between 0.1 – 20 % (but ideally between 0.5 – 10 %) on a metal oxide support, preferably ceria. The supported gold catalyst is particularly effective at converting Cashmeran-alcohol into Cashmeran.<sup>15</sup>



**Scheme 1.2.** Desired partial hydrogenation of GHC to THPMI and subsequent undesired full hydrogenation into HHPMI.

The current optimal production of Cashmeran is summarised above (Scheme 1.1), where THPMI of approximately 65 mol% purity, depending on batch, is reacted with flowing air of residence time 47 h without solvent in a semi-batch process. Co-bis(2-ethylhexanoate) is added as a catalyst/radical initiator at a loading of close to 0.15 wt% relative to the starting material. The reaction is run to approximately 50 % conversion as above this level of conversion the selectivity to the desired allylic oxidation products decreases (Figure 1.3). The THPMI is only around 65 mol% pure as it is produced from the selective hydrogenation of GHC (Scheme 1.2), the remainder of the THPMI solution is unreacted GHC and HHPMI,<sup>16,17</sup> neither of which are oxidised under the standard reaction conditions to produce Cashmeran. Under current procedures there are two major limitations on the efficiency of the process to produce Cashmeran: the limited air flow that can be applied to the industrial reactor and the selectivity of the reaction. The air flow is deliberately limited due to safety concerns regarding a build-up of oxygen at the top of the reactor. If the air flow is increased in a safe way the rate of reaction could be increased, however this would only decrease the time of reaction rather than improve the yield of the Cashmeran. The imperfect selectivity to Cash-total products (Cashmeran and Cashmeran-alcohol) is a more realistic target with regards to improving overall yield and is the subject of this thesis. A representation of the typical trend of conversion (of THPMI) against Cash-total selectivity is shown below (Figure 1.3) and demonstrates why it is more efficient to stop the reaction at close to 50 % conversion as selectivity drops off above this point. The

reaction will quench regardless if the reaction is run for too long, which is discussed more in section (1.6). If a greater conversion of THPMI can be achieved whilst maintaining a high Cash-total selectivity, then the efficiency of the process for producing Cashmeran will be significantly more economically favourable. To achieve this goal significant research is needed to understand why this conversion-selectivity relationship is observed and how the current reaction conditions need to be adapted to improve the reaction yield. Adaptations could involve reaction temperature, catalyst(s), radical initiators, radical scavengers, choice of oxidant, mass transfer or other additives to the reaction including solvents. Before this undertaking is investigated it is important to understand the background of oxidation reactions, discussed below.

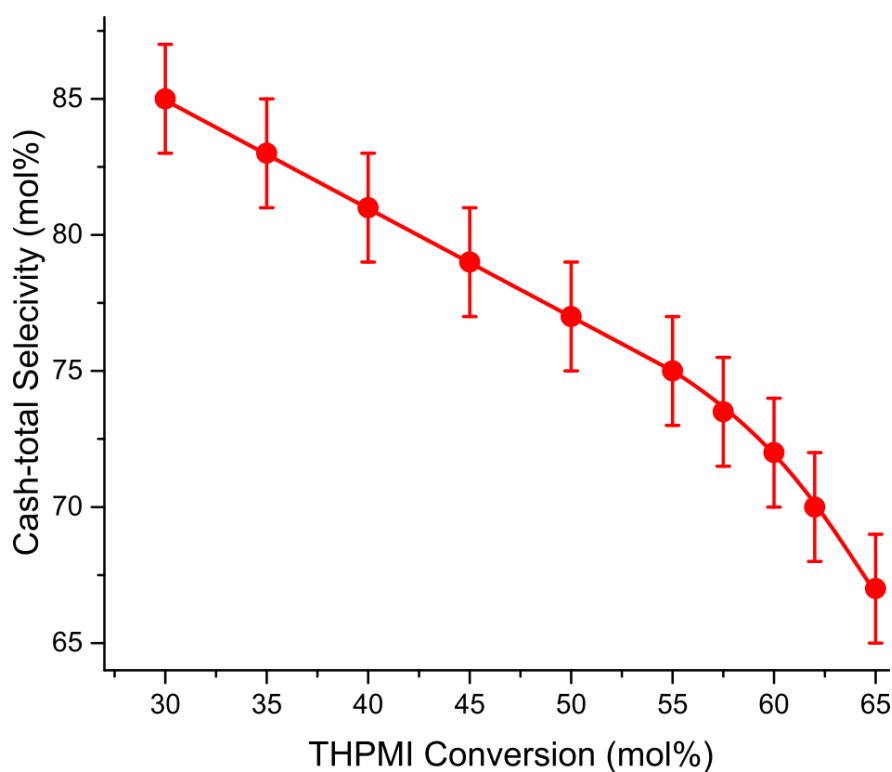


**Figure 1.3.** A typical representation of conversion against Cash-total selectivity for the oxidation of THPMI by IFF.

## 1.4 Oxidation

To build an understanding of the chemistry involved in the oxidation of THPMI into Cashmeran, it is first important to have a detailed understanding of oxidation in general. Partial oxidation of chemicals such as butane,<sup>18</sup> xylene,<sup>19</sup> propane,<sup>20</sup> and cyclohexane,<sup>21</sup> to name a few, yield molecules that can be used in industries varying from pharmaceuticals to agriculture.<sup>22</sup> Total oxidation of volatile organic compounds (VOCs) is of great importance as a means of converting highly toxic industrial pollutants into clean and safe CO<sub>2</sub> and H<sub>2</sub>O,<sup>23,24</sup> including the total oxidation of CO and hydrocarbons in catalytic converters in automobiles.<sup>25</sup> Aerobic

oxidations, where the oxidant is O<sub>2</sub>, are highly desired in chemical synthesis. This is because O<sub>2</sub> is the most readily available, cheapest, least toxic and is the least environmentally damaging oxidant available.<sup>26</sup>

Most industrial oxidation reactions are catalysed by metals, either in the form of supported nanoparticles, metal oxides, or metal complexes. The fundamental need for catalysts stems from the nature of O<sub>2</sub> in its ground state ( $^3\Sigma_g^-$ ), which is a triplet spin state.<sup>27</sup> This is of importance as reactions between reactants in a singlet state, such as organic molecules including olefins, and reactants in triplet states, such as O<sub>2</sub>, are forbidden if their products are only in the singlet state.<sup>28,29</sup> Essentially this means that for O<sub>2</sub> to react with an organic substrate, either O<sub>2</sub> needs to be activated into a different spin multiplicity, usually by a metal catalyst, or the organic substrate needs to be radicalised to yield a substrate which can react with O<sub>2</sub> whilst obeying Wigner's spin selection rule.<sup>30</sup> It should be noted that O<sub>2</sub> has two accessible singlet states at higher energy that would be reactive to organic molecules,  $^1\Sigma_g^+$  and  $^1\Delta_g$  (Figure 1.4), which are approximately 157 and 94 kJ mol<sup>-1</sup> above the ground state,  $^3\Sigma_g^-$ , respectively.<sup>31</sup> The  $^1\Delta_g$  singlet state is accessible by using photo-excited sensitisers,<sup>32,33</sup> however due to its high reactivity its applications are limited to specific organic synthesis such as cycloaddition of furans.<sup>34,35</sup> The vast majority of oxidation reactions, particularly those in industry, can be summarised in one of two ways: ground, triplet state O<sub>2</sub> being activated by a metal centre in a 2-electron process (heterolytic activation)<sup>36</sup> or ground, triplet state O<sub>2</sub> reacting with an organic radical, which is formed from an autoxidation process, possibly initiated by a single metal centre (homolytic activation).<sup>37</sup>

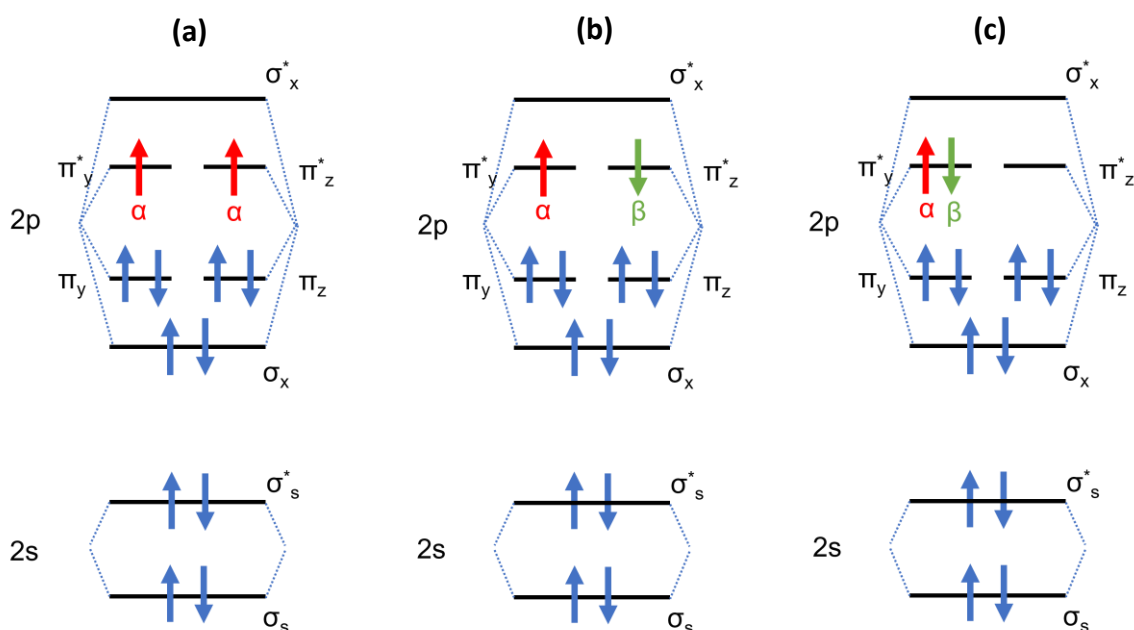
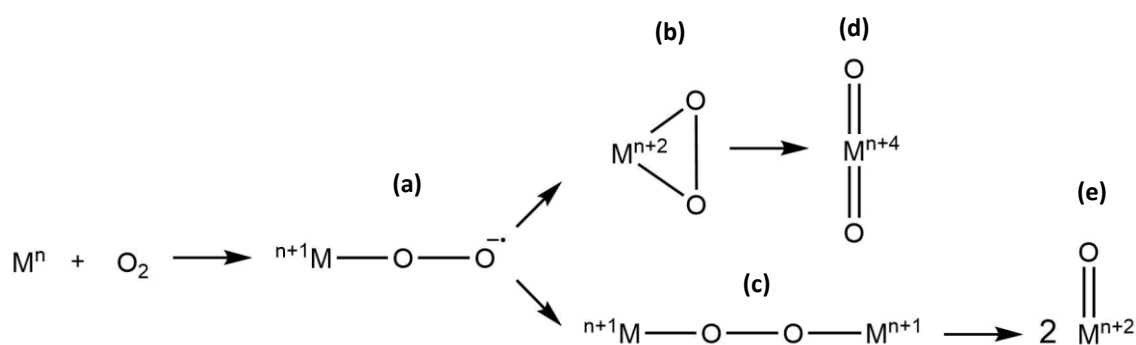


**Figure 1.4.** Electronic configurations of O<sub>2</sub>, (a) triplet state  $^3\Sigma_g^-$ , (b) singlet state  $^1\Sigma_g^+$  and (c) singlet state  $^1\Delta_g$ .

### 1.4.1 Heterolytic Oxygen Activation

Due to spin selection rules, a paramagnetic metal centre of oxidation state  $n$  ( $M^n$ ) is allowed to react with ground state  $O_2$  ( $^3\Sigma_g^-$ ) to form a superoxo metal complex ( $M^{n+1}-O_2^{\bullet-}$ ).<sup>38</sup> The peroxy-metal complex can also form an  $\eta$ -peroxy species or a  $\mu$ -peroxy species, which can further oxidise into a dioxo-metal or two oxo-metal species, respectively (Scheme 1.3).<sup>22,39</sup> These metal-oxygen species are utilised in catalytic oxidation reactions as they can react with organic compounds to form oxidised products. An Fe superoxo metal complex ( $[(TMS)Fe^{3+}-OO]^{2+}$ ), where TMS = 1,4,8,11-tetramethyl-1,4,8,11-tetraazacyclotetradecane, was found to be reactive towards the oxidation of cyclohexene.<sup>40</sup>  $\eta$ -Peroxy species have been proven to be reactive in the Sharpless epoxidation of alkenes<sup>41,42</sup>. Metal-oxo species are active for various oxidation reactions that occur *via* the Mars and van Krevelen mechanism,<sup>43</sup> such as the total oxidation of VOCs by cerium oxides.<sup>44</sup> An elegant use of heterolytic oxygen activation is the Wacker process, where  $PdCl_2$  is used as a catalyst to oxidise ethylene with  $O_2$  to acetaldehyde. This is done by cycling through from  $Pd^{2+}$  to  $Pd^0$ ; the  $Pd^{2+}$  is then reformed by reaction with an electron transfer mediator,  $CuCl_2$ .<sup>45</sup> This heterolytic oxygen activation mechanism is also present in enzymatic processes such as oxidations catalysed by monooxygenases,<sup>46</sup> often involving metal centres of Fe or Cu<sup>47</sup> and an electron transfer mediator like flavin.<sup>48</sup> Although there are many very useful oxidation reactions that occur *via* heterolytic oxygen activation, this will not be a focus of this study as homolytic oxygen activation is more relevant to the current industrial oxidation of THPMI to Cashmeran.



**Scheme 1.3.** Various forms of metal (M) -oxygen species which form during heterolytic activation of oxygen. (a) metal superoxo species, (b)  $\eta$ -peroxy species, (c)  $\mu$ -peroxy species, (d) dioxo-metal species and (e) oxo-metal species.

### 1.4.2 Homolytic Oxygen Activation

The fundamental difference between heterolytic and homolytic activation mechanisms is that homolytic activation mechanisms involve radical species as the reactive intermediate.<sup>37</sup> Uncatalyzed autoxidation proceeds *via* a homolytic process where an initiator, often an alkyl

peroxide, thermally decomposes and forms a radical species capable of initiating a radical chain reaction.<sup>22</sup> A generalised scheme for this process is shown in equations (1) – (3); where ‘In’ refers to an initiator and ‘R’ refers to an organic molecule. The initiator, often a thermally decomposed hydroperoxide, reacts with the organic molecule to abstract the most labile hydrogen producing an organic radical (1). This radical can then activate ground state O<sub>2</sub> to produce a peroxide radical (2) which is spin allowed,<sup>30</sup> which itself can propagate further oxidation by abstracting another hydrogen atom from the original organic substrate (3).<sup>49</sup> In the case of cumene hydroperoxide the onset temperature of decomposition was determined to be 80 °C.<sup>50</sup> This is of significance as it demonstrates that any oxidation reaction performed at elevated temperatures could result in the decomposition of hydroperoxide species, starting a chain radical process potentially affecting selectivity.

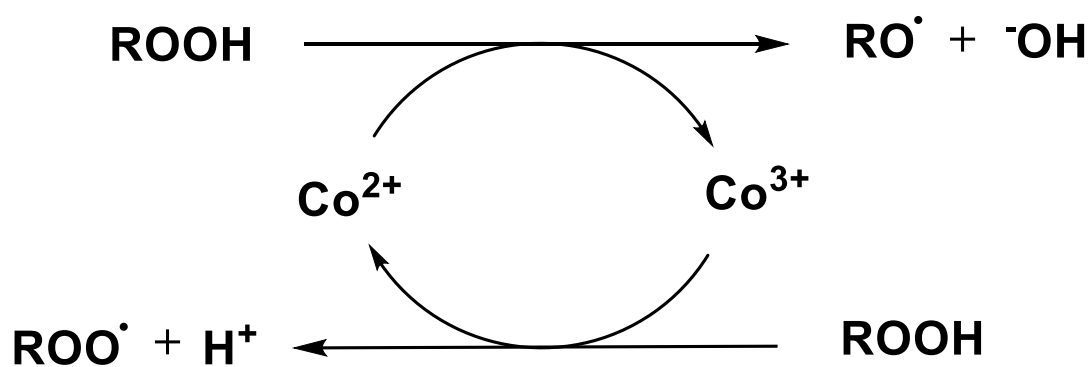


Metal centres such as Mn, Fe, Ni, Cu, and Co can be used to deliberately trigger a radical autoxidation reaction by inducing cleavage of a hydroperoxide species.<sup>51–53</sup> A more detailed analysis of cobalt for this use is given in section 1.5. It is important to note that in these systems the metal is not necessarily acting as a catalyst, but as a promoter or initiator for radical autoxidation, meaning there is little direct control of selectivity.<sup>54</sup>

## 1.5 Homogeneous Cobalt-Catalysed Oxidation Reactions

Cobalt is well known to be useful in a variety of industrial oxidation reactions. Cobalt has been utilised for decades in the aerobic oxidation of cyclohexane into a mixture of cyclohexanone and cyclohexanol known as KA oil,<sup>55</sup> which can then be further oxidised with strong acids into adipic acid, an important precursor for the formation of Nylon 6,6.<sup>56</sup> The autoxidation of n-butane into acetic acid was historically catalysed by cobalt acetate,<sup>57</sup> before being replaced by the rhodium-catalysed carbonylation of methanol.<sup>58</sup> How these systems operate is of importance to this investigation, as the Co-bis(2-ethylhexanoate) along with the operating conditions are largely similar to those historically used for the oxidation of cyclohexane using Co-stearate and Co(II)-naphthenate.<sup>59</sup> Co(II)-naphthenate acts as a radical

initiator for the autoxidation of cyclohexane *via* the homolytic cleavage of cyclohexane hydroperoxide (CHHP), as part of the Haber-Weiss cycle (Scheme 1.4).<sup>60,61</sup> This greatly increases selectivity as it has been shown that the uncontrolled decomposition of CHHP is the major cause of unwanted by-products.<sup>61-66</sup> The radical products of the Haber-Weiss cycle then undergo a series of propagation and termination steps, resulting in the desired products of cyclohexanone and cyclohexanol. The specific mechanism of these steps is debated in the literature, however it is generally agreed that once cobalt has catalysed the formation of the radical species, it plays little role in the reaction and the products are determined by the free radical autoxidation.<sup>60,64,67</sup> This is not to say that cobalt is not affecting the selectivity of the reactions, as the free radical chain reaction it catalyses results in greater levels of selectivity than would otherwise be seen without the catalyst.



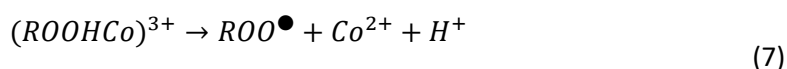
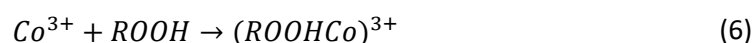
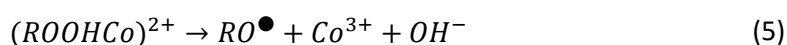
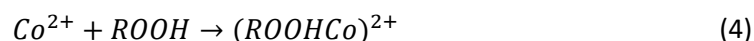
**Scheme 1.4.** The Haber-Weiss cycle for the decomposition of cyclohexane hydroperoxide (CHHP) by Co<sup>2+</sup>/Co<sup>3+</sup>, where R denotes C<sub>6</sub>H<sub>11</sub>.

Cobalt has also been used as a catalyst for alkene oxidations, historically cobalt naphthenate has been used in the aerobic, pressurised oxidation of methylpentene to afford the allylic ketone product.<sup>68,69</sup> Cobalt naphthenate has also been used in the aerobic oxidation of cyclohexene into 2-cyclohexen-1-one and 2-cyclohexen-1-ol selectively, below the autoxidation temperature in a solvent of chloroform.<sup>70</sup> Co(acac)<sub>2</sub> was tested for cyclohexene oxidation at 100 °C, well above the autoxidation temperature, in a solvent of acetic acid with no conversion being observed unless accompanied by NHPI (*N*-hydroxyphthalimide) as a co-catalyst.<sup>71</sup> From these studies it is apparent that solvent and ligand choice can play a large role in determining the activity and selectivity of the cobalt centre. Unfortunately, few studies exist which focus on cyclohexene oxidation using conditions which are analogous to the present work on THPMI. There are numerous studies which utilise cobalt as a catalyst for cyclohexene oxidation, however these often require the use of peroxides as an oxidant and/or promoter,<sup>72-74</sup> and/or the use of a solvent.<sup>70,75</sup> Studies which employ air as the oxidant, under solventless conditions and activated only by the cobalt species are very rare in the literature. However, Wei *et al.*<sup>76</sup> developed a Co<sup>II</sup>-

L-glutamic acid complex capable of oxidising cyclohexene to almost exclusively allylic oxidation products at over 80 % conversion, solventless and in an atmosphere of pure O<sub>2</sub>. Although the reaction proceeds *via* a radical pathway; when cobalt acetate was used as a catalyst almost no conversion was observed. It would be expected that Co<sup>2+</sup> ions would initiate the free radical oxidation of cyclohexene like in the many examples discussed above. However if the cyclohexene used in this example was stabilised it is possible that no initiators were present for Co<sup>2+</sup> ions to react with. The conclusion of this research was the Co<sup>II</sup>-L-glutamic acid complex catalysed oxidation by activation of O<sub>2</sub> directly, therefore circumventing the need for an initiator species like a hydroperoxide. There are also examples of cyclohexene oxidation under aerobic and solventless conditions, catalysed by heterogeneous catalysts, however this literature will be discussed in section 1.7.

## 1.6 Quenching of Oxidation Reactions

Since the 1950's, it has been known that oxidation catalysts can rapidly transform into inhibitors in the very same reaction. Cobalt and manganese decanoate, used in the oxidation of tetralin, will rapidly inhibit the reaction if a certain concentration is reached.<sup>77-80</sup> In the case of n-decane oxidation, a similar effect is observed where the oxidation is suddenly inhibited when a particular loading of the catalyst, copper stearate, is reached.<sup>81</sup> The sudden transition from catalyst to inhibitor only occurs in solvents of low polarity and is not observed in polar solvents such as acetic acid.<sup>82</sup> Research published by ExxonMobil suggests that the cause of this switch is an abundance of 'free' Co<sup>2+</sup> ions relative to hydroperoxide species.<sup>81</sup> To understand this, it is important to appreciate the initiation, propagation and termination steps of cobalt catalysed autoxidations. Initiation occurs when the hydroperoxide species forms a complex with cobalt and decomposes into either the hydroxy or peroxy radical, *via* the Haber-Weiss cycle, shown in equations (4 - 7). Propagation occurs when the radical species produced from initiation abstract

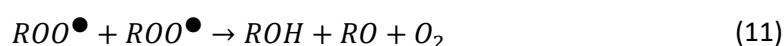


hydrogen atoms from the starting material, producing allylic radicals. In the case of alkene oxidation either an alcohol (8) or peroxide (9) molecule is produced depending on the reacting

radical. The allylic radical can then react with oxygen to form more peroxy radicals, propagating the reaction further (10). Generally, termination is considered to occur from two reactions, the first being a combination of two peroxy radicals to form one alcohol and one ketone product (11), known as a Russell termination.<sup>83,84</sup> This of course would limit oxidation as the peroxide molecules cannot undergo further propagation. The second termination is considered the explanation for deactivation in the cases of cobalt and manganese (12); for copper<sup>85-87</sup> and iron<sup>88</sup>



the higher valence ion would likely contribute to this step. The concept described by equation (12) was initially proposed in 1946<sup>89</sup> and was cited as a possible cause of deactivation in the case of tetralin oxidation.<sup>77</sup> The reason this termination step rapidly increases in rate at the point of deactivation is related to the ratio of free cobalt cations to cobalt cations complexed to hydroperoxide molecules. If the hydroperoxide is in excess concentration relative to cobalt, then the concentration of free cobalt will be too low for reaction (12) to be of significance. This explains why subtle increases in the concentration of cobalt catalysts can trigger reaction quenching.<sup>81</sup> This also explains why, in acetic acid or other polar solvents,<sup>82</sup> this effect is not seen as acetic acid binds strongly to cobalt and so at any cobalt concentration there is not enough free cobalt for reaction (9) to occur in significance.

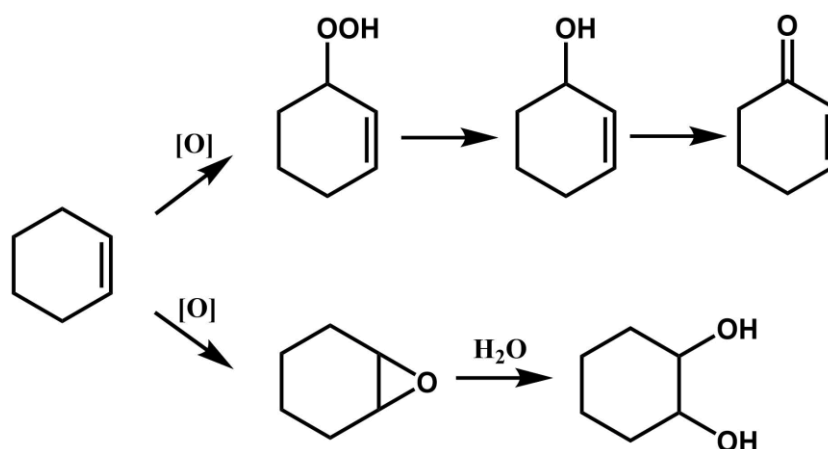


In the industrial oxidation of THPMI, oxidation will cease when approximately 65 % conversion is reached. This is not a major concern for IFF as reaction is limited to 50 %, as higher conversions result in un-economic selectivities. However, understanding this reaction quenching and how it is caused may provide vital knowledge leading to the improvement of the overall system.

## 1.7 Heterogeneous Catalysts for Oxidation of Alkenes

### 1.7.1 Considering Reaction Conditions

The oxidation of THPMI is not a reaction with rich abundance in the literature. The patent for the current industrial process demonstrates a high yield when cobalt salts were used as catalysts however gold supported on ceria performed very poorly with a much slower rate of reaction.<sup>15</sup> Cyclohexene oxidation is a much more explored reaction in the literature since the development of the Asahi process, which uses a Ruthenium catalyst to efficiently hydrogenate benzene into cyclohexene.<sup>90</sup> The conditions applied in the oxidation of cyclohexene vary significantly across literature. Many studies use highly reactive peroxides such as TBHP<sup>91-93</sup> or H<sub>2</sub>O<sub>2</sub><sup>94,95</sup> in excess as their oxygen sources (and *de facto* initiators),<sup>22</sup> but this is mainly to direct epoxidation rather than allylic oxidation (Scheme 1.5). These types of oxidations will not be considered in this overview as the oxidation of THPMI is already an aerobic process. The introduction of peroxides as oxidants would constitute a backwards step both environmentally and in terms of safety and would most likely direct oxidation away from the desired allylic products. Even when O<sub>2</sub> is used as the source of oxygen, either in its pure form or delivered in compressed air, there are many significant variations in reaction conditions that can affect oxidation. The use of solvent varies significantly in the literature, if used at all. DCM,<sup>96</sup> chloroform,<sup>70</sup> ethylbenzene,<sup>97</sup> cyclohexane,<sup>98</sup> toluene,<sup>99,100</sup> dimethylbenzene,<sup>99,100</sup> and others have been used, however acetonitrile<sup>100-103</sup> is the most common. Although it was found in autoxidation of cyclohexane that polarity of solvent has minimal effect on rate constant of propagation,<sup>104</sup> for other reactions the rate of termination (11) decreases with increasing polarity of solvent,<sup>105,106</sup> likely the reason acetonitrile is a popular choice of solvent. The papers which have studied various solvents under otherwise identical conditions found that there were



**Scheme 1.5.** Cyclohexene oxidation and its primary oxidation routes. Top: allylic oxidation. Bottom: epoxidation.

remarkable differences in selectivity depending on which solvent was employed.<sup>99,100</sup> Hughes *et al.*<sup>99</sup> demonstrated that, in the presence of a gold catalyst, changing the solvent from toluene to tetramethylbenzene results in switching from almost exclusively allylic oxidation to primarily epoxidation (Scheme 1.5). In the same study a more significant change of solvent to water resulted in almost exclusively total oxidation, with only CO<sub>2</sub>, formic and oxalic acid being formed. Wang *et al.*<sup>100</sup> showed that, with a supported gold catalyst, switching from toluene to acetonitrile can direct formation of the epoxide and diol products, rather than allylic oxidation products. To summarise, the choice of solvent will have a significant effect on selectivity and so when looking at relevant literature to this project it is more relevant to concentrate on reactions which are solventless. Solventless reactions are also much more relevant industrially as when no solvent is used, more reactor space can be designated to producing profitable chemicals and it removes the need for costly separation steps.

Aside from solvent and oxidant, the third condition that must be considered when assessing literature is the use of an initiator. Hydroperoxide species such as TBHP<sup>99,107–109</sup> or H<sub>2</sub>O<sub>2</sub><sup>101</sup> have been used in low loadings varying from 0.06 – 5 mol % in catalysed oxidations of cyclohexene. Used in conjunction with a metal catalyst of variable oxidation state, even trace amounts of hydroperoxide can act as an initiator for a free-radical chain oxidation.<sup>22</sup> For this reason it is important not to ignore literature where small amounts of hydroperoxide initiator are used, as any sample of alkene that does not contain stabilisers is likely to have small amounts of hydroperoxide present and therefore can be thought of as being ‘self-initiating’. The final condition that needs to be considered is temperature. Autoxidation of cyclohexene does not occur at a significant rate below 70 °C,<sup>110</sup> therefore at ≥ 70 °C thermal initiation of hydroperoxides should be considered as an activation mechanism.

## 1.7.2 Gold Catalysts for Oxidation

Many metals have been tested for the oxidation of cyclohexene with the most commonly used being gold<sup>94–96,99,100,107,108,111–113</sup>, copper<sup>102,114–116</sup> and cobalt<sup>70,97,98,102,117</sup>. Alshammari *et al.*<sup>107</sup> demonstrated that gold supported on graphite or metal oxide was active for the aerobic, solventless oxidation of cyclohexene, initiated by low loadings of TBHP. Gold was observed to be more active than either palladium or gold-palladium alloys when supported on graphite, particularly when smaller gold nanoparticles were formed (< 10 nm). Conclusions on selectivity should be avoided as conversion reached was < 10 % for all reactions in this study, however all reactions were below the autoxidation temperature, so any selectivity is directly due to the catalyst. Cai *et al.*<sup>111</sup> utilised gold supported on halloysite nanotubes and found activity under

solventless and aerobic conditions at 80 °C. Conversion of 12 % in the blank reaction increased to up to 30 % with the catalyst, and selectivity to the allylic products increased from 37 % with no catalyst to up to 85 % with the gold catalyst. It was again found that smaller nanoparticles corresponded to greater activity. Under similar conditions Hamdy *et al.*<sup>108</sup> demonstrated that gold nanoparticles supported on mesoporous silica are active for cyclohexene oxidation with 80 % selectivity to allylic products at 50 % conversion. As with previously mentioned studies, smaller nanoparticle size was linked to greater activity. Ovoshchnikov *et al.*<sup>112</sup> demonstrated that the cyclohexene epoxidation can be favoured by using WO<sub>3</sub> as a support for gold nanoparticles, or as a co-catalyst with Au/SiO<sub>2</sub>. If the metal organic framework 'MIL-101' is used as a co-catalyst with Au/SiO<sub>2</sub> then cyclohexene-hydroperoxide decomposition into 2-cyclohexene-1-one will be favoured. As with other examples the conditions were solventless, aerobic and at 65 °C. This work also demonstrated that leached gold is inactive for cyclohexene oxidation. Under similar conditions Rogers *et al.*<sup>113</sup> demonstrated how graphite and graphene can be effective supports for gold nanoparticles for the oxidation of cyclohexene, and again smaller nanoparticles were linked to greater activity. The work enhanced on Ovoshchnikov's by using water to hydrolyse the epoxide into the diol. To summarise, various forms of gold catalysts have been employed for the oxidation of cyclohexene, all under aerobic and solventless conditions, with some using small amounts of TBHP as initiator. Various types of supports have been tested; however, Au nanoparticles are always active for oxidation with activity increasing as nanoparticle size decreases. Unless epoxidation is deliberately enhanced by catalyst design or co-catalyst, selectivity will be primarily directed towards the allylic alcohol and ketone products. This is due to relatively small rings such as C<sub>6</sub> cyclohexene needing to pass through a greater energetic barrier to form the epoxide products, compared to larger rings such as C<sub>8</sub> cyclooctane which passes through a relatively lower energy barrier, due to lower ring strain.<sup>118</sup> Although gold clearly catalyses the oxidation of cyclohexene below autoxidation levels, the overall allylic selectivities obtained are no better than simply running the reaction above autoxidation with no catalyst, where at 50 % conversion approximately 90 % of all products were allylic.<sup>110</sup> None of the work described in the literature above demonstrates a greater yield of allylic products compared to a blank reaction; however generally the make-up of the allylic products from gold catalysis constitutes less peroxide and more alcohol and ketone.

### 1.7.3 Copper and Other Catalysts for Oxidation

Copper is another commonly used metal for the catalysed oxidation of cyclohexene, with some examples in the literature under conditions that are solvated<sup>102,115</sup> or non-aerobic.<sup>119</sup>

However, there are examples utilising aerobic and solventless conditions such as a study by Sang *et al.*<sup>114</sup> who used a mesoporous CuO catalyst. This work demonstrated that mesoporous CuO has high activity for cyclohexene oxidation, with joint allylic selectivities of 90 % at conversions of 65 -75 %, much greater than commercial CuO. The selectivity was claimed to be entirely made up of 2-cyclohexen-1-ol and 2-cyclohexen-1-one with no detection of the hydroperoxide intermediate or any other products such as the epoxide or cyclohexene dimers. It should also be noted that running the reaction up to 10 hours resulted in 67 % conversion, however running the reaction for a further 2 or 5 hours results in no more conversion. This is not explained in the paper or even mentioned; however it could be a result of some quenching mechanism, as discussed in section 1.6, or from the formation of a biphasic mixture that separates the catalyst from the cyclohexene.<sup>113</sup> Da Silva *et al.*<sup>116</sup> demonstrated that copper oxide nanoparticles supported on silica-coated iron oxide are active for the solventless, aerobic oxidation of cyclohexene. Total allylic selectivities of over 90 % were reported, at conversions of up to 90 %. It was concluded that CuO was more active than Cu<sub>2</sub>O and running the reaction at higher temperatures directed selectivity away from epoxidation and towards allylic oxidation. However, cyclohexene peroxide concentration levels were not analysed and after several runs the catalyst lost activity rapidly, although copper leaching was not detected. Denekamp *et al.*<sup>102</sup> produced a catalyst consisting of copper nanoparticles, supported on a highly porous, nitrogen doped carbon material. This material catalysed the aerobic oxidation of cyclohexene in a solvent of acetonitrile at 70 °C. Selectivity to allylic oxidation products was between 66 – 70 % at between 71 – 85 % conversion. A more interesting trait of this catalyst was ability to maintain these conversion and selectivity values in the presence of the radical scavenger, butylated hydroxytoluene (BHT). This is thought to be possible due to the bulky BHT molecules being too large to enter the pores of the support, and so the copper active sites within the pores could catalyse the reaction without the release of radical species into the solution.

Although tested for cyclohexane oxidation, not cyclohexene oxidation as with other catalysts in this section, Molybdenum Blue has demonstrated useful traits which may be of use for THPMI oxidation. Molybdenum Blue is a complex polyoxometalate<sup>120-122</sup> which has applications in quantification assays for phosphate ions<sup>123</sup> and reducing sugars.<sup>124</sup> Molybdenum Blue has demonstrated catalytic properties for cyclohexane oxidation into cyclohexanol and cyclohexanone which was tuneable with heat treatment.<sup>125</sup> More importantly, the selectivity of material is thought to be a result of the catalytic decomposition of CHHP into the alcohol and ketone products.<sup>122</sup> Another useful property of Molybdenum Blue was continued activity in spite of addition of the radical scavenger CBrCl<sub>3</sub>.<sup>125</sup>

## 1.7.4 Summary of Heterogeneous Catalysts for Oxidation

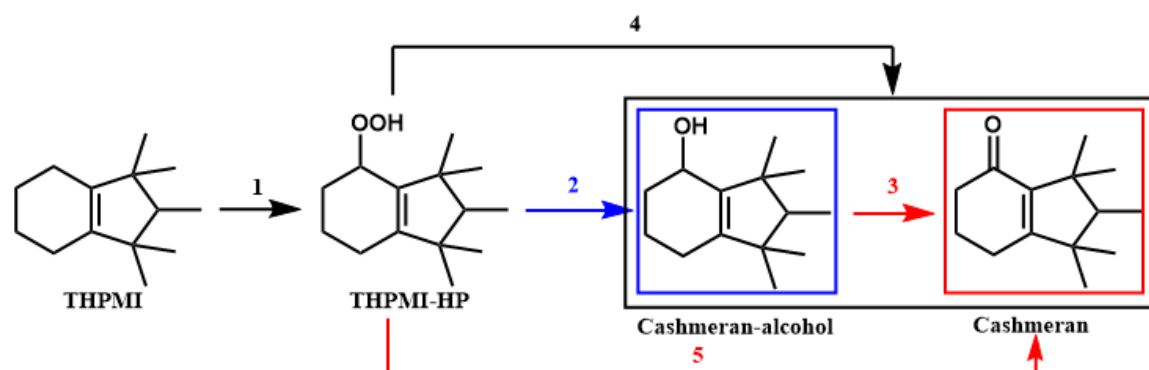
Although a wealth heterogeneous metal catalysts have been tested for the oxidation of cyclohexene, very few of these papers investigate or suggest the possible mechanism of reaction. It is well known that the autoxidation of alkenes proceeds *via* a radical mechanism<sup>126</sup> and will primarily result in allylic oxidation products.<sup>110</sup> Often work on this reaction will focus on designing catalytic systems that directs oxidation away from allylic routes into epoxidation.<sup>94,95,112,113</sup> However, this thesis is focused on maximising the already favoured allylic route, often not a concern in the literature. Much of the literature cited above will seem to demonstrate very high selectivity towards the allylic products, however it is possible that, similar to  $\text{Co}^{2+}$  ions, the heterogeneous catalysts mentioned are simply initiating a self-propagating radical chain mechanism. When considering this literature in the context of improving the oxidation of THPMI into Cashmeran, it is important to glean inspiration for new catalysts whilst considering reaction conditions such as solvent, temperature, oxidant, initiators, promoters, and substrate. An alteration of any of these conditions could change the outcome of the reaction in terms of both selectivity and activity, and results in literature will not necessarily yield similar results when used in new reactions.

## 1.8 Summary

The improvement in selectivity (and so yield) in the oxidation of THPMI into Cashmeran could result in a significant improvement in its producers profit margin, but perhaps more importantly would satisfy the first principle of the 12 principles of green chemistry, 'Prevention'.<sup>127</sup> By avoiding the conversion of THPMI into undesired products, less waste will have to be disposed of, less THPMI, and fewer energy intensive reactions will be required to produce the same mass of Cashmeran.

Currently Cashmeran and Cashmeran-alcohol are produced in an aerobic oxidation, mediated by Co-bis(2-ethylhexanoate). The typical routes to form these products is shown in Scheme 1.6 and there is precedent in the literature for all routes. It is expected the cobalt functions as an initiator of a chain radical oxidation method; as with the oxidation of cyclohexane where the hydroperoxide species, CHHP, is decomposed by  $\text{Co}^{2+}$  and  $\text{Co}^{3+}$  as part of the Haber-Weiss cycle (Scheme 1.4).<sup>60,61</sup> This satisfies routes **1** and **2**, although at current industrially used temperature of 110 °C autoxidation of THPMI could occur, which would also result in THPMI-HP.<sup>126</sup> Another mechanism for the route **1** would be the abstraction of the allylic hydrogen by a  $\text{Co}^{3+}$  species, as with the autoxidation of n-butane<sup>57,128</sup> and cyclohexane<sup>129,130</sup> by cobalt acetate

in acetic acid. There is also suggestion that route **2** may occur by reaction between one THPMI molecule and one THPMI-HP molecule to form two Cashmeran-alcohol molecules.<sup>102</sup> Route **3** could occur by a  $\text{Co}^{3+}$  species catalysing the oxidation of the secondary alcohol group into a ketone, as with  $\text{Co}^{\text{III}}$  acetate, as described in the literature.<sup>131,132</sup> Route **3** could also occur spontaneously through autoxidation, producing a Cashmeran and a  $\text{H}_2\text{O}_2$  molecule for every Cashmeran-alcohol molecule oxidised.<sup>133,134</sup> Route **4** represents a termination step where two peroxide molecules combine to form one Cashmeran-alcohol and one Cashmeran molecule, known as a Russell termination, a step that is typical in autoxidation processes.<sup>83,84</sup> Route **5** is an idealised route whereby THPMI-HP is oxidised directly into Cashmeran *via* a condensation reaction. This could be catalysed by  $\text{Co}^{2+}$ , as with the oxidation of cyclohexene by cobalt acetate in acetic acid mentioned earlier.<sup>129,130</sup> However, it is more likely to result from the abstraction of the weakly bonded alpha hydrogen from THPMI-HP by a radical species, leading to the formation of one Cashmeran molecule and a hydroxy radical.<sup>135</sup> Due to the radical mechanism the autoxidation of organic molecules, including THPMI, can be vastly complicated and it is almost impossible to decipher exactly what is occurring on a molecular level. When studying this system, it is vital to consider as many of these radical, possibly catalysed, processes as possible to analyse any data. The aim of this report is to try and uncover the benefits of using Co-bis(2-EH) in the oxidation of THPMI into Cashmeran and investigate ways to improve this process or to find alternative catalysts or systems that may improve the overall yield.



**Scheme 1.6.** Various routes to oxidise THPMI into the desired products: Cashmeran and Cashmeran-alcohol. Route **1** represents the formation of the initial intermediate, THPMI-HP, by the oxidation of the starting material, THPMI. Route **2** represents the breakdown of THPMI-HP into Cashmeran-alcohol. Route **3** represents the oxidation of Cashmeran-alcohol to Cashmeran. Route **4** represents a Russell termination where two THPMI-HP molecules form one Cashmeran-alcohol and one Cashmeran molecule. Route **5** represents the conversion of THPMI-HP to Cashmeran, directly.

## 1.9 References

- 1 P. Kraft, J. A. Bajgrowicz, C. Denis and G. Fráter, *Angew. Chemie - Int. Ed.*, 2000, **39**, 2980–3010.

- 2 W. H. Perkin, *J. Chem. Soc.*, 1868, **21**, 53–63.
- 3 K. Reimer, *Eur. J. Inorg. Chem.*, 1876, **9**, 423–424.
- 4 B. G. Lake, *Food Chem. Toxicol.*, 1999, **37**, 423–453.
- 5 M. B. Hocking, *J. Chem. Educ.*, 1997, **74**, 1055–1059.
- 6 G. A. Martău, L. F. Călinoiu and D. C. Vodnar, *Trends Food Sci. Technol.*, 2021, **109**, 579–592.
- 7 P. Chattopadhyay, G. Banerjee and S. K. Sen, *J. Clean. Prod.*, 2018, **182**, 272–279.
- 8 I. Felker, G. Pupo, P. Kraft and B. List, *Angew. Commun.*, 2015, **54**, 1960–1964.
- 9 United States Patent Office, US3773836, 1973.
- 10 P. Kraft, V. Di Cristofaro and S. Jordi, *Chem. Biodivers.*, 2014, **11**, 1567–1596.
- 11 P. Kraft, S. Jordi, N. Denizot and I. Felker, *European J. Org. Chem.*, 2014, **2014**, 554–563.
- 12 N. Armanino, J. Charpentier, F. Flachsmann, A. Goeke, M. Liniger and P. Kraft, *Angew. Chemie - Int. Ed.*, 2020, **59**, 2–37.
- 13 United States Patent Office, US 20050009729A1, 2005.
- 14 United States Patent Office, US3847993, 1974.
- 15 European Patent Office, EP2305628, 2011.
- 16 United States Patent Office, US2020/0001274A1, 2020.
- 17 European Patent Office, EP3257831A3, 2018.
- 18 M. Eichelbaum, R. Glaum, M. Hävecker, K. Wittich, C. Heine, H. Schwarz, C. Dobner, A. Trunschke and R. Schlögl, *ChemCatChem*, 2013, **5**, 2318–2329.
- 19 R. Y. Saleh, I. E. Wachs, S. S. Chan and C. C. Chersich, *J. Catal.*, 1986, **98**, 102–114.
- 20 C. Hess, M. H. Looi, S. B. A. Hamidb and R. Schlogl, *Chem. Commun.*, 2006, 451–453.
- 21 U. Schuchardt, D. Cardoso, R. Sercheli, R. Pereira, S. Rosenira, M. C. Guerreiro, D. Mandelli, E. V Spinacé and E. L. Pires, *Appl. Catal. A Gen.*, 2001, **211**, 1–17.
- 22 X. Liu, Y. Ryabenkova and M. Conte, *Phys. Chem. Chem. Phys.*, 2015, **17**, 715–731.
- 23 C. He, J. Cheng, X. Zhang, M. Douthwaite, S. Pattison and Z. Hao, *Chem. Rev.*, 2019, **119**, 4471–4568.

- 24 P. M. Shah, A. N. Day, T. E. Davies, D. J. Morgan and S. H. Taylor, *Appl. Catal. B Environ.*, 2019, **253**, 331–340.
- 25 E. Kritsanaviparkporn, F. M. Baena-Moreno and T. R. Reina, *Chemistry (Easton)*, 2021, **3**, 630–646.
- 26 C. A. Hone and C. O. Kappe, *Top. Curr. Chem.*, 2019, **377**, 1–44.
- 27 R. Prabhakar, P. E. M. Siegbahn, B. F. Minaev and H. Ågren, *J. Phys. Chem. B*, 2002, **106**, 3742–3750.
- 28 C. Carbogno, J. Behler, A. Groß and K. Reuter, *Phys. Rev. Lett.*, 2008, **101**, 1–4.
- 29 H. Winter, *Phys. Scr.*, 1983, **T3**, 159–162.
- 30 K. Kang, M. Park and J. Choi, *Phys. Chem. Chem. Phys.*, 2011, **13**, 8122–8126.
- 31 A. H. Haines, in *Alkanes, Alkyl Groups, and Hydrocarbon Residues, Alkanes, Alkenes, Alkynes and Arenes*, ed. Academic Press, 1985, p. 29.
- 32 M. Kristiansen, R. D. Scurlock, K. Lu and P. R. Ogilby, *J. Phys. Chem.*, 1991, **95**, 5190–5197.
- 33 M. A. J. Rodgers, *J. Am. Chem. Soc. Chem. Soc.*, 1983, **105**, 6201–6205.
- 34 K. Gollnick and A. Griesbeck, *Tetrahedron*, 1985, **41**, 2057–2068.
- 35 C. S. Foote, *Science*, 1968, **162**, 963–970.
- 36 R. A. Sheldon, I. W. C. E. Arends and H. E. B. Lempers, *Catal. Today*, 1998, **41**, 387–407.
- 37 G. Rothenberg, L. Feldberg, H. Wiener and Y. Sasson, *J. Chem. Soc. Perkin Trans. 2*, 1998, 2429–2434.
- 38 M. H. Dickman and M. T. Pope, *Chem. Rev.*, 1994, **94**, 569–584.
- 39 J. M. Mayer, *Inorg. Chem.*, 1988, **27**, 3899–3903.
- 40 Y. Lee, S. Hong, Y. Morimoto, W. Shin, S. Fukuzumi and W. Nam, *J. Am. Chem. Soc.*, 2010, **132**, 10668–10670.
- 41 Y. Wu and D. K. W. Lai, *J. Am. Chem. Soc.*, 1995, **117**, 11327–11336.
- 42 K. B. Sharpless, J. M. Townsend and D. R. Williams, *J. Am. Chem. Soc.*, 1972, **94**, 295–296.
- 43 P. Mars and D. W. van Krevelen, *Chem. Eng. Sci.*, 1954, **3**, 41–59.
- 44 S. Scirè, S. Minicò, C. Crisafulli, C. Satriano and A. Pistone, *Appl. Catal. B Environ.*, 2003, **40**, 43–49.

- 45 J. Piera and J. E. Bäckvall, *Angew. Chemie - Int. Ed.*, 2008, **47**, 3506–3523.
- 46 D. E. Torres Pazmiño, M. Winkler, A. Glieder and M. W. Fraaije, *J. Biotechnol.*, 2010, **146**, 9–24.
- 47 A. Decker and E. I. Solomon, *Curr. Opin. Chem. Biol.*, 2005, **9**, 152–163.
- 48 D. H. Lang, C. K. Yeung, R. M. Peter, C. Ibarra, R. Gasser, K. Itagaki, R. M. Philpot and A. E. Rettie, *Biochem. Pharmacol.*, 1998, **56**, 1005–1012.
- 49 W. Partenheimer, *Catal. Today*, 1995, **23**, 69–158.
- 50 Y. Duh, C. Kao, H. Hwang and W. W. Lee, *Process Saf. Environ. Prot.*, 1998, **76**, 271–276.
- 51 A. Bakac, *Coord. Chem. Rev.*, 2006, **250**, 2046–2058.
- 52 N. Lehnert, R. Y. N. Ho, L. Que and E. I. Solomon, *J. Am. Chem. Soc.*, 2001, **123**, 8271–8290.
- 53 P. Chen, E. I. Solomon and R. Phm, *J. Am. Chem. Soc.*, 2004, **126**, 4991–5000.
- 54 M. Conte, X. Liu, D. M. Murphy and G. J. Hutchings, *Phys. Chem. Chem. Phys.*, 2012, **14**, 16279–16285.
- 55 J. W. M. Stebman, S. Kaae and P. J. Hoftyzer, *Chem. Eng. Sci.*, 1961, **14**, 139–149.
- 56 A. Castellan, J. C. J. Bart and S. Cavallaro, *Catal. Today*, 1991, **9**, 301–322.
- 57 R. A. Sheldon and J. K. Kochi, in *Metal-catalyzed Oxidations of Organic Compounds*, Academic Press, 1981, pp. 345–346.
- 58 D. Forster, *Adv. Organomet. Chem.*, 1979, **17**, 255–267.
- 59 I. V. Berezin, E. T. Denisov and N. M. Emanuel, in *The Oxidation of Cyclohexane*, 1966, pp. 163–211.
- 60 B. P. C. Hereijgers and B. M. Weckhuysen, *J. Catal.*, 2010, **270**, 16–25.
- 61 A. Ramanathan, M. S. Hamdy, R. Parton, T. Maschmeyer, J. C. Jansen and U. Hanefeld, *Appl. Catal. A Gen.*, 2009, **355**, 78–82.
- 62 E. J. Silke, W. J. Pitz, C. K. Westbrook and M. Ribaucour, *J. Phys. Chem.*, 2007, 3761–3775.
- 63 B. Modén, B. Zhan, J. Dakka, J. G. Santiesteban and E. Iglesia, *J. Catal.*, 2006, **239**, 390–401.
- 64 I. Hermans, J. Peeters and P. A. Jacobs, *J. Phys. Chem.*, 2008, 1747–1753.

- 65 I. Hermans, P. A. Jacobs and J. Peeters, *Chem. - A Eur. J.*, 2007, 754–761.
- 66 I. Hermans, P. A. Jacobs and J. Peeters, *Chem. - A Eur. J.*, 2006, 4229–4240.
- 67 C. Nussbaumer, G. Fráter and P. Kraft, *Helv. Chim. Acta*, 1999, **82**, 1016–1024.
- 68 R. A. Sheldon and J. K. Kochi, in *Metal-catalyzed Oxidations of Organic Compounds*, Academic Press, 1981, p. 274.
- 69 United States Patent Office, 3258491, 1966.
- 70 C. S. Sharma, S. C. Sethi and S. Dev, *Synthesis*, 1974, 45–46.
- 71 Y. Ishii, T. Iwahama, S. Sakaguchi and K. Nakayama, 1996, **3263**, 4520–4526.
- 72 Z. Bıyıklıo, E. Tu, S. Gökc and H. Kantekin, *J. Mol. Catal. A Chem.*, 2013, **378**, 156–163.
- 73 P. Chutia, S. Kato, T. Kojima and S. Satokawa, *Polyhedron*, 2009, **28**, 370–380.
- 74 M. Salavati-niasari, P. Salemi and F. Davar, *J. Mol. Catal. A Chem.*, 2005, **238**, 215–222.
- 75 K. Kasuga, K. Tsuboi, M. Handa, T. Sugimori and K. Sogabe, *Inorg. Chem. Commun.*, 1999, **2**, 507–509.
- 76 Y. N. Wei, H. Li, F. Yue, Q. Xu, J. D. Wang and Y. Zhang, *RSC Adv.*, 2016, **6**, 107104–107108.
- 77 Y. Kamiya and K. U. Ingold, *Can. J. Chem.*, 1964, **42**, 2424–2433.
- 78 Y. Kamiya, S. Beaton, A. Lafortune and U. Ingold, *Can. J. Chem.*, 1963, **41**, 2020–2033.
- 79 Y. Kamiya, S. Beaton, A. Lafortune and K. U. Ingold, *Can. J. Chem.*, 1963, **41**, 2034–2053.
- 80 Y. Kamiya and K. U. Ingold, *Can. J. Chem.*, 1963, **42**, 1027–1043.
- 81 J. F. Black, *J. Am. Chem. Soc.*, 1978, **100**, 527–535.
- 82 B. Arthur, E. Woodward and R. B. Mesrobian, *J. Am. Chem. Soc.*, 1953, **75**, 6189–6195.
- 83 U. N. Gupta, N. F. Dummer, S. Pattisson, R. L. Jenkins, D. W. Knight, D. Bethell and G. J. Hutchings, *Catal. Letters*, 2015, **145**, 689–696.
- 84 G. A. Russell, *J. Am. Chem. Soc.*, 1957, **79**, 3871–3872.
- 85 J. K. Kochi, *Tetrahedron*, 1962, **18**, 483–497.
- 86 J. K. Kochi, *J. Am. Chem. Soc.*, 1963, **225**, 1862–1872.
- 87 J. K. Kochi, *J. Organic Chem.*, 1962, **85**, 1958–1968.
- 88 C. Walling, *Acc. Chem. Res.*, 1975, **8**, 125–131.

- 89 P. George and A. Robertson, *Trans. Faraday Soc.*, 1946, **42**, 217–224.
- 90 H. Nagahara, M. Ono, M. Konishi and Y. Fukuoka, *Appl. Surf. Sci.*, 1997, **122**, 448–451.
- 91 C. H. A. Tsang, Y. Liu, Z. Kang, D. Duo, N. Wong and S. Lee, *Chem. Commun.*, 2009, **0**, 5829–5831.
- 92 S. El-Korso, S. Bedrane, A. Choukchou-Braham and R. Bacir, *RSC Adv.*, 2016, **6**, 110375–110382.
- 93 A. K. Rathi, M. B. Gawande, J. Pechousek, J. Tucek, C. Aparicio, M. Petr, O. Tomanec, R. Krikavova, Z. Travnicek, R. S. Varma and R. Zboril, *Green Chem.*, 2016, **18**, 2363–2373.
- 94 N. Yu, Y. Ding, A. Lo, S. Huang, P. Wu, C. Liu and D. Yin, *Microporous Mesoporous Mater.*, 2011, **143**, 426–434.
- 95 P. Bujak, P. Bartczak and J. Polanski, *J. Catal.*, 2012, **295**, 15–21.
- 96 X. He, L. Chen, X. Zhou and H. Ji, *Catal. Commun.*, 2016, **83**, 78–81.
- 97 W. Zhong, M. Liu, J. Dai, J. Yang, L. Mao and D. Yin, *Appl. Catal. B Environ.*, 2018, **225**, 180–196.
- 98 F. P. Silva, M. J. Jacinto, R. Landers and L. M. Rossi, *Catal. Letters*, 2011, **141**, 432–437.
- 99 M. D. Hughes, Y. Xu, P. Jenkins, P. McMorn, P. Landon, D. I. Enache, A. F. Carley, G. A. Attard, G. J. Hutchings, F. King, E. H. Stitt, P. Johnston, K. Griffin and C. J. Kiely, *Nature*, 2005, **437**, 1132–1135.
- 100 L. Wang, H. Wang, P. Hapala, L. Zhu, L. Ren, X. Meng, J. P. Lewis and F. Xiao, *J. Catal.*, 2011, **281**, 30–39.
- 101 T. Liu, H. Cheng, W. Lin, C. Zhang, Y. Yu and F. Zhao, *Catalysts*, 2016, **6**, 24.
- 102 I. M. Denekamp, M. Antens, T. K. Slot and G. Rothenberg, *ChemCatChem*, 2018, **10**, 1035–1041.
- 103 P. Zhang, H. Lu, Y. Zhou, L. Zhang, Z. Wu, S. Yang, H. Shi, Q. Zhu, Y. Chen and S. Dai, *Nat. Commun.*, 2015, **6**, 1–10.
- 104 E. T. Denisov and R. L. Vardanyan, *Bull. Acad. Sci. USSR, Div. Chem. Sci.*, 1972, **21**, 2396–2399.
- 105 K. Tanaka and J. Imamura, *Chem. Lett.*, 1974, **3**, 1347–1348.
- 106 R. A. Sheldon and J. K. Kochi, in *Metal-catalyzed Oxidations of Organic Compounds*,

Academic Press, 1981, p. 30.

- 107 H. Alshammari, P. J. Miedziak, D. W. Knight, D. J. Willock and G. J. Hutchings, *Catal. Sci. Technol.*, 2013, **3**, 1531–1539.
- 108 M. S. Hamdy, *Microporous Mesoporous Mater.*, 2016, **220**, 81–87.
- 109 I. Y. Skobelev, A. B. Sorokin, K. A. Kovalenko, V. P. Fedin and O. A. Kholdeeva, *J. Catal.*, 2013, **298**, 61–69.
- 110 S. M. Mahajani, M. M. Sharma and T. Sridhar, *Chem. Eng. Sci.*, 1999, **54**, 3967–3976.
- 111 Z. Cai, M. Zhu, H. Dai, Y. Liu, J. Mao, X. Chen and C. He, *Adv. Chem. Eng. Sci.*, 2011, **1**, 15–19.
- 112 D. S. Ovoshchnikov, B. G. Donoeva, B. E. Williamson and V. B. Golovko, *Catal. Sci. Technol.*, 2014, **4**, 752–757.
- 113 O. Rogers, S. Pattison, J. Macginley, S. H. Taylor and G. J. Hutchings, *Catalysts*, 2018, **8**, 311.
- 114 X. Sang, J. Zhang, T. Wu, B. Zhang, X. Ma, L. Peng, B. Han, X. Kang, C. Liu and G. Yang, *RSC Adv.*, 2015, **5**, 67168–67174.
- 115 R. Zhang and R. Tang, *J. Mater. Sci.*, 2016, **51**, 5802–5810.
- 116 F. P. da Silva, R. V. Goncalves and L. M. Rossi, *J. Mol. Catal. A Chem.*, 2017, **426**, 534–541.
- 117 A. Reza, S. Mosazadeh and F. Ashouri, *J. Colloid Interface Sci.*, 2017, **506**, 10–26.
- 118 H. Alshammari, P. J. Miedziak, D. W. Knight, D. J. Willock and G. J. Hutchings, *Catal. Sci. Technol.*, 2013, **3**, 1531–1539.
- 119 C. H. A. Tsang, Y. Liu, Z. Kang, D. Duo, N. Wong and S. Lee, *Chem. Commun.*, 2009, **39**, 5829–5831.
- 120 C. Serain, *Acc. Chem. Res.*, 2000, **33**, 2–10.
- 121 A. Müller, J. Meyer, E. Krickemeyer and E. Diemann, *Angew. Chemie - Int. Ed.*, 1996, **35**, 1206–1208.
- 122 M. Conte, X. Liu, D. M. Murphy, S. H. Taylor, K. Whiston and G. J. Hutchings, *Catal. Letters*, 2016, **146**, 126–135.
- 123 Z. He and C. W. Honeycutt, *Commun. Soil Sci. Plant Anal.*, 2007, **36**, 1373–1383.
- 124 S. P. Deng and M. A. Tabatabai, *Soil Biol. Biochem.*, 1994, **26**, 473–477.

- 125 X. Liu, M. Conte, W. Weng, Q. He, R. L. Jenkins, M. Watanabe, D. J. Morgan, D. W. Knight, D. M. Murphy, K. Whiston, C. J. Kiely and G. J. Hutchings, *Catal. Sci. Technol.*, 2015, **5**, 217–227.
- 126 R. A. Sheldon and J. K. Kochi, in *Metal-catalyzed Oxidations of Organic Compounds*, Academic Press, 1981, pp. 271–274.
- 127 P. T. Anastas and J. C. Warner, in *Green Chemistry: Theory and Practice*, Oxford University Press, New York, 1998, p. 30.
- 128 A. Onopchenko and J. G. D. Schulz, *J. Organic Chem.*, 1973, **38**, 909–912.
- 129 A. Onopchenko and J. G. D. Schulz, *J. Organic Chem.*, 1973, **38**, 3729–3733.
- 130 R. A. Sheldon and J. K. Kochi, in *Metal-catalyzed Oxidations of Organic Compounds*, Academic Press, 1981, p. 347.
- 131 R. A. Sheldon and J. K. Kochi, in *Metal-catalyzed Oxidations of Organic Compounds*, Academic Press, 1981, pp. 353–356.
- 132 Great Britain Patent Office, GB1275699A, 1972.
- 133 United States Patent Office, 2869989, 1959.
- 134 R. A. Sheldon and J. K. Kochi, in *Metal-catalyzed Oxidations of Organic Compounds*, Academic Press, 1981, pp. 350–352.
- 135 I. Hermans, P. Jacobs and J. Peeters, *Chem. - A Eur. J.*, 2007, **13**, 754–761.

# 2 Experimental Section

## 2.1 Introduction

This chapter details the methods used to run and analyse reactions, prepare and test catalysts, and describes techniques used to characterise catalysts. Some background theory behind all techniques is also provided.

## 2.2 Oxidation of THPMI

THPMI (10 mL, 65 mol% crude, IFF), hexadecane as internal standard (1 mL, 99 %, Sigma Aldrich), and any catalyst (e.g. 13 mg Co-bis(2-ethylhexanoate) (50 - 70 % in naphtha, IFF) for a standard 0.15 wt% loading) were added to a 2-neck, 50 ml round bottom flask. A magnetic stirrer bar was added and the side neck was sealed by a rubber stopper. An air delivery tube was inserted through the side neck stopper into the liquid, being rested on the bottom of the glass flask. The middle neck was fitted with an adapter to prevent loss of liquid through agitation, but was left open to the air to allow pressure release. Air flow for all reactions was set to 100 mL min<sup>-1</sup> using a gas flow meter to give an air residence time of 0.11 min, unless stated otherwise. This set up was placed in a preheated oil bath to the desired temperature and the reaction was run for the required time (Figure 2.1). When a sample was taken the stirring was stopped and a few drops of the reaction mixture were added to two GC vials, one containing triphenylphosphine (TPP) (99 %, Sigma-Aldrich), then both vials are filled with acetone. If a solid catalyst was present in the reaction, the sample was filtered using a syringe filter to remove any catalyst. Each sample was analysed using gas chromatography (GC), as described in section (2.4.2).

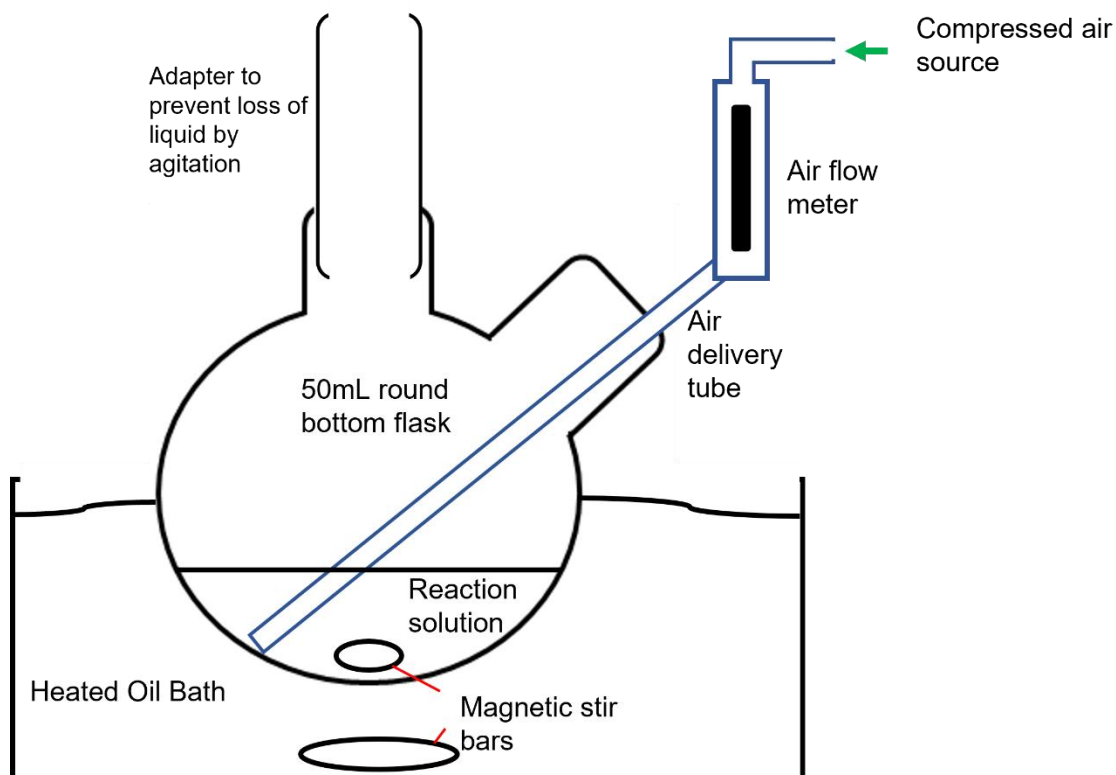


**Figure 2.1.** Schematic of the reactor for the oxidation of THPMI.

## 2.3 Preparation of Heterogeneous Catalysts

### 2.3.1 Preparation of CoO/SiO<sub>2</sub>

Procedure modified from the literature:<sup>1,2</sup> (3-aminopropyl)triethoxysilane (4.5 mL, 99 % Sigma-Aldrich) was dissolved in toluene (150 mL). SiO<sub>2</sub> (3 g, silica gel from Sigma-Aldrich, lot number MKBJ0366V) was added and stirred for 2 h at room temperature. The solid was then separated *via* centrifugation, washed with toluene and dried at 110 °C for 16 h to produce the aminated silica support. This aminated silica (2 g) was added to Co(NO<sub>3</sub>)<sub>6</sub>H<sub>2</sub>O (aqueous, 3.3 mmol L<sup>-1</sup>, 500 mL, ≥98 % Sigma-Aldrich) and left to stir at room temperature for 1 h. The solid was separated *via* centrifugation and washed with H<sub>2</sub>O (2 L). The solid was then re-dispersed in H<sub>2</sub>O (100 mL) and NaOH (2 M, aqueous, ≥98 % Sigma-Aldrich) was added until pH 11 was obtained. The mixture was then stirred at 100 °C for 2 h. The solid was then separated *via* centrifugation and washed with H<sub>2</sub>O (2 L). The solid was then dried under vacuum at 25 °C for 16 h. For details on characterisation of CoO/SiO<sub>2</sub>, please refer to section 4.3.1.

### 2.3.2 Preparation of $\text{Co}_3\text{O}_4$

Using a Metrohm 902 Titrando autotitrator, cobalt nitrate hexahydrate (0.25 M, aqueous) was added to a reaction vessel heated to 80 °C *via* a jacketed water heater. After a 30 min period,  $\text{Na}_2\text{CO}_3$  (2 M, aqueous) was added until pH 8.3 was attained, at which point the autotitrator added nitrate and carbonate at such a rate so that the pH was maintained at 8.3. Once all the nitrate solution was added the mixture was left to age for 30 min at 80 °C. After this the solid precursor was isolated by filtration and washed with warm  $\text{H}_2\text{O}$  (2 L) and dried for 16 h at 110°C. The solid was then calcined at 300 °C (based TGA analysis, see section 4.4.1) for 2 h (2 °C  $\text{min}^{-1}$ ) in static air to form  $\text{Co}_3\text{O}_4$ . For details on characterisation of  $\text{Co}_3\text{O}_4$ , please refer to section 4.4.2.

### 2.3.3 Preparation of Molybdenum Blue

Procedure modified from literature:<sup>3,4</sup>  $\text{H}_2\text{O}_2$  (2.12 g, stabilised, 50 wt%, aqueous, Sigma-Aldrich) was diluted up to 50 ml with  $\text{H}_2\text{O}$  and to this solution molybdenum metal (1.04 g) was added and the mixture was stirred for 16 h. The dark blue mixture was then filtered, and the water was removed from the filtrate under vacuum, leaving the dark blue solid. For details on characterisation of Molybdenum Blue, please refer to section 4.6.1.

## 2.4 Analysis of Reaction Products by Gas-Chromatography

### 2.4.1 Theory

Gas-chromatography (GC) was first developed in the 1950's by James and Martin.<sup>5</sup> The principal theory is the same as any other mode of chromatography whereby a mobile phase, in this case an inert gas, carries a mixture of analytes through a stationary phase, a silica coated column, and the interaction between the analytes and the stationary phase determine the time it takes for each analyte to travel through the column and reach the detector (the retention time). The basic components of a GC instrument are gas inlets, an injector, the column, the oven(s), and the detector (Figure 2.2). GC analysis is suitable for mixtures of relatively volatile organic compounds in organic solvents. In modern instruments an auto-sampler is used in conjunction with a robotic injector so that multiple samples can be queued and analysed automatically. Immediately after injection the sample is vaporised into the gas phase and the carrier gas flows the sample through the column. The column is a capillary tube that is lined with the stationary phase. As the components of the sample interact with the stationary phase to varying degrees, certain components will travel through the column at different speeds. Once

each component leaves the column it will reach the detector, in the case of this work a flame-ionisation detector (FID). At the FID the components of the sample are ionised in a hydrogen-air flame, these ions cause a current that can be detected and visualised by a computer. As each component leaves the column, the detector will pick up each one and a gas-chromatogram is produced.<sup>6</sup>

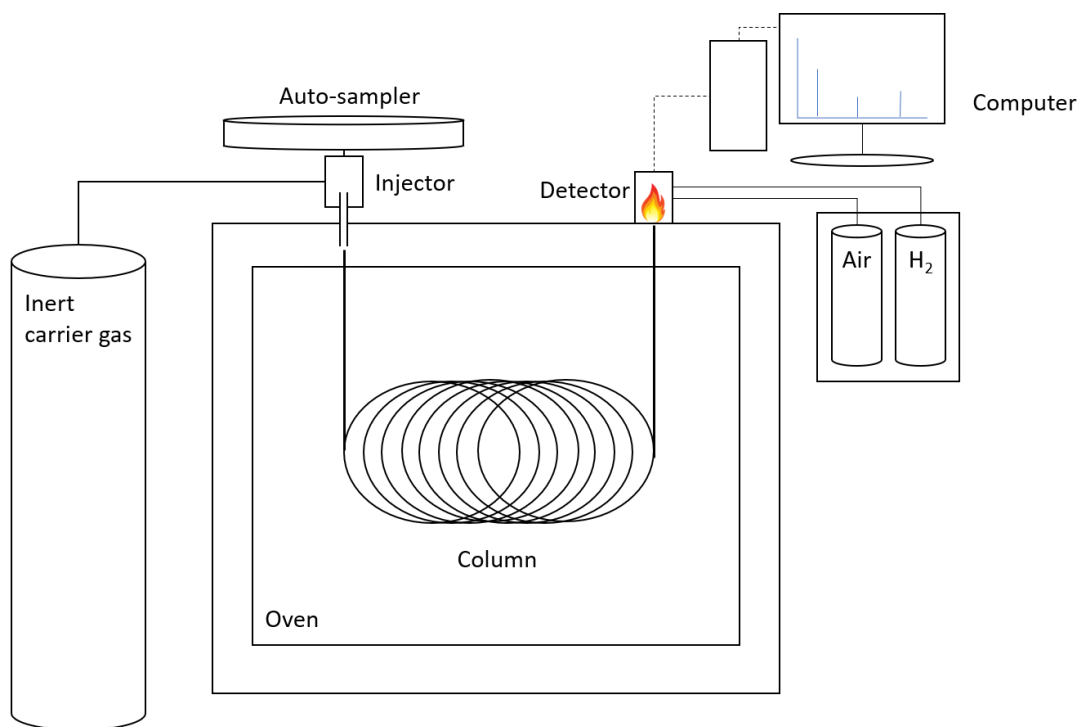


**Figure 2.2.** General scheme for a gas chromatogram with an FID detector.

The auto-sampler will line up the selected sample for injection and a robotic needle will draw around 1  $\mu\text{L}$  of sample and inject. There are various types of injectors but the most commonly used is the split/splitless injector. A 'split' refers to the venting of some of the sample after dilution with the mobile phase, which prevents a significant portion of the sample entering the column. This is useful for solventless or more concentrated solvated samples where a lower concentration being injected will result in sharper, more separated peaks. A splitless injection is more appropriate where trace samples are being analysed. In either case a needle will pierce a septum to deliver the sample to the glass liner. The septum is a silicone disc that allows the introduction of the sample whilst maintaining a leak free seal; this is so that the elevated pressure in the injector is maintained even after many injections. Once the sample is in the glass liner the elevated temperature will result in vaporisation; it is here that the sample is mixed with

the carrier gas, and some will be vented off through the split vent. The rest of the sample will pass through the glass liner and onto the column (Figure 2.3).<sup>7</sup>

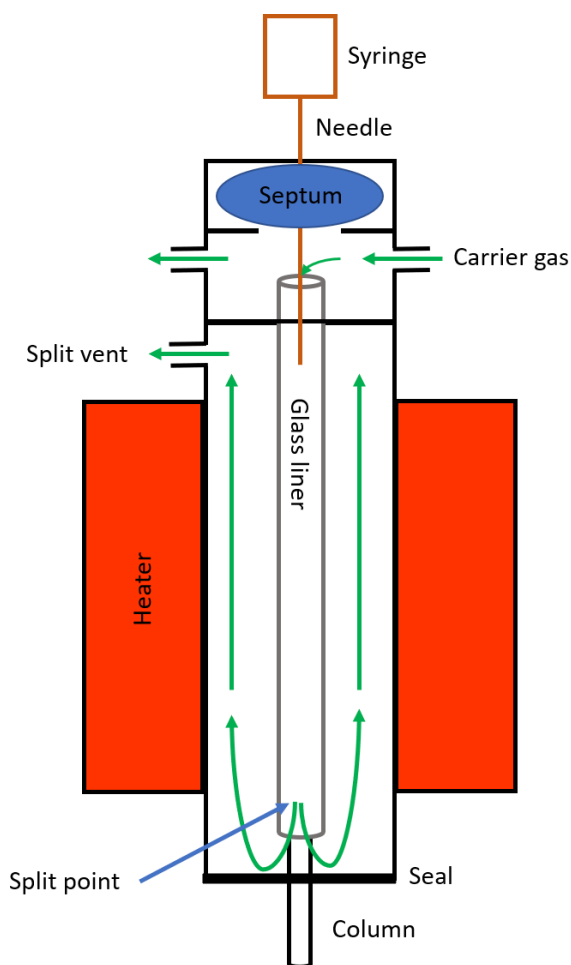


**Figure 2.3.** Schematic of a split injector.

Modern GC instruments typically use capillary columns with diameters of between 0.18 – 0.53 mm and a length of 10 – 100 m. The stationary phase is coated on the inside of the column and is usually a silica, silica derivative, or in the case of this work polyethylene glycol. The type of column that is employed will be determined on the properties of compounds that need to be separated. For instance some stationary phases, such as polyethylene glycol, are particularly effective at separating compounds that vary in polarity, while others will be more effective at separating products that vary in boiling temperatures.<sup>8</sup>

On exiting the column, compounds enter the detector of which there are various types including: electron capture detector (ECD), flame ionisation detector (FID), thermal conductivity detector (TCD) or a mass spectrometer. For the purposes of this work an FID (Figure 2.4) was used due to its high sensitivity and ability to detect carbon containing compounds. Hydrogen gas is used as the fuel for the flame which burns with the addition of compressed air and results

in a very low background noise. When an analyte leaves the column and reaches the flame, it is ionised and causes a change in the current in the detector, which results in a quantifiable peak in the chromatogram. The disadvantages of FIDs are that they cannot detect water, CO<sub>2</sub> and other inorganic molecules that do not contain carbon atoms.<sup>9</sup>

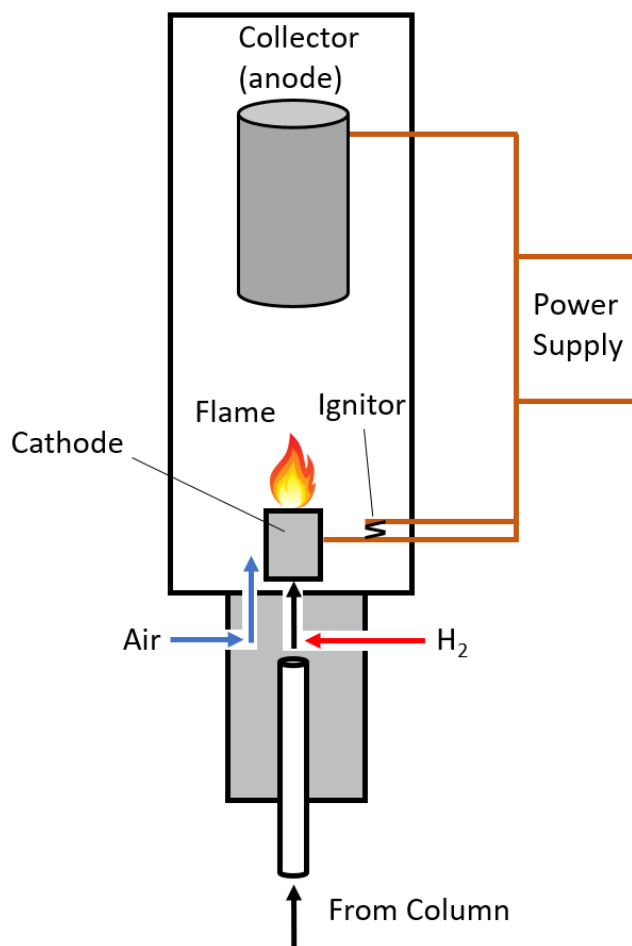


Figure 2.4. Flame ionisation detector (FID).

## 2.4.2 Experimental

A few drops of sample were added to two GC vials, one containing an excess of TPP, which were then filled with acetone to just above the halfway mark and shaken to ensure full dissolution of the sample and effective reaction between the TPP and any THPMI-HP present. Samples were then analysed using an Agilent 7820A gas chromatograph with a CP-Wax 52 CB capillary column and an FID detector. A 1  $\mu\text{L}$  syringe was used to inject 0.2  $\mu\text{L}$  of sample at an injector temperature of 250  $^{\circ}\text{C}$  and a split ratio of 50:1. The initial oven temperature was set at 70  $^{\circ}\text{C}$ , which was increased to 150  $^{\circ}\text{C}$  at a rate of 20  $^{\circ}\text{C min}^{-1}$  and then held for 3 minutes. The temperature was then increased to 230  $^{\circ}\text{C}$  at 10  $^{\circ}\text{C min}^{-1}$ , at which point the rate of heating was increased to 20  $^{\circ}\text{C min}^{-1}$  until 250  $^{\circ}\text{C}$ . This was held for 30 minutes if no TPP was present in the sample and for 54 minutes if TPP was present.

Using hexadecane as an internal standard, calibrations were performed on pure samples of THPMI and Cashmeran to calculate their response factors. Mixtures of THPMI and Cashmeran in varying known masses and hexadecane in a consistent, known mass were made and analysed by GC. Using the data from these GC traces and the known moles of THPMI, Cashmeran and hexadecane added, the response factors were calculated from the gradients of the plots shown below (Figure 2.5). The response factors and retention times for GC analysis have been collated (Table 2.1). For products which could not be obtained in pure samples, an averaged response factor from THPMI and Cashmeran was used. It is assumed that the response factor for Cashmeran and Cashmeran-alcohol is the same.

**Table 2.1.** Retention times and response factors for GC analysis of the reaction products.

<b>Product</b>	<b>Retention Time (s)</b>	<b>Response Factor</b>
THPMI	9.4	0.79
	9.9	
Cashmeran-alcohol	17.1	0.77
Cashmeran	17.6	0.77
Ethyl-Cashmeran	16.5	0.77
Hydroxy-Cashmeran-alcohol	28.5	0.78 <sup>a</sup>
Hydroxy-Cashmeran	29.6	0.78 <sup>a</sup>
Cashmeran-ketone	32.5	0.78 <sup>a</sup>

<sup>a</sup>refers to an averaged response factor.

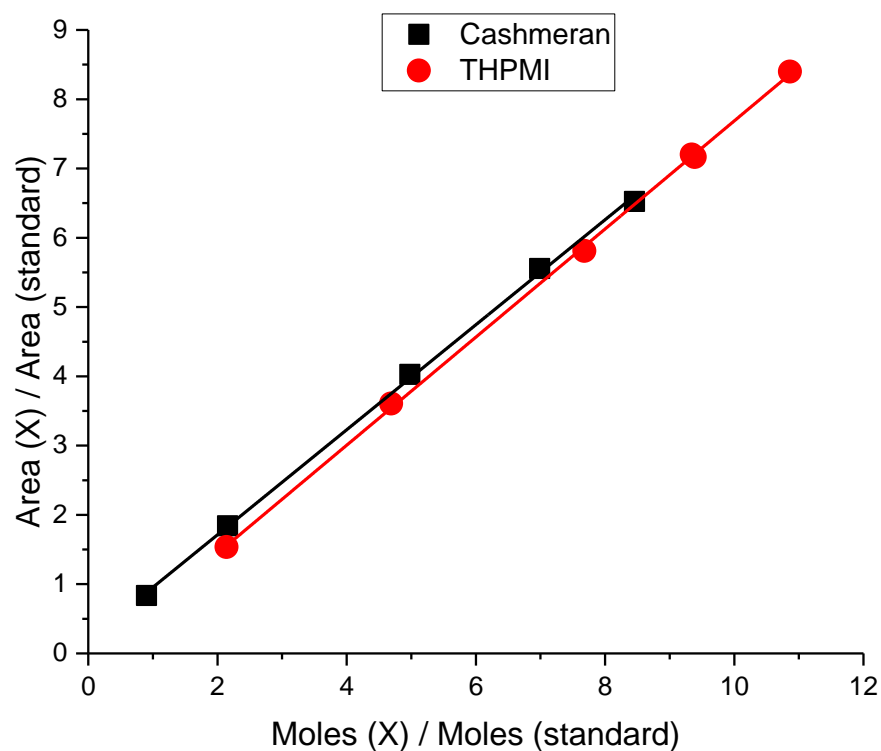


**Figure 2.5.** Calculation of response factors for THPMI and Cashmeran based on calibrations. X = Cashmeran or THPMI.

#### 2.4.2.1 Calculation of Conversion

The response factors calculated above were used to calculate conversion at time 't' of THPMI by calculating the concentration of THPMI that has reacted by time 't' as a percentage of the total amount of THPMI at the start of the reaction or 't0' (13).

$$Conversion (\%) = \frac{[THPMI]_{t0} - [THPMI]_t}{[THPMI]_{t0}} \times 100 \quad (13)$$

#### 2.4.2.2 Calculation of Selectivity

Selectivity to each product is calculated by dividing the concentration of that product by the THPMI that has been converted since the start of the reaction (14).

$$Selectivity (\%) = \frac{[Product]}{[THPMI]_{t0} - [THPMI]_t} \times 100 \quad (14)$$

The mass balance of the oxidation of THPMI was calculated by dividing the sum of all observed products and THPMI at time 't' by the concentration of THPMI at the start of reaction or 't0' (15).

$$\text{Mass Balance (\%)} = \frac{\sum[\text{THPMI, Products}]_t}{[\text{THPMI}]_{t0}} \times 100 \quad (15)$$

#### 2.4.2.3 Error Bars

Error bars shown in figures in chapters 3 and 4 are calculated based on repeats of reactions sampled at the same times. For data points with one repeat (2 values) the error is calculated by subtracting the mean of the data points by the lower data point. For data points with 2 or more repeats (3 or more values), the error was calculated as being 1 standard deviation. For data points where no error bar is shown, no repeats were conducted for that sampling time. For most reactions repeats were conducted, although the sampling times varied for each reaction. For information on the number of repeats conducted, refer to each figure caption.

## 2.5 Gas Chromatography Mass Spectrometry (GC-MS)

### 2.5.1 Theory

GC-MS instruments are commonly described as either being a GC with an MS detector or an MS with a GC inlet. These descriptions are not entirely accurate due to the considerable drop in pressure required when moving from a GC to an MS instrument.<sup>10</sup> The principle of GC-MS is simple, the GC separates a mixture of analytes as described in section 2.4, and each analyte is characterised by MS. This system is a powerful tool in analytical chemistry as it allows complex mixtures of volatile organic compounds to be characterised rapidly. When the analytes leave the GC column they enter the GC-MS interface which is a heated area where the pressure needs to be reduced from 200 – 700 kPa in the GC column to around 1 Pa in the MS. This reduction in pressure is achieved by limiting the amount of analyte that enters the MS, along with a vacuum pump.<sup>11</sup> After the analytes enter the MS, they are ionised by one of several possible methods, however electron ionisation (EI) was used in this work. EI results in positively charged molecular ions ( $M^{*+}$ ) after bombardment of the analyte with electrons. These ions can further fragment to produce a 'fragmentation pattern'. The fragments and the original ions are separated in the instrument by their mass to charge ratio ( $m/z$ ). As nearly all the ions have a single charge the  $m/z$  values will refer to the mass of the fragments. There are several types of  $m/z$  analyser,

however this work used a quadrupole mass filter which uses direct and alternating currents to separate fragments based on their  $m/z$ . Once the  $m/z$  analyser has separated each ion, they will hit an ion detector which produces a cascade of electrons or photons to produce a signal which is proportional to the concentrations of ions which are being detected.<sup>12</sup>

## 2.5.2 Experimental

Samples for GC-MS were manually injected (1  $\mu\text{L}$  in a 10  $\mu\text{L}$  syringe) into a Shimadzu GCMS-QP2010 SE gas chromatograph mass spectrometer. The temperature of the injector was 230  $^{\circ}\text{C}$  and a 50:1 split ratio was applied. The initial oven temperature was 70  $^{\circ}\text{C}$ , which was increased to 150  $^{\circ}\text{C}$  at a rate of 10  $^{\circ}\text{C min}^{-1}$  and then held at 150  $^{\circ}\text{C}$  for 5 minutes. The temperature was raised to 230  $^{\circ}\text{C}$  at a rate of 10  $^{\circ}\text{C min}^{-1}$  and held at 230  $^{\circ}\text{C}$  for 15 minutes, by which point all reaction products had left the column. The interface temperature between the GC and MS was 250  $^{\circ}\text{C}$  and the ion source temperature was 200  $^{\circ}\text{C}$ . Scans were taken every 0.2 seconds between a range of 20 – 300  $m/z$  (a range of 20 – 1000  $m/z$  was initially used to confirm that heavy products were not present in samples).

## 2.6 Thermogravimetric Analysis (TGA)

### 2.6.1 Theory

TGA is a technique used to observe changes in mass of a sample that is heated under controlled conditions. A sample is placed on a highly sensitive balance in an oven and the mass is monitored as the temperature is increased. The technique is used to determine various chemical and physical changes that can occur including decomposition, oxidation or loss or solvent.<sup>13</sup> In terms of the work presented here, TGA was used to determine the temperature at which cobalt carbonate will decompose, aerobically, into cobalt oxide.<sup>14,15</sup> This temperature was then applied to the calcination conditions used for the cobalt carbonate generated from precipitation (2.3.2).

### 2.6.2 Experimental

TGA was carried out using a PerkinElmer Thermogravimetric Analyser TGA 4000. Approximately 10 mg of sample was placed in a ceramic crucible, which was positioned on the balance. A flow of compressed air was applied at 50  $\text{ml min}^{-1}$  to the system, and a temperature

of 30 °C was held for 2 minutes. The oven was then heated from 30 – 600 °C at a rate of 5 °C min<sup>-1</sup> as the mass was monitored.

## 2.7 Microwave Plasma Atomic Emission Spectroscopy (MP-AES)

### 2.7.1 Theory

MP-AES is a technique used to quantify elements in a sample. As with other forms of atomic emission spectroscopy the electrons in a sample are energised and are excited into a higher energy level. As the electrons return to their ground states energy is released (Figure 2.6), and the specific amount of energy released is unique for each element of the periodic table. In the case of MP-AES all samples must be in liquid or gaseous form; if a solid is being analysed then it must be digested and dissolved prior to analysis. A magnetically excited microwave nitrogen plasma is used as the source of energy and will atomise and excite the sample. As the electrons return to the ground state, the energy released will pass through a monochromator and to a detection system, in this case a charge-coupled device. This allows each wavelength emitted to be detected individually and so a quantification of each element is possible with high sensitivity.<sup>16</sup>

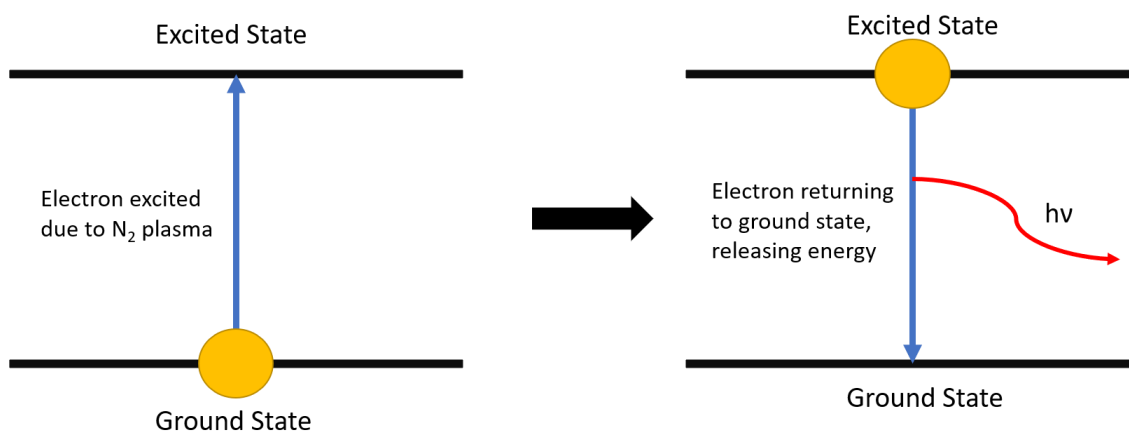


**Figure 2.6.** Atomic emission occurring during MP-AES.

### 2.7.2 Experimental

All MP-AES was conducted by Dr Samuel Patisson on an Agilent 4100 MP-AES. Solid samples were digested in *aqua regia* (3:1 mixture of hydrochloric acid to nitric acid) and diluted further

in distilled water before being analysed. Quantification of elements present was achieved by calibration against bought analytical standards.

## 2.8 X-ray Photoelectron Spectroscopy (XPS)

### 2.8.1 Theory

XPS is a surface sensitive technique which can reveal the elemental composition and the oxidation states on a catalyst surface. XPS works *via* the photoelectric effect whereby an electron with energy,  $h\nu$ , will hit an atom causing a core or valence electron of energy,  $E_b$ , to be ejected with kinetic energy,  $E_k$ . This is shown in equation (16) where 'h' is Planck's constant and 'v' is the frequency of radiation.

$$E_k = h\nu - E_b \quad (16)$$

When a photoelectron is emitted from a core energy level, a vacancy is created that can be filled by a valence electron. This results in the release of energy as x-rays which can either be emitted or can strike another electron which will be ejected; this is known as an Auger electron and can also provide information on the oxidation state of elements in the sample (Figure 2.7).<sup>17</sup>

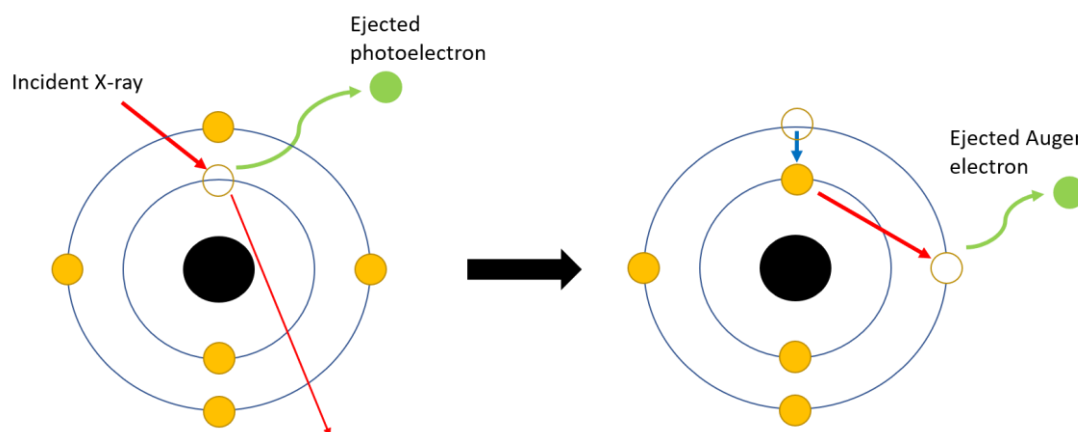


**Figure 2.7.** Photoelectron emission and subsequent Auger emission from XPS.

### 2.8.2 Experimental

All XPS analysis was carried out by Dr David Morgan on a Thermo Fisher Scientific K-alpha<sup>+</sup> spectrometer. Samples were analysed using a micro-focused monochromatic Al X-ray source (72 W) using the "400-micron spot" mode, which provides an analysis defining elliptical X-ray

spot of 400 x 600 microns. Data were recorded at pass energies of 150 eV for survey scans and 40 eV for high resolution scan, with 1 eV and 0.1 eV step sizes, respectively. Charge neutralisation of the sample was achieved using a combination of both low energy electrons and argon ions. Data analyses were performed in CasaXPS using a Shirley-type background and Scofield cross sections, with an energy dependence of -0.6.

## 2.9 Powder X-ray Diffraction (XRD)

### 2.9.1 Theory

XRD is a technique used to determine bulk, crystalline phases in solid materials. X-Rays, due to their wavelength, are capable of penetrating solid materials and consequently can reveal information about chemical order. When X-rays interact with atoms of a material they are scattered and, if the atoms are in a periodic lattice, the scattered X-rays will constructively interfere with one another and produce a strong signal (Figure 2.8). If the atoms are arranged amorphy then destructive interference will occur and no signal or only a weak signal will be observed. The lattice spacings ( $d$ ) can be derived from the Bragg relationship (17), which must be obeyed if constructive interference of the scattered X-rays occurs.

$$n\lambda = 2d \sin\theta \quad (17)$$

Where:

$\lambda$  = wavelength of X-rays

$n$  = an integer number

$d$  = the interplanar distance

$\Theta$  = the angle of incident X-rays to the reflecting lattice plane

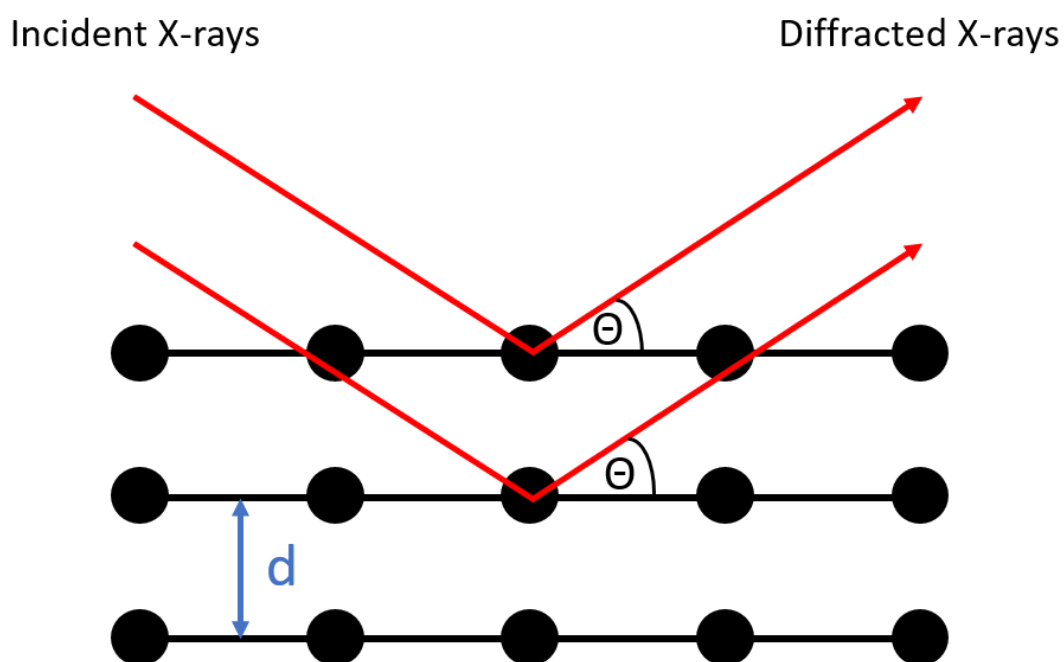


**Figure 2.8.** Diffraction of X-rays by crystalline materials.

The Bragg relationship was first discovered in 1913<sup>18</sup> and is the cornerstone of XRD analysis as it demonstrates that, if a sample is analysed at a variety of angles,  $d$  spacings and other information about the analyte can be obtained.<sup>19</sup> A typical powder XRD device works by a stationary X-ray source delivering radiation to a rotating, but otherwise stationary sample. The detectors will move to alter angle to obtain a greater range of  $\Theta$  values (Figure 2.9).

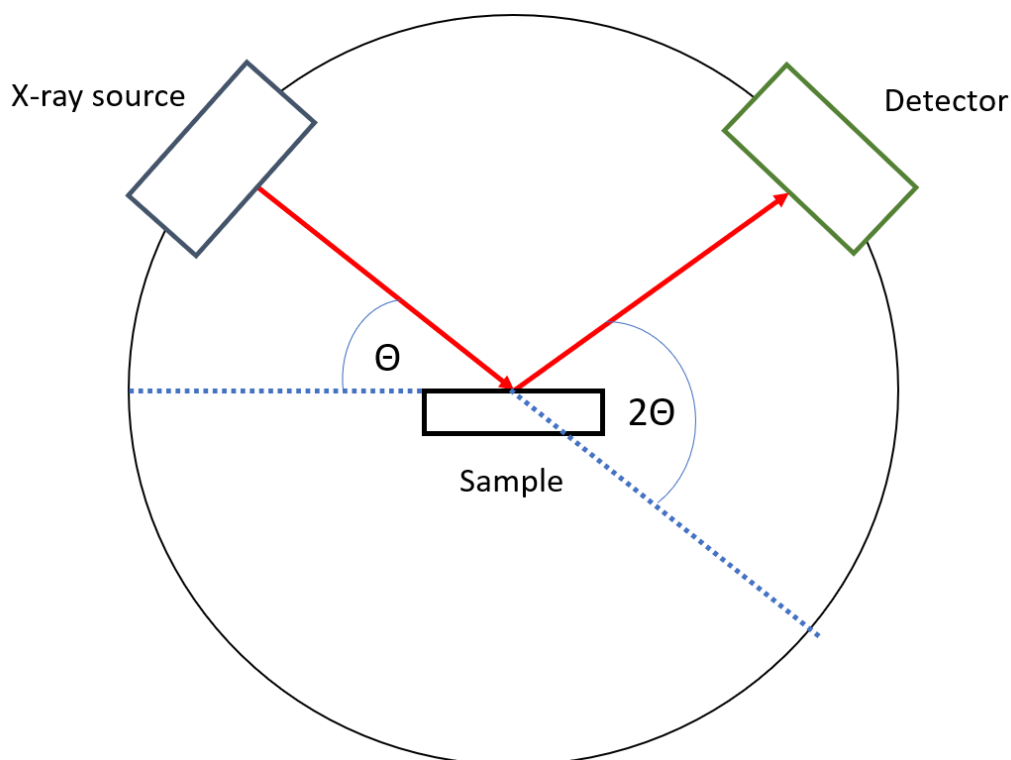


**Figure 2.9.** Schematic of an X-ray diffractometer.

## 2.9.2 Experimental

Powder X-ray diffraction was performed using a Panalytical X'Pert diffractometer equipped with a Cu X-ray source operating at 40 kV and 40 mA. Samples were ground to a fine powder and placed on metal holders and a 5 – 80°  $2\Theta$  angle range was scanned. Patterns were analysed by matching the phases observed with entries from the International Centre for Diffraction Data (ICDD) database.

## 2.10 Scanning Electron Microscopy (SEM)/Energy Dispersive X-ray Spectroscopy (EDX)

### 2.10.1 SEM Theory

SEM is a technique capable of revealing information regarding morphology, composition, crystallography, and other properties of a solid catalyst. A finely focused beam of electrons of energy 0.1 – 30 keV will pass through a series of magnetic lenses and electromagnetic coils to further focus the beam. The beam will impact a series of close yet discrete locations on the surface of the analyte. When the beam interacts with the surface of the analyte some of the

electrons will be scattered by the electric field of the surface atoms with enough of their incident energy to escape and be detected, these are known as back scattered electrons (BSE). Electrons on the analyte surface can also be ejected by the electron beam, which can also be detected and are known as secondary electrons (SE). The BSE and SE are detected and produce a signal which is digitised and converted into a pixel by a computer. The pixels from each individual area are combined to a complete image of the area that is being scanned by the SEM. Heavier elements will scatter electrons more effectively and so will produce brighter pixels in the end image. The system must operate under high vacuum conditions in the region of  $10^{-4}$  Pa as if the electron beam encounters any gaseous atoms, it will cause undesired scattering. Samples that could develop an electrical charge due to the electron beam need to be coated with a conductive material, often Au-Pd, to ensure grounding and an escape for electrical discharge.<sup>20</sup>

## 2.10.2 EDX Theory

Along with the BSE and SE that are emitted during SEM discussed earlier (2.10.1), X-rays are also emitted. The electron beam used in SEM is capable of removing core shell electrons from the sample as well as the valence electrons that are typically detected (Figure 2.10). When the core shell electrons are removed, a valence shell electron will drop down an energy level and energy will be released in the form of X-rays; this is very similar to the Auger emission observed in XPS (2.9.1). The X-rays that are emitted will be characteristic to the atoms which are emitting them, this way the elements present in the SEM image can be mapped and quantified.<sup>21</sup>

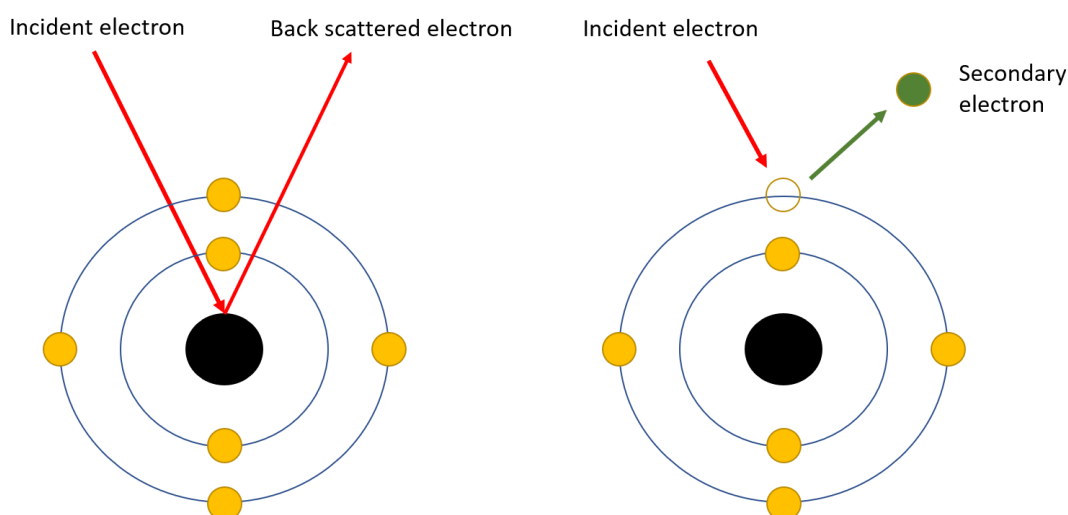


**Figure 2.10.** The formation of back scattered electrons (left) and secondary electrons (right) in SEM.

### 2.10.3 SEM/EDX Experimental

All SEM/EDX was conducted by Dr Thomas Morgan. Samples were coated with 15 nm Au-Pd prior to analysis. Samples were mounted on adhesive carbon Lite discs and analysed on a TESCAN MAIA3 FEG-SEM at 15 kV. EDX was performed using Oxford Instruments SD detector X-Max<sup>N</sup> 80 and interpreted using the Aztec software.

## 2.11 Infra-red Spectroscopy (IR)

### 2.11.1 Theory

IR spectroscopy is a technique that can be used to determine certain chemical bonds that are present in a molecule or in a solid lattice. If a photon interacts with a chemical bond, it will be absorbed providing it has an appropriate wavelength, which causes the bond to vibrate. The specific wavelength required for vibration will depend on the type of bond between specific elements, however they all fall in the mid infra-red range of  $200 - 4000 \text{ cm}^{-1}$ . A vibration will only occur if a dipole moment changes during the rotation; this means that molecules such as  $\text{H}_2$  and  $\text{N}_2$  will not be IR active, O-H, C=O or N=O bonds are particularly active and C-C or N=N bonds in molecules will be active but much weaker. There are a few variations of IR spectroscopy, however the most common is transmission IR spectroscopy where IR light passes through a sample and is measured on the other side as a transmission percentage (Figure 2.11).

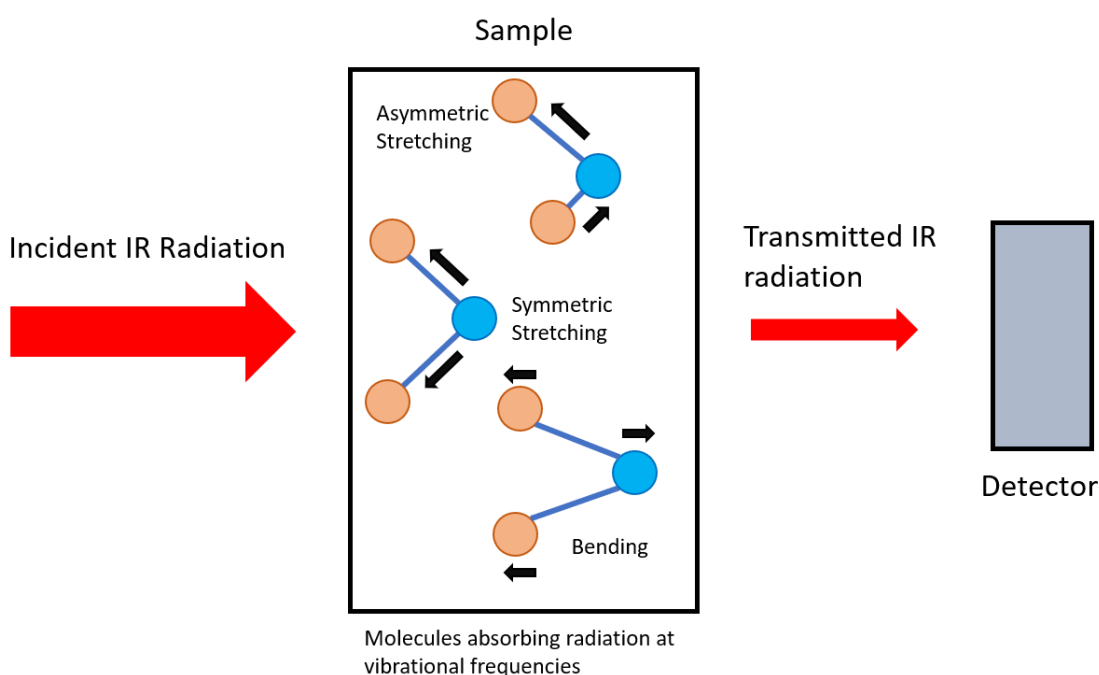


**Figure 2.11.** Basic schematic of transmission infra-red spectroscopy with some examples of simple molecular vibrations.

If a particular functional group is present, for instance a C-O bond, light of  $2143\text{ cm}^{-1}$  will be absorbed due to stretching and so less of this light will be transmitted to the detector and a lower transmission % will be observed.<sup>22</sup>

## 2.11.2 Experimental

All IR spectroscopy was conducted on an Agilent Technologies Cary 630 FTIR device. Scans between  $650 - 4000\text{ cm}^{-1}$  were conducted.

## 2.12 Brunauer-Emmett-Teller Surface Area Analysis (BET)

### 2.12.1 Theory

The theory of BET first arose in 1938,<sup>23</sup> building from the concepts of gas adsorption introduced by Langmuir in 1918.<sup>24</sup> The technique involves the adsorption of gas onto the surface of a material, whilst measuring the pressure, which can provide information on the sample surface area and porosity. The relationship between the relative vapour pressure,  $p/p_0$ , where  $p_0$  is saturation pressure, is known as the adsorption isotherm<sup>25</sup> of which there are 6 types, designated by the IUPAC (Figure 2.12).<sup>26</sup> Langmuir's early work assumed only monolayer coverage and is represented by isotherm 'I'. The BET model expanded on this and accounts for mono and multi-layer coverage of adsorbents, represented by isotherms 'II' or 'IV'. The BET equation can be expressed by equation (18):

$$\frac{p}{n_{ads}(p_0 - p)} = \frac{1}{cn_m} + \frac{(c - 1)}{cn_m} x \frac{p}{p_0} \quad (18)$$

Where:

$p$  and  $p_0$  = pressure and saturation pressure respectively

$n_{ads}$  = volume of gas adsorbed on the surface

$n_m$  = volume of a monolayer of gas

$c$  = BET constant, described by (19)

$$c = \exp\left(\frac{E_1 - E_L}{RT}\right) \quad (19)$$

Where:

$E_1$  = heat of adsorption for monolayer formation

$E_2$  = heat of adsorption for multilayer formation

R = gas constant

T = temperature

If ' $\frac{p}{n_{ads}(p_0-p)}$ ' is plotted on the y axis and ' $\frac{p}{p_0}$ ' is plotted on the x axis, then the gradient of the straight-line graph is ' $\frac{(c-1)}{cn_m}$ ' and the intercept is ' $\frac{1}{cn_m}$ '. Using these values ' $n_m$ ' can be calculated and through equation (20) there surface area of the material can be obtained.

$$S_{BET} = \frac{n_m}{M} N_A \sigma \quad (20)$$

Where:

$S_{BET}$  = Surface area

M = molecular weight of adsorbate

$N_a$  = Avogadro's number

$\sigma$  = surface area covered by one molecule

$n_m$  = volume of a monolayer of gas

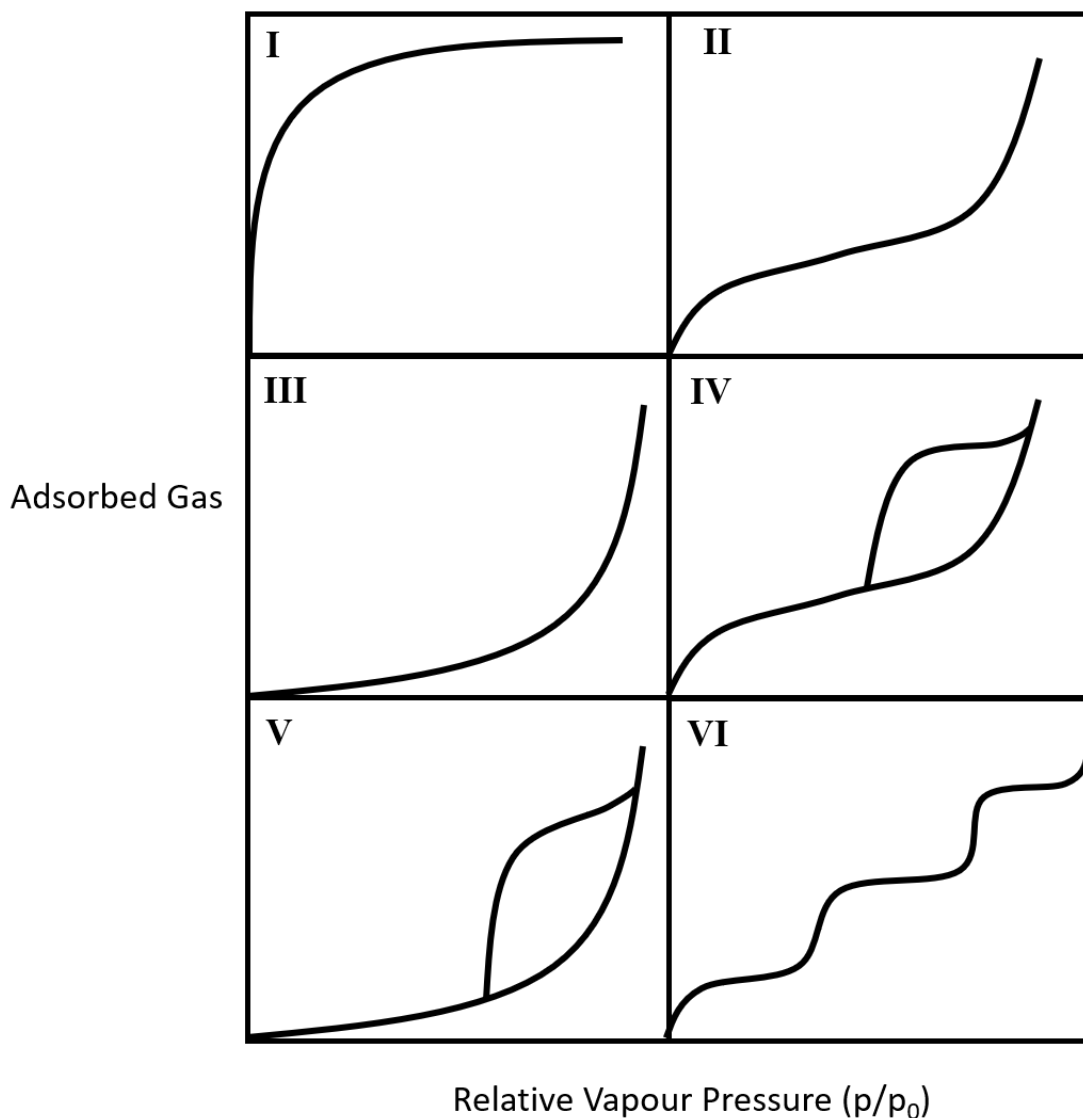


**Figure 2.12.** The six isotherms for adsorption, 'I' being the Langmuir isotherm and 'II' being the BET isotherm.

### 2.12.2 Experimental

BET analyses were performed using a Quantachrome NOVA 2200e Surface Area & Pore Size Analyser. A sample for analysis, usually between 0.5 – 1 g, was weighed accurately and added to a 9 mm quartz tube with a bulb. Samples were then pre-treated under a vacuum at 150 °C for 3 hours to remove surface species. After pre-treatment the samples were submerged in liquid nitrogen to reduce their temperature and the analysis began. Nitrogen gas was flowed through the sample and nitrogen adsorption was recorded between a relative pressure ( $P/P_0$ ) range of 0.05 – 0.3. The surface area was determined by the BET method, as described above (2.12.1).

## 2.13 References

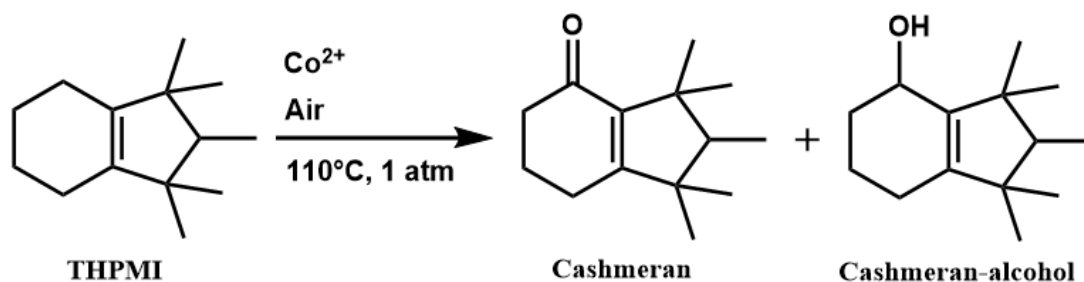
- 1 M. J. Jacinto, P. K. Kiyohara, S. H. Masunaga, R. F. Jardim and L. M. Rossi, *Appl. Catal. A Gen.*, 2008, **338**, 52–57.
- 2 F. P. Silva, M. J. Jacinto, R. Landers and L. M. Rossi, *Catal. Letters*, 2011, **141**, 432–437.
- 3 M. Conte, X. Liu, D. M. Murphy, S. H. Taylor, K. Whiston and G. J. Hutchings, *Catal. Letters*, 2016, **146**, 126–135.
- 4 X. Liu, M. Conte, W. Weng, Q. He, R. L. Jenkins, M. Watanabe, D. J. Morgan, D. W. Knight, D. M. Murphy, K. Whiston, C. J. Kiely and G. J. Hutchings, *Catal. Sci. Technol.*, 2015, **5**, 217–227.
- 5 A. T. James and A. J. P. Martin, *Biomed. J.*, 1951, **50**, 679–690.
- 6 D. Sparkman, Z. E. Penton and F. G. Kiston, in *Gas Chromatography and Mass Spectrometry*, Elsevier, 2nd edn., 2011, pp. 15–16.
- 7 D. Sparkman, Z. E. Penton and F. G. Kiston, in *Gas Chromatography and Mass Spectrometry*, 2nd edn., 2011, pp. 16–22.
- 8 D. Sparkman, Z. E. Penton and F. G. Kiston, in *Gas Chromatography and Mass Spectrometry*, Elsevier, 2nd edn., 2011, pp. 49–57.
- 9 D. Sparkman, Z. E. Penton and F. G. Kiston, in *Gas Chromatography and Mass Spectrometry*, 2nd edn., 2011, pp. 66–68.
- 10 D. Sparkman, Z. E. Penton and F. G. Kiston, in *Gas Chromatography and Mass Spectrometry*, Elsevier, 2nd edn., 2011, pp. 3–13.
- 11 D. Sparkman, Z. E. Penton and F. G. Kiston, in *Gas Chromatography and Mass Spectrometry*, Elsevier, 2nd edn., 2011, pp. 85–88.
- 12 D. Sparkman, Z. E. Penton and F. G. Kiston, in *Gas Chromatography and Mass Spectrometry*, Elsevier, 2nd edn., 2011, pp. 89–92.
- 13 A. W. Coats and J. P. Redfern, *Analyst*, **88**, 906–924.
- 14 P. Porta, R. Dragone, G. Fierro, M. Inversi, M. Lo Jacono and G. Moretti, *J. Chem. Soc. Faraday Trans.*, 1992, **88**, 311–319.
- 15 R. K. Pinnell, PhD Thesis, Cardiff University, 2014.
- 16 V. Balaram, *Microchem. J.*, 2020, **159**, 105483.

- 17 J. W. Niemantsverdriet, in *Spectroscopy in Catalysis: An Introduction*, Weinheim, 3rd edn., 2007, pp. 41–44.
- 18 W. H. Bragg and W. L. Bragg, *Proc. R. Soc. A*, 1913, **88**, 428–438.
- 19 J. W. Niemantsverdriet, in *Spectroscopy in Catalysis: An Introduction*, Weinheim, 3rd edn., 2007, pp. 148–152.
- 20 J. I. Goldstein, D. E. Newbury, J. R. Michael, N. W. M. Ritchie, J. H. J. Scott and D. C. Joy, in *Microscopy and X-Ray Microanalysis*, Springer, 4th edn., 2018, p. VII.
- 21 J. I. Goldstein, D. E. Newbury, J. R. Michael, N. W. M. Ritchie, J. H. J. Scott and D. C. Joy, in *Microscopy and X-Ray Microanalysis*, Springer, 4th edn., 2018, p. X.
- 22 J. W. Niemantsverdriet, in *Spectroscopy in Catalysis: An Introduction*, Weinheim, 3rd edn., 2007, pp. 218–224.
- 23 S. Brunauer, P. H. Emmett and E. Teller, *J. Am. Chem. Soc.*, 1938, **60**, 309–319.
- 24 I. Langmuir, *J. Am. Chem. Soc.*, 1918, **40**, 1361–1403.
- 25 C. Weidenthaler, *Nanoscale*, 2011, **3**, 792–810.
- 26 K. S. W. Sing, D. H. Everett, R. A. W. Haul, L. Moscou, R. A. Pierotti, J. Rouquerol and T. Siemieniewska, *Pure Appl. Chem.*, 1985, **57**, 603–619.

# 3 The Effect of Co-bis(2-ethylhexanoate) on the Aerobic Oxidation of THPMI

## 3.1 Introduction

The aim of this chapter is to investigate the effect of the metal salt Co-bis(2-ethylhexanoate), herein referred to as Co-bis(2-EH) for brevity, on the industrial oxidation reaction of 4,5,6,7-tetrahydro-1,1,2,3,3-pentamethylindane (THPMI) into 1,2,3,5,6,7-hexahydro-1,1,2,3,3-pentamethyl-4H-inden-4-one (Cashmeran) and 1,2,3,5,6,7-hexahydro-1,1,2,3,3-pentamethyl-4H-inden-4-ol (Cashmeran-alcohol) (Scheme 3.1).<sup>1</sup> The enhanced understanding of this reaction and, in particular, of the catalyst is vital to improving selectivity and yield for the large scale industrial process. Analysing the positive and negative impacts of the catalyst will provide insights into either possible improvement of the current process or highlight the need for replacement of the catalyst with a superior alternative.



**Scheme 3.1.** Oxidation of THPMI into Cashmeran and Cashmeran-alcohol.

This work focuses on the beneficial effects of Co-bis(2-EH) (Figure 3.1) on the oxidation of THPMI into Cashmeran. Scheme 3.2 shows the expected reaction route which, as with the aerobic oxidations of cyclohexane<sup>2-8</sup> and cyclohexene,<sup>9-14</sup> proceeds through the principal oxidation product of THPMI-hydroperoxide, herein referred to as THPMI-HP. The sequential breakdown of THPMI-HP will primarily yield Cashmeran-alcohol and/or Cashmeran depending on the mechanism in play. Routes **2**,<sup>2,3,15</sup> **3**,<sup>16-19</sup> **4**<sup>20,21</sup> or **5**<sup>7,22,23</sup> (Scheme 3.2) need to be enhanced to maximise selectivity to the desired, allylic, oxidation products, with examples of these routes being discussed in more detail in section (1.8). Along with promoting desired routes, idealised

reaction conditions will suppress the (undesired) oxidation of Cashmeran-alcohol and any oxidation of Cashmeran to produce 'over-oxidised' products.

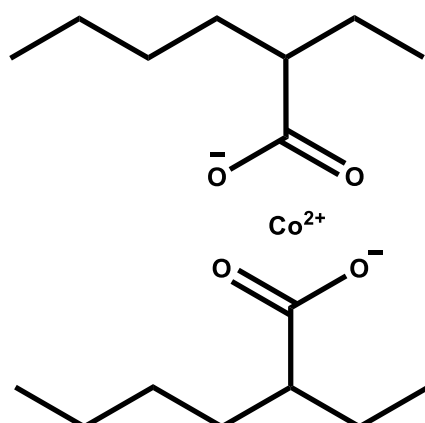
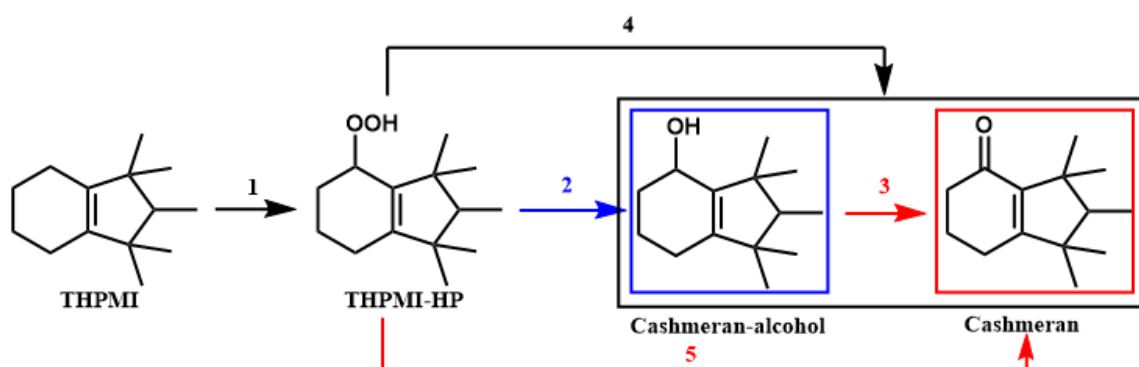


Figure 3.1. Structure of Co-bis(2-ethylhexanoate).

In the industrial oxidation of THPMI, oxidation will cease when approximately 65 % conversion is reached. This is not a major concern for IFF as reaction is stopped at 50 % because higher conversions result in lower selectivities. This means it is more economical to stop the reaction at 50 % conversion and recycle the unreacted THPMI. This type of reaction quenching has been reported in the literature,<sup>24–28</sup> which is discussed in section (1.6). However, understanding this quenching phenomenon and how it is caused may provide vital knowledge leading to the improvement of the overall system.



Scheme 3.2. Reaction route for the oxidation of THPMI into the desired allylic oxidation products.

## 3.2 Development of Reaction Conditions

Initial experiments without the deliberate introduction of air resulted in little to no oxidation. Even in an environment of 3 bar of pure O<sub>2</sub> and rapid stirring, very little conversion was observed. THPMI has a low oxygen solubility, as expected for hydrocarbons with this many carbons,<sup>29,30</sup> and so it was decided that an air delivery tube must be placed into the THPMI as close to the bottom of the flask as possible without disturbing the magnetic stirrer. Approximately 2.3 mmol of O<sub>2</sub> is delivered to the reaction mixture every minute at the most rapid air delivery rate (100 mL min<sup>-1</sup>), compared to the 29 mmol of THPMI in a reaction. This makes the level of dissolved O<sub>2</sub> always sub-stoichiometric compared to THPMI, even before considering that O<sub>2</sub> will rapidly leave the reactor and the limited interaction between the liquid and gas phase depending on the size of the air bubbles. Therefore, both the rate of air delivered into the reactor and the stirrer speed will have significant kinetic effects.<sup>31</sup> The conditions chosen were based on a series of experiments conducted at 50 °C, with Co-bis(2-EH) as the catalyst. A temperature of 50 °C was chosen as it is below any significant levels of autoxidation, which is

$$\text{Air residence time (min)} = \frac{\text{Volume of liquid in reactor (mL)}}{\text{Airflow (mL min}^{-1}\text{)}} \quad (21)$$

only of significance at temperatures of 70 °C and above (3.5.1). It should also be noted that the boiling temperature of THPMI is close to 250 °C and so loss of product through evaporation is not considered important in this study. The rate of stirring was varied, along with the air flow, and the level of conversion was measured after 5 hours (Figure 3.2). The rate of airflow is described by the air residence time given by equation (21); the air residence time and airflow are inversely related to one another, and so increasing the flow of air results in a lower air residence time. Decreasing the air residence time from 0.92 to 0.11 minutes at a constant stir rate of 300 rpm increased conversion from 31 % to 42 %. Likewise, at a constant stir speed of 900 rpm, decreasing the air residence time from 0.92 to 0.33 minutes increased the conversion from 40 to 45 %; however, when the air residence time was decreased further from 0.33 to 0.15 or 0.11 minutes, no further increase in conversion was observed. When the air residence time was kept constant at 0.11 minutes and stir speed was increased from 300 to 900 rpm, no change in the rate of reaction was observed as it was already at maximum. When a greater air residence time of 0.92 minutes was kept constant and the stir speed was increased from 300 to 900 rpm, an increase in conversion from 31 to 40 % was observed. It should also be noted that the maximum conversion observed of 45 % was not simply the end point of the reaction as if the reaction is run for a further hour a conversion of 51 % was observed. This demonstrated that a conversion of 45 % after 5 h under these conditions represents the most efficient mass transfer

possible. To summarise, under the conditions chosen for this study, an air residence time of 0.11 minutes and a stir speed of 900 rpm is sufficient to provide maximum rate of reaction and therefore avoid mass transfer limitation for the reaction. If further catalyst testing was conducted under mass transfer limited conditions, improvements in a new catalyst may not be observed.

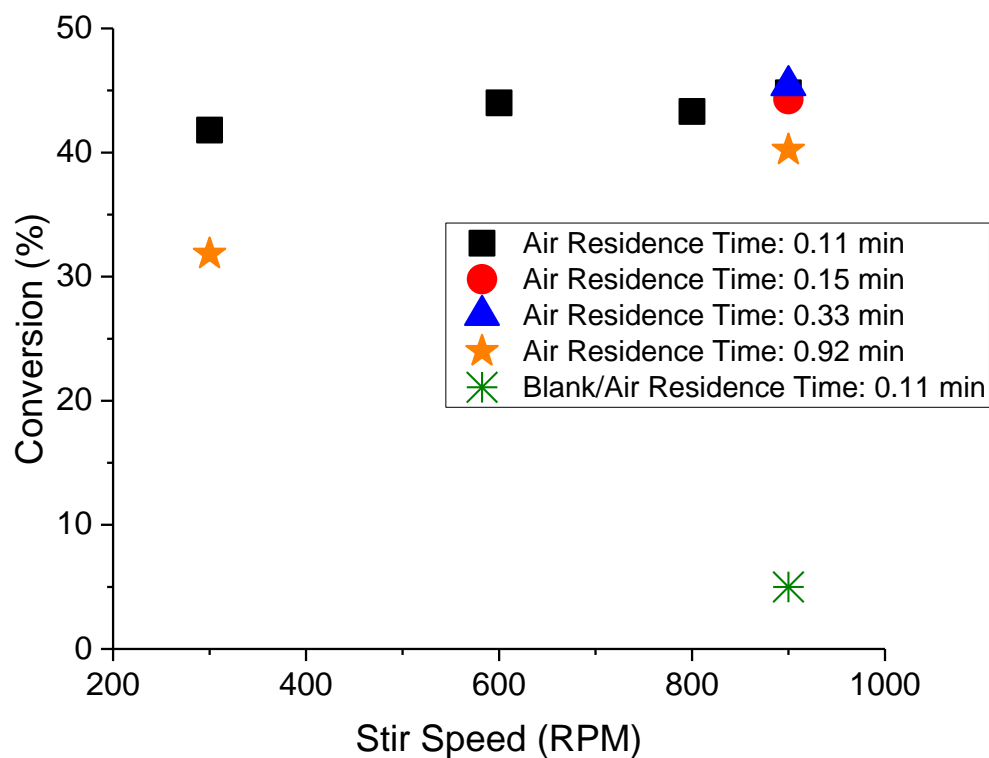
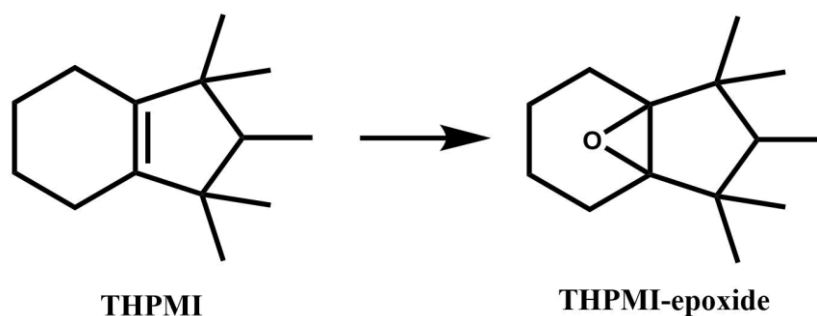


**Figure 3.2.** Conversion at various stir speeds and air residence times. Conditions: 5 h, 50 °C, 5 h, THPMI (10 mL), hexadecane (1 mL), 0.15 wt% Co-bis(2-ethylhexanoate), air residence time (0.11 - 0.92 min) and stir speed (300 – 900 rpm).

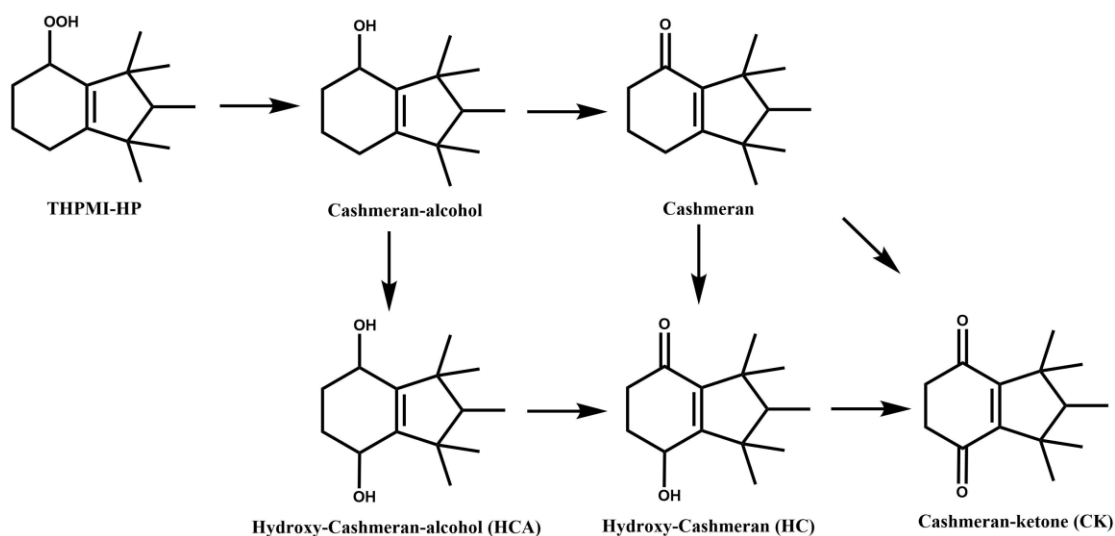
### 3.3 Characterisation of Undesired Products

Other than the desired allylic oxidation products, prior to this study, it was unclear what other products can form during the oxidation of THPMI. GC-MS studies on reaction mixtures demonstrated evidence of three distinct over-oxidation products of masses 224, 222 and 220, respectively referring to; hydroxy-Cashmeran-alcohol (HCA), hydroxy-Cashmeran (HC) and



**Scheme 3.4.** Formation of suspected THPMI-epoxide product.

Cashmeran-ketone (CK) (Scheme 3.3). The formation of these products is discussed in more detail in section (3.4), however it can be stated that their concentrations are only of significance at conversions greater than 40 %.



**Scheme 3.3.** Formation of over-oxidised products.

Evidence was also obtained for the formation of another undesired product, THPMI-epoxide (Scheme 3.4). The suspected product demonstrated a mass of 208 from GC-MS analysis, which is identical to Cashmeran-alcohol, however the peak for THPMI-epoxide elutes at 13.8 minutes which is much closer to THPMI (9.9 minutes) than Cashmeran-alcohol (17.1 minutes). This is very similar to the elution time of cyclohexene oxide which elutes at 5.8 minutes, much closer to cyclohexene (2 minutes) than to cyclohexen-1-ol (12.4 minutes) (Figure 3.3). Although this does not confirm definitively if the peak relates to THPMI-epoxide, it is very likely and it will be assumed that it is the case throughout the report. THPMI-epoxide is always a minor product in the oxidation of THPMI and it never constitutes more than 5 % selectivity, usually making up less than 3 % of the total products. The selectivity to THPMI-epoxide is explored in more detail in section 3.4.1.



**Figure 3.3.** Products from cyclohexene oxidation.

### 3.4 Aerobic Oxidation of THPMI at Industry Temperature

The standard operating conditions for the industrial oxidation of THPMI consist of a temperature of 110 °C, an air residence time of 3 minutes (lab scale) or 47 hours (industrial scale), a Co-bis(2-EH) loading of 0.15 wt%, and a run time of 5-5.5 hours, which yields approximately 50 % conversion and 81 - 83 % Cash-total (Cashmeran and Cashmeran-alcohol combined) selectivity. The reaction is run in a batch reactor with a highly optimised stirrer, and air is delivered from the bottom. Mass transfer in this system is limited by rate of airflow due to safety concerns of oxygen build up in the headspace of the reactor. The mass transfer limitations of the reactions in this investigation have been minimised (see section 3.2) due to a decreased air residence time; causing an expected increase in the dissolved O<sub>2</sub> concentration. This was chosen so that all catalytic effects of cobalt and any other catalysts tested can be fully investigated, without being masked by mass transfer limitations. A standard replication of the

reaction at industrial temperature is shown below, with comparison to an equivalent reaction with no Co-bis(2-EH) (Figure 3.4 and Figure 3.5).

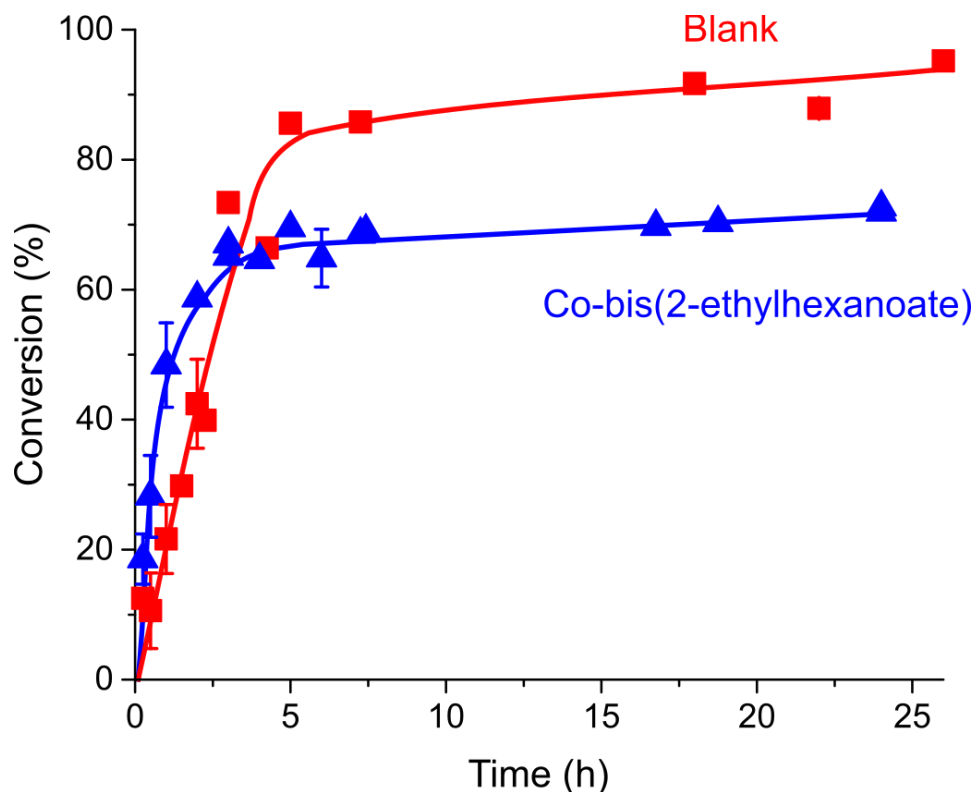


**Figure 3.4.** Conversion against time for standard replica of industrial conditions, with and without Co-bis(2-EH). Conditions: THPMI (10 mL), hexadecane (1 mL), Co-bis(2-ethylhexanoate) (13 mg/0.15 wt%) or no catalyst for blank, 110°C, 0.25 – 26 h, air residence time (0.11 min), 900 rpm. Data for the blank reaction was taken from 5 separate reactions, and data for Co-bis(2-EH) was taken from 6 separate reactions.

The first observation of the reaction is that the blank reaction shows significant activity, demonstrating that 110 °C is well above the autoxidation temperature for THPMI (Figure 3.4). Even at above autoxidation temperature Co-bis(2-EH) provided a boost in activity relative to the blank reaction. After 1 hour with Co-bis(2-EH), 48 % ( $\pm 9$ ) conversion was observed, compared to only 24 % ( $\pm 3$ ) in the blank. Similarly, after 2 hours with Co-bis(2-EH) 49 % conversion was reached compared to only 36 % in the blank. Although Co-bis(2-EH) enhanced the rate of reaction between 0 and 2 hours, it had the opposite effect from 2 hours onwards where the rate of reaction dropped to close to 0. This effect did not occur so early in the reaction in the case of the blank and after 5 hours the blank reaction demonstrated 86 % conversion and the reaction with Co-bis(2-EH) showed only 70 % conversion, which was the largest conversion observed under these conditions. It is not uncommon for oxidations involving cobalt to demonstrate this reaction quenching effect,<sup>24,28,32</sup> where the rate of oxidation is significantly reduced at a certain point in the reaction. This quenching effect is explored in more detail in sections 3.5 and 3.6.

Cash-total selectivity here refers to a combination of all 3 allylic oxidation products: THPMI-HP, Cashmeran-alcohol and Cashmeran. The inclusion of the THPMI-HP is not part of the Cash-total grouping industrially as any residual THPMI-HP in the reaction mixture will decompose after being exposed to the elevated temperatures in the distillation process. It is important in these studies to calculate and include the concentration of THPMI-HP as its concentration could play a key role in determining selectivity, this data would be missed if only Cashmeran and Cashmeran-alcohol yield was measured. The selectivities observed in both the blank (Figure 3.5a) and catalysed reactions (Figure 3.5b) are shown below.

The blank reaction generally favours allylic oxidation products, which is to be expected as this is seen for cyclohexene autoxidation<sup>33</sup> and THPMI is more sterically favoured towards these products. After 20 % conversion, 68 % Cash-total selectivity was observed, this decreased to 58 % selectivity at 50 % conversion and further to 46 % at 80 % conversion. When conversion increased beyond 80 %, the Cash-total selectivity rapidly decreased from 46 % at 80 % conversion to 20 % at 95 % conversion. The composition of the Cash-total selectivity was initially made up of only THPMI-HP (44 % at 20 % conversion) and Cashmeran-alcohol (18 % at 20 % conversion). As conversion increased, the relative concentration of THPMI-HP decreased (30 % at 50 % conversion) and the relative concentration of Cashmeran increased (10 % at 50 % conversion). As conversion is further increased, the relative concentration of THPMI-HP decreases to 0 % and Cashmeran increases to 20 % with Cashmeran-alcohol being maintained at around 20 % until post 80 % conversion where the concentration dropped to 0 %. These trends are not unexpected as THPMI-HP, Cashmeran-alcohol and Cashmeran are consecutive oxidation products and so as the reaction proceeds the relative concentration of Cashmeran will increase. These results also suggest that reaction route **2** is favoured over the Russell termination (**4**) or dehydration (**5**) (Scheme 3.2), as selectivity towards Cashmeran is at 0 % early in the reaction and only starts to increase when Cashmeran-alcohol is oxidised later in the reaction.

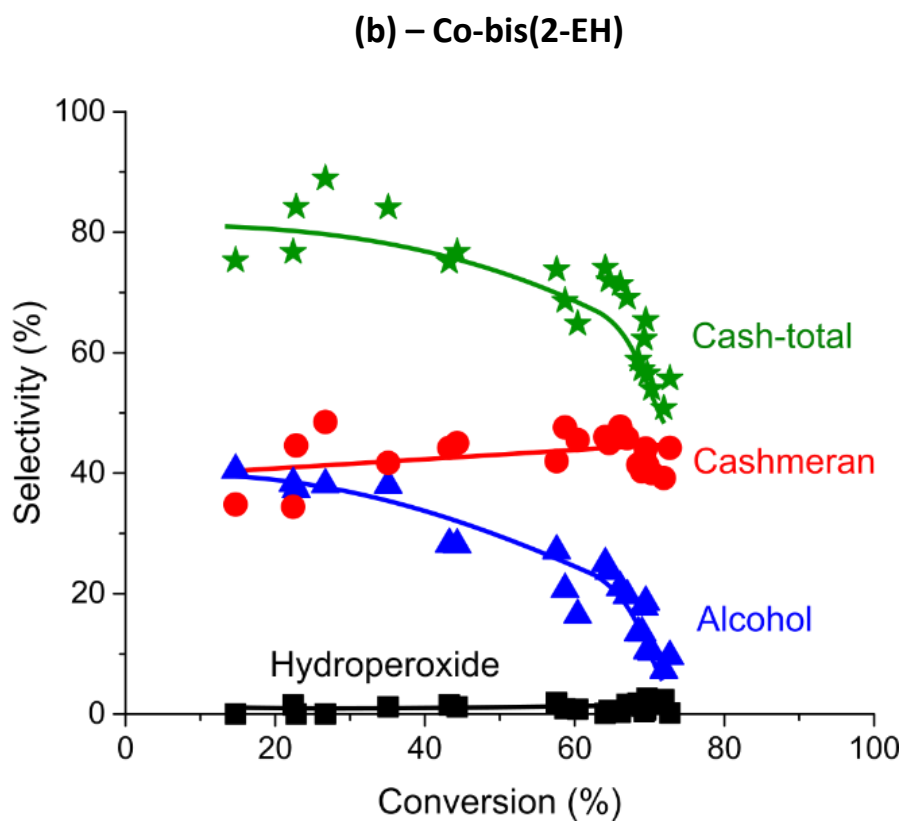
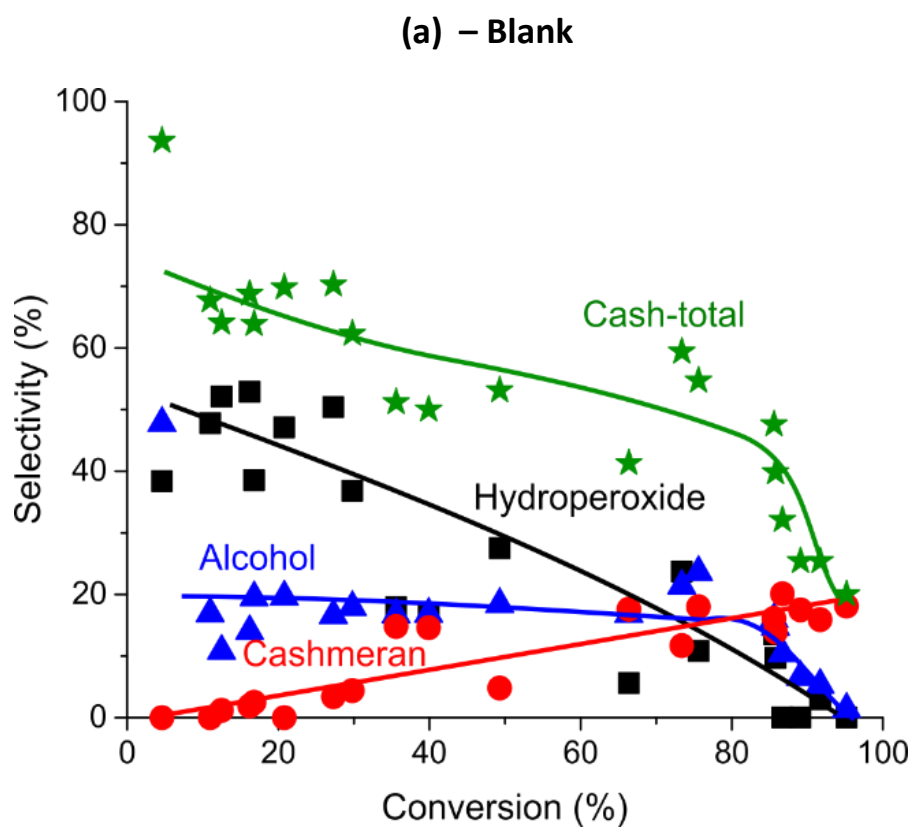


**Figure 3.5.** Selectivity against conversion for oxidation of THPMI (a): without catalyst and (b): with Co-bis(2-ethylhexanoate) (b). Conditions: THPMI (10 mL), hexadecane (1 mL), Co-bis(2-ethylhexanoate) ((b) only) (13 mg/0.15 wt%), 110 °C, 0.25 – 26 h, air residence time (0.11 min), 900 rpm. Data for the blank reaction was taken from 5 separate reactions, and data for Co-bis(2-EH) was taken from 6 separate reactions.

The introduction of Co-bis(2-EH) into this reaction had significant effects on the selectivity (Figure 3.5b). The Cash-total was consistently greater with the catalyst (81 % at 20 % conversion and 74 % at 50 % conversion), although dropped off more significantly beyond approximately 60 % conversion and a Cash-total of 61 % ( $\pm 4$ ) was observed at 70 % conversion. The composition of the Cash-total was also significantly altered with the introduction of Co-bis(2-EH) where, unlike the blank reaction, concentration of THPMI-HP was  $< 3\%$  throughout the reaction. Cashmeran is always in relatively high concentration, being between 40 – 45 % throughout the reaction. Cashmeran-alcohol drops from 40 % at 15 % conversion to 8 % at 70 % conversion, and as with the Cash-total this drop is more significant later in the reaction.

The results described above demonstrate that Co-bis(2-EH) has three distinct effects on the aerobic oxidation of THPMI; firstly, an increased initial rate of oxidation relative to the blank, more evidence for this is provided in section 3.5. Secondly, Co-bis(2-EH) affects the selectivity in two ways, by increasing the Cash-total selectivity, by 16 % at 50 % conversion relative to the blank, and by significantly increasing the proportion of Cashmeran within the Cash-total value. Thirdly, Co-bis(2-EH) seems to promote a quenching effect on the reaction after approximately 2 hours, something discussed in more detail in sections 3.5 and 3.6. Decomposition of THPMI-HP is to be expected given the extensive literature on the effect of cobalt ions on cyclohexyl hydroperoxide (CHHP) in the oxidation of cyclohexane.<sup>2-8,34</sup> This property of Co-bis(2-EH) likely also results in the increased rate of reaction observed, given that the breakdown of peroxide species will likely produce radicals capable of propagating further oxidation of THPMI. Another route for THPMI activation may stem from the formation of a  $\text{Co}^{3+}$  species as part of the Haber-Weiss cycle (1.5), where  $\text{Co}^{3+}$  abstracts the allylic hydrogen from THPMI forming  $\text{Co}^{2+}$  and a proton; similar to the oxidation of butane by  $\text{Co}^{3+}$ .<sup>35,36</sup> The increase in Cash-total selectivity is likely linked to the rapid decomposition of THPMI-HP, considering hydroperoxides are very reactive species and their decomposition can lead to highly reactive radical species. It is possible that high concentrations of THPMI-HP in the blank reaction will increase the rate of undesired reaction routes. This is similar to cyclohexane oxidation where it is shown that CHHP is the major cause of unwanted side products.<sup>3-8</sup> Co-bis(2-EH) also increases the Cashmeran to Cashmeran-alcohol ratio relative to the blank reaction. There are some possibilities for this; Co-bis(2-EH) could be catalysing the rapid oxidation of the alcohol into Cashmeran (reaction route **3**, Scheme 3.2). This is supported by literature where  $\text{Co}^{\text{III}}$  acetate is thought to oxidise secondary alcohols into ketones.<sup>16,17</sup> It is also possible that the hydroperoxide is being decomposed directly into Cashmeran *via* a dehydration reaction (reaction route **5**, Scheme 3.2). The fact that at 20 % conversion a near 1:1 Cashmeran to Cashmeran-alcohol ratio is observed suggests the possibility that Co-bis(2-EH) is promoting the Russell termination (reaction route **4**, Scheme 3.2) which

yields one Cashmeran and one Cashmeran-alcohol for each two THPMI molecules reacted, although this mechanism is usually uncatalysed.<sup>20,21</sup> If reaction route **5** is favoured, the explanation could lie in the ligand of Co-bis(2-EH). Excess 2-ethylhexanoic acid is present in the catalyst mixture which could result in the acid catalysed condensation of THPMI-HP into Cashmeran; this theory is discussed more in section 3.8.

### 3.4.1 Undesired Products

Although in both reactions the allylic oxidation products are the major products, the exact composition of side products is unclear. The development of primary over-oxidation products HCA, HC and CK (Scheme 3.3) are shown below for the blank (Figure 3.6a) and catalysed reactions (Figure 3.6b). In the blank reaction, HCA and HC were produced to similar selectivities (up to 4 %) at up to 70 % conversion, after this point the HCA was rapidly oxidised into HC. Some (< 1 %) CK was produced at THPMI conversion above 80 %. The composition of over-oxidised products for the blank increased from 0 – 10 % as the reaction proceeded to 95 % conversion, with only 3 – 4 % over-oxidation at 50 % conversion, near the point the industrial process is stopped.

When Co-bis(2-EH) was present in the reaction (Figure 3.6b) the overall concentration of over-oxidised products was similar to the blank with 3 – 4 % observed at 50 % conversion, increasing to 5 – 6 % at 70 % conversion. There is a slight trend of a greater proportion of HC compared to HCA compared to the blank reaction, however this is difficult to say definitively due to large error in selectivities at this low level of concentration. If this trend of greater HC compared to HCA is accurate then it could be further evidence of Co-bis(2-EH) acting as a catalyst for oxidation of alcohols into ketones, already evidenced by the oxidation of Cashmeran-alcohol into Cashmeran (section 3.4).

THPMI-epoxide was also detected in both catalysed and non-catalysed reactions (Figure 3.7). In the blank reaction, selectivity to THPMI-epoxide was detected at between 0 – 5 % from 11 – 90 % conversion, with a general trend of increasing THPMI-epoxide as conversion increased. In the reaction with Co-bis(2-EH), THPMI-epoxide was detected at a consistent level of 1 % between 22 – 73 % conversion. This may partially explain the difference in selectivity between the catalysed and non-catalysed reactions as the blank reaction is marginally more selective towards the undesired epoxide, at 50 % conversion 1 % more epoxide was observed in the blank reaction.

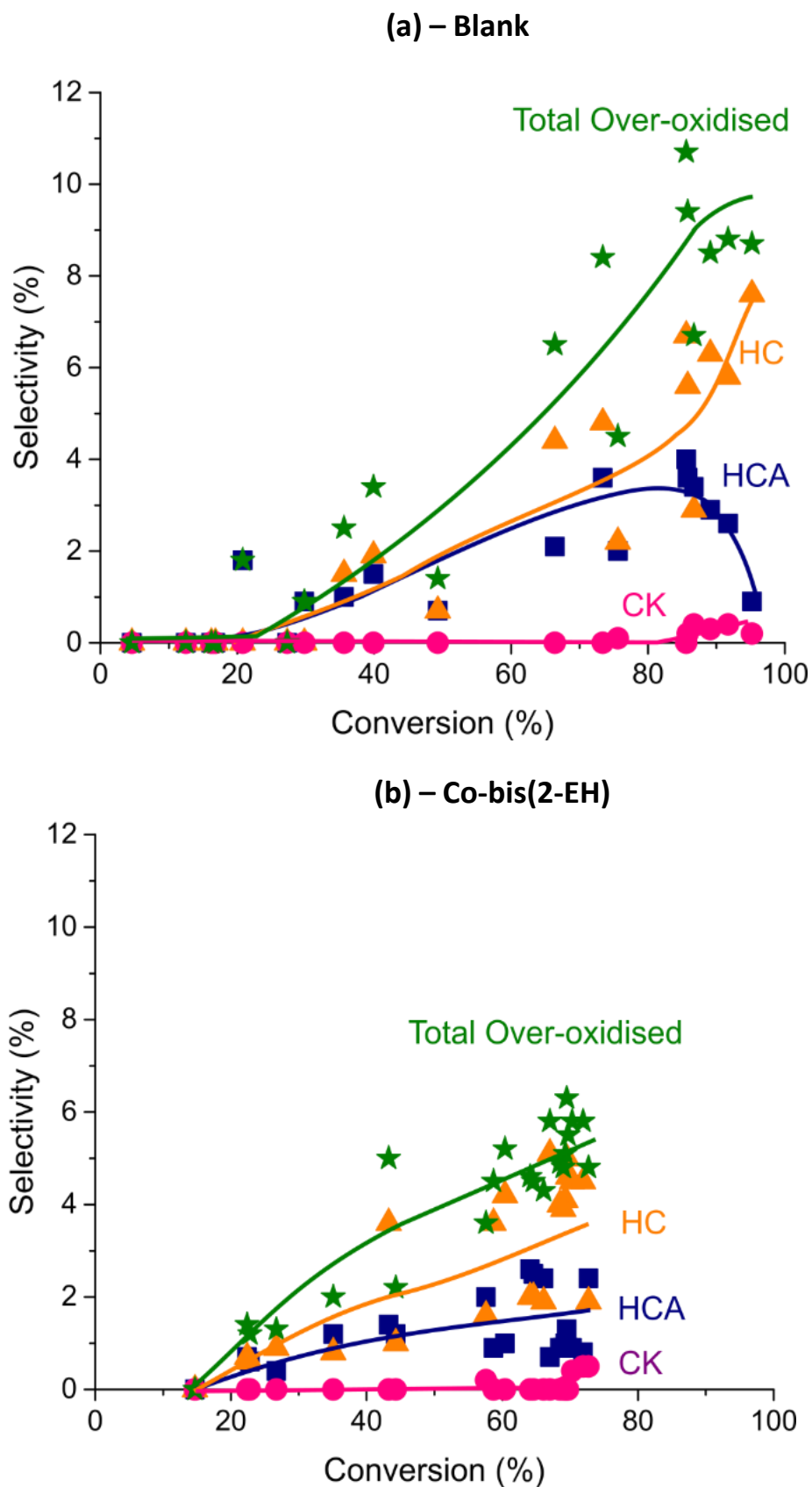


**Figure 3.6.** (a) Selectivity against conversion for overoxidation products produced in the blank reaction. (b) selectivity against conversion for over-oxidation products produced by the catalysed reaction. HC - hydroxy-Cashmeran, HCA – hydroxy-Cashmeran-alcohol, CK – Cashmeran-ketone. Conditions: THPMI (10 mL), hexadecane (1 mL), Co-bis(2-ethylhexanoate) ((b) only) (13 mg/0.15 wt%), 110 °C, 0.25 – 26 h, air residence time (0.11 min), 900 rpm. Data for the blank reaction was taken from 5 separate reactions, and data for Co-bis(2-EH) was taken from 6 separate reactions.

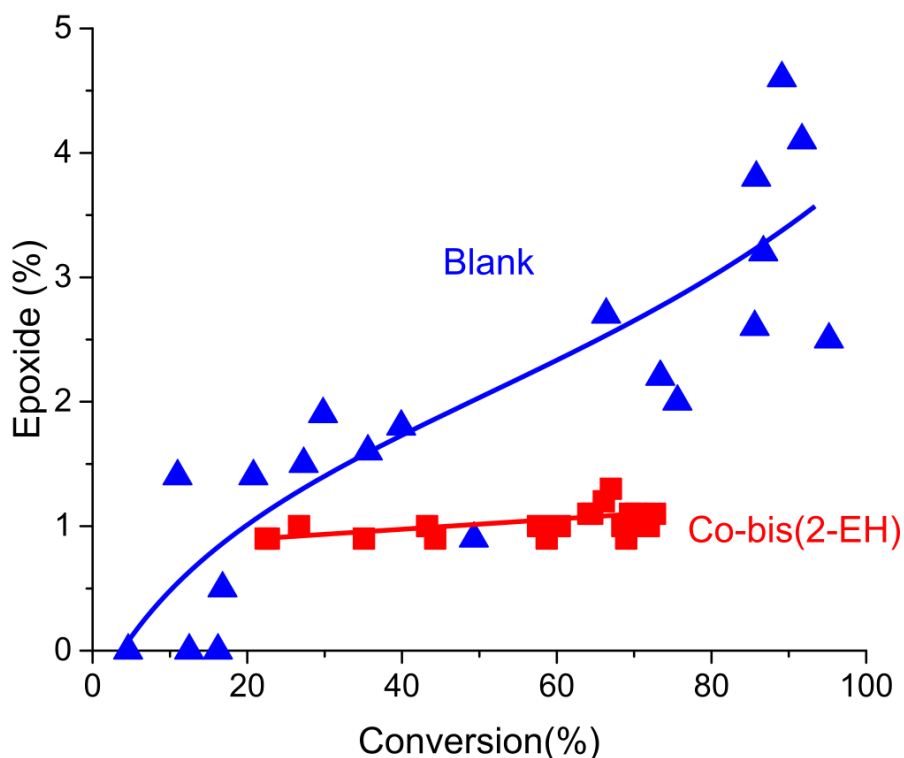


**Figure 3.7.** Selectivity towards epoxide for the blank reaction and the reaction with Co-bis(2-ethylhexanoate). Conditions: THPMI (10 mL), hexadecane (1 mL), Co-bis(2-ethylhexanoate) (13 mg/0.15 wt%) or no catalyst for blank, 110 °C, 0.25 – 26 h, air residence time (0.11 min), 900 rpm. Data for the blank reaction was taken from 5 separate reactions, and data for Co-bis(2-EH) was taken from 6 separate reactions.

Even with the quantification of over-oxidised and THPMI-epoxide products, there are still a large number of unknowns. For the standard reaction with Co-bis(2-EH) at 50 % conversion 74 % is made up of Cash-total products, 4 % from over-oxidised products and 1 % THPMI-epoxide, this only accounts for 79 % of products, leaving a deficit of 21 %. Several small peaks appear on the GC trace which combined will make up near 3 % selectivity at 50 % conversion, however these peaks are currently unassigned. The rest of the products that are unaccounted for could be oligomerised materials, which are too heavy to detect by GC analysis, as observed in the industrial oxidation of THPMI. Alternatively, these could be highly oxidised or totally oxidised gaseous products which would not appear by standard GC analysis as they would have escaped the reactor. Further evidence for this theory is provided in the next section.

### 3.4.2 Mass Balance

When interpreting the mass balance for both the blank and catalysed reactions, a clear trend of decreasing mass balance with increasing conversion is observed (Figure 3.8). The catalysed reaction demonstrated mass balances as low as 73 % (at 72 % conversion), and the blank reactions demonstrated a mass balance as low as 45 % (at 95 % conversion). The decrease in

mass balance was more significant for the blank reaction compared to the catalysed reaction when similar conversions are compared. This suggests that mass balance decreases more at lower selectivity. This could be a result of the blank reaction promoting routes that result in products not observable by GC analysis, or stated in another manner, Co-bis(2-EH) is suppressing these undesired reaction routes. The data here promote the theory that gaseous, high volatility, or polymerised products are produced as they will not appear by GC analysis and so a deficit of products and an incomplete mass balance is observed.

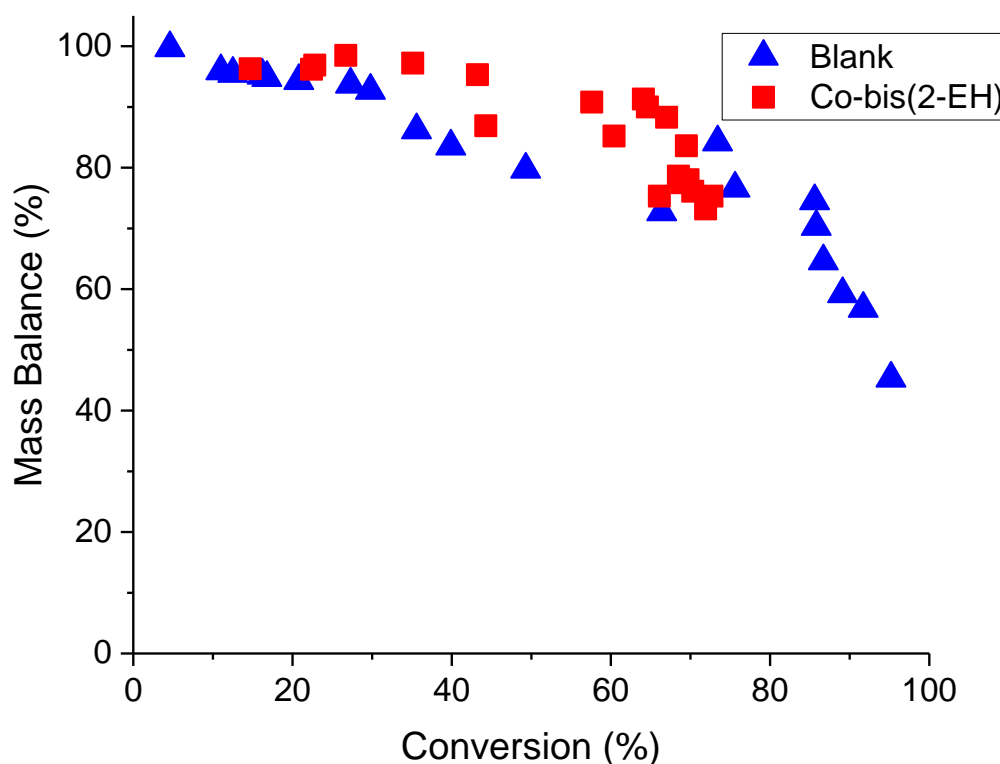


**Figure 3.8.** Mass balance against conversion for blank reactions and reactions with Co-bis(2-ethylhexanoate). Conditions: Conditions: THPMI (10 mL), hexadecane (1 mL), Co-bis(2-ethylhexanoate) (13 mg/0.15 wt%) or no catalyst for blank, 110 °C, 0.25 – 26 h, air residence time (0.11 min), 900 rpm. Data for the blank reaction was taken from 5 separate reactions, and data for Co-bis(2-EH) was taken from 6 separate reactions.

## 3.5 Effect of Varying Temperature

### 3.5.1 Blank Reaction

Internal research at IFF into THPMI oxidation was limited to a temperature regime of 100 - 120 °C, where 110 °C was found to be, on average, 2 % higher in Cash-total selectivity. It was hypothesised that by reducing the reaction temperature significantly, the beneficial activating and selectivity directing properties of cobalt can be maintained, whilst slowing down the undesired side reactions. First, a temperature range of 50 – 110 °C was tested for the blank reactions with no catalysts (Figure 3.9). At 50 °C no THPMI was converted for the first 5 hours of

reaction and only 6 % was converted after 24 hours of reaction. At 70 °C only 5 % THPMI was converted after 5 hours and 20 % conversion was observed after 23 hours. These results demonstrate that autoxidation is of little to no significance for reactions performed at 50 °C and of only minor significance for those undertaken at 70 °C, this is similar to the literature for cyclohexene autoxidation where < 5 % conversion was observed at 70 °C after 5 hours.<sup>33</sup> The autoxidation is likely a result of residual THPMI-HP O—O bond cleavage, resulting in alkoxy and peroxy radicals. The onset of decomposition for cumene hydroperoxide occurs at 80 °C,<sup>37</sup> a similar temperature range for the autoxidation of THPMI. If catalysts are tested at 70 °C or below then any significant levels of conversion can be associated with the inclusion of the catalyst rather than the blank, background reaction. The rate of reaction increased significantly at 90 °C with 24 % conversion being reached at 5.5 hours, increasing to 74 % after 16.25 hours. The rate was again enhanced with increase of temperature to 110 °C where 86 % conversion was reached

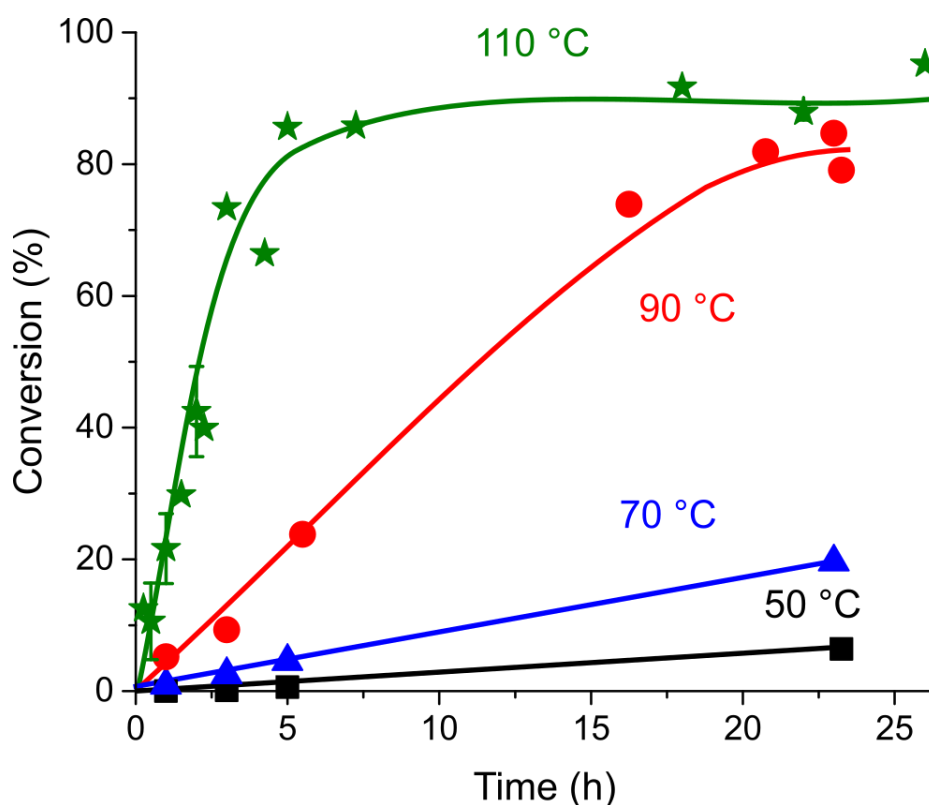


**Figure 3.9.** Conversion against time for blank reactions between 50 – 110 °C. Conditions: THPMI (10 mL), hexadecane (1 mL), 50 - 110°C, 0.25 – 24 h, air residence time (0.11 min), 900 rpm. Data for the 110 °C reaction was taken from 5 separate reactions, data for the 50 and 70 °C were taken from 1 reaction, and the data for the 90 °C was taken from 2 separate reactions.

after only 5 hours. These results are very similar to the uncatalysed, autoxidation of cyclohexene, where similar rates of conversion were observed at equivalent temperatures.<sup>33</sup> These results signify that at temperatures above 70 °C autoxidation must be taken into

consideration and any catalyst testing at these temperatures will primarily show effects on selectivity rather than activity.

The selectivity data for the blank reactions at 70 °C (Figure 3.10a) and 90 °C (Figure 3.10b) are shown below. Due to lack of activity, data for the reaction 50 °C is not provided and the data for the reaction at 110 °C has already been discussed in section 3.4 (Figure 3.5b). Although only one reliable data point was obtained for the reaction at 70 °C, it showed 45 % Cash-total selectivity at 20 % conversion, made up mostly of THPMI-HP (32 % selectivity). This constitutes a significant reduction in Cash-total compared to the blank reaction at 110 °C where near 68 % selectivity was observed at 20 % conversion. The composition of the Cash-total is however similar with a large majority of the products being THPMI-HP and only 2 % Cashmeran observed. Cash-total selectivity seemed to be improved at 90 °C, relative to 70 °C, with 59 % selectivity at 24 % conversion. Once again, this selectivity was directed primarily to THPMI-HP (44 % selectivity). At 90 °C the Cash-total selectivity dropped to 29 % at 80 % conversion, again lower than the 46 % observed for the 110 °C. At all three temperatures the same trend was observed where THPMI-HP concentration decreases, Cashmeran concentration increases, and Cashmeran-alcohol concentration remains consistent. Although more data points are required to determine definitive trends, from the data that has been obtained it seems that for the blank reaction greater temperatures result in greater selectivity to Cash-total products.

The reduction in selectivity at 70 °C was not explained by a relatively higher rate of over-oxidation, as over-oxidation products were present at negligible levels at the lower temperature (Figure 3.11a). No change in the proportions of over-oxidation products was observed between reaction at 90 °C (Figure 3.11b) and 110 °C (Figure 3.6a) and so any change in selectivity caused by temperature is likely not caused by an enhanced directing of selectivity towards the three detected over-oxidation products. It can also be noted that the selectivity towards THPMI-epoxide was not significantly different at lower temperatures compared to the reaction at 110 °C (Figure 3.7).

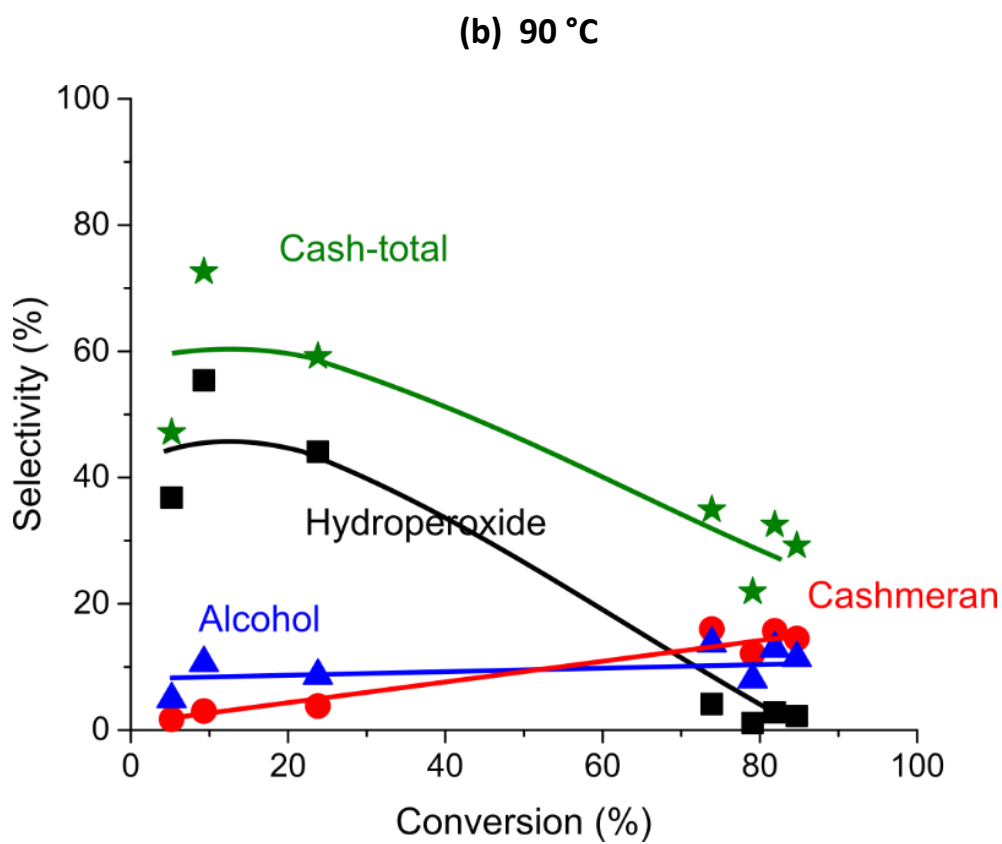
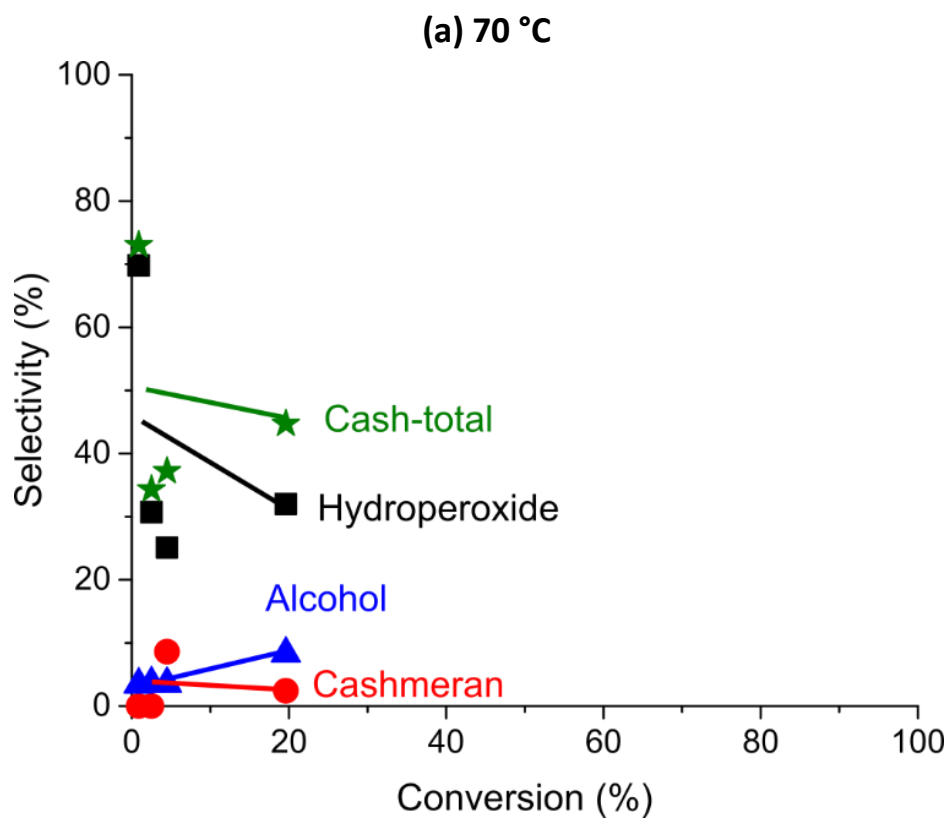
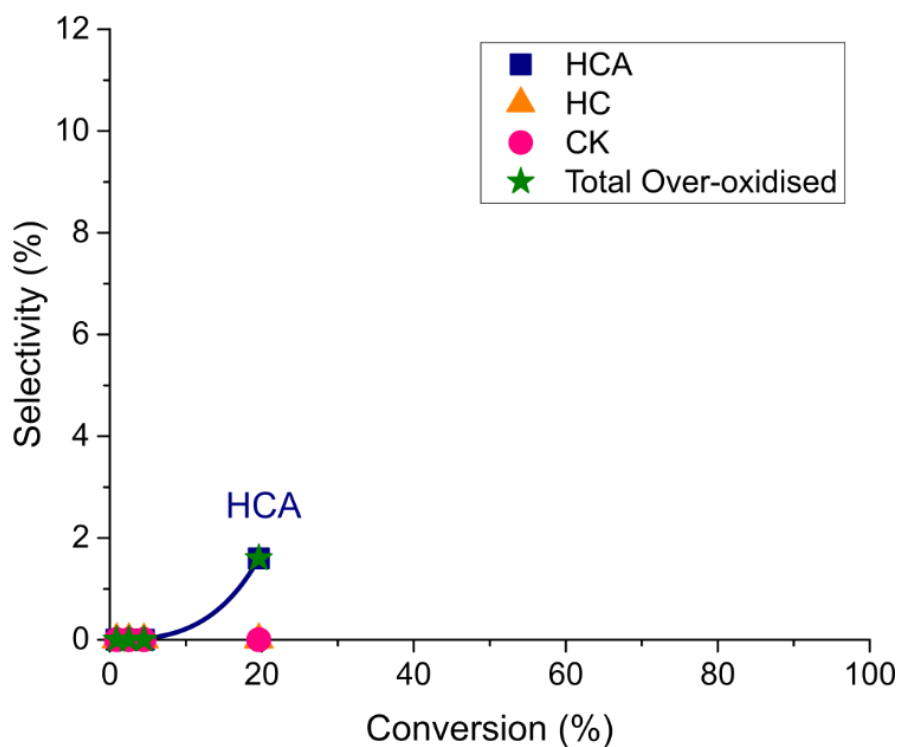


**Figure 3.10.** Selectivity for blank reactions at (a): 70 °C and (b): 90 °C. Conditions: THPMI (10 mL), hexadecane (1 mL), 770 or 90 °C, 0.25 – 24 h, air residence time (0.11 min), 900 rpm. Data for the 50 and 70 °C plots were taken from 1 reaction, and the data for the 90 °C was taken from 2 separate reactions.

(a) 70 °C



(b) 90 °C

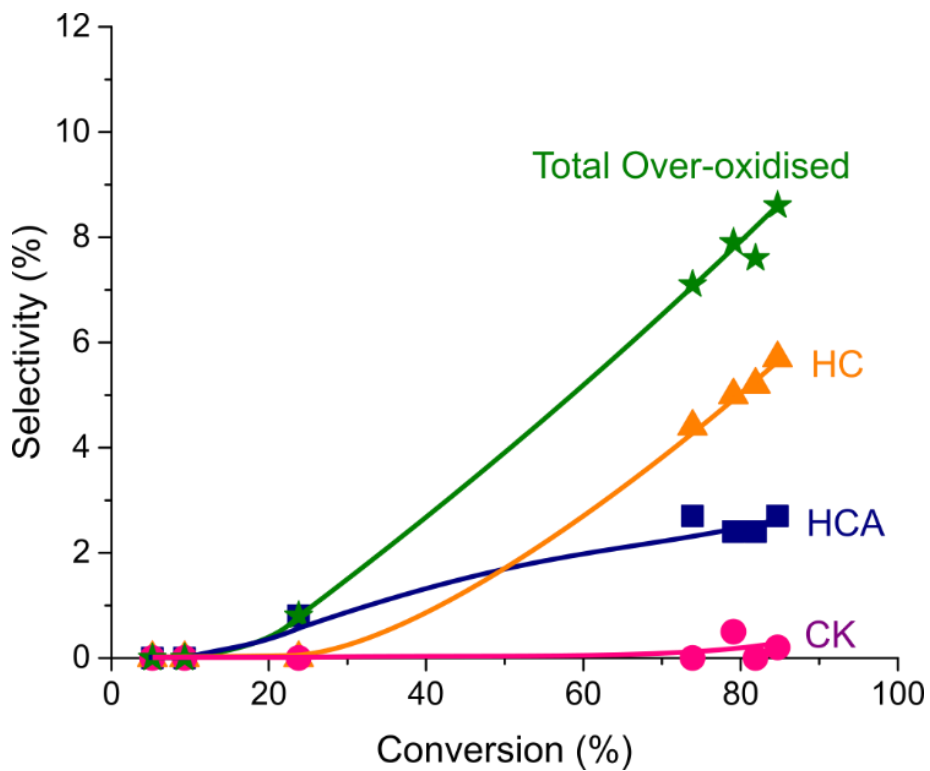


**Figure 3.11.** Selectivity to over-oxidation products for blank reactions at (a): 70 °C and (b): 90 °C. Conditions: THPMI (10 mL), hexadecane (1 mL), 70 or 90 °C, 0.25 – 24 h, air residence time (0.11 min), 900 rpm. Data for the 50 and 70 °C plots were taken from 1 reaction, and the data for the 90 °C was taken from 2 separate reactions.

### 3.5.2 Reactions with Co-bis(2-ethylhexanoate)

A range of 50 – 130 °C was also tested for the catalysed oxidation of THPMI (Figure 3.12). Even at 50 °C, below significant rates of autoxidation, Co-bis(2-EH) is effective at initiating radical oxidation *via* decomposition of THPMI-HP and/or abstraction of the allylic hydrogen. The rate of reaction was significantly increased by raising the temperature to 70 °C and then increased slightly further by going to 110 °C or 130 °C. After 1 hour the reaction at 50 °C reached 19 % ( $\pm 2$ ) conversion, this increased to 35 % at 70 °C, increased (within error) to 45 % ( $\pm 13$ ) at 90 °C but did not increase when the temperature was raised to 110 °C (48 %  $\pm 7$ ) or 130 °C (40 %). The most distinctive effect of alteration in temperature is the rate at which the reaction begins to quench; there is a clear correlation between a greater temperature and a faster rate of quenching. At 50 °C the reaction did not seem to quench at any point, while at 70 °C the reaction slowed down significantly after 5 hours. It is unclear if the reaction at 70 °C reduced in rate due to quenching or due to reaction kinetics, as a reduction in THPMI concentration would result in a lower rate of reaction of THPMI. At 90 °C and 110 °C the reaction was quenched by 3 hours and at 130 °C the reaction was quenched by 2 hours. This effect was also demonstrated by the fact that the maximum conversion reached by the end of the reaction is inversely proportional to the temperature, providing the reaction was run for a long enough time. It is important to

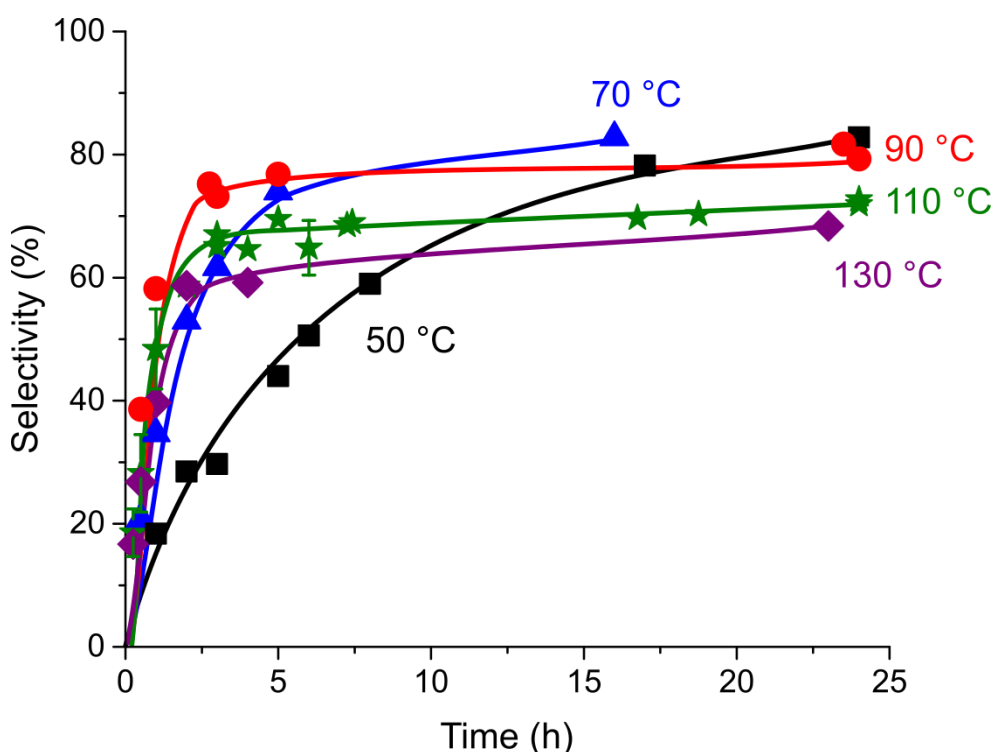


**Figure 3.12.** Conversion against time for oxidation of THPMI with Co-bis(2-ethylhexanoate) at temperatures between 50 – 130 °C. Conditions: THPMI (10 mL), hexadecane (1 mL), Co-bis(2-ethylhexanoate) (13 mg/0.15 wt%), 110 °C, 0.25 – 24 h, air residence time (0.11 min), 900 rpm. Data for the 50 °C plot was taken from 2 separate reactions, data from the 70 °C plot was taken from 1 reaction, data for the 90 °C plot was taken from 2 separate reactions, data for the 110 °C plot was taken from 5 separate reactions and data for the 130 °C plot was taken from 1 reaction.

note that after the point of quenching the reaction slows down significantly, but does not stop entirely. These data demonstrate that there is a clear relationship between temperature and reaction quenching, and considering data for the blank reaction, Co-bis(2-EH) is also likely involved in the process which is discussed more in section (3.6).

The comparisons of selectivity at various temperatures for the catalysed reaction are shown below (Figure 3.13 and Figure 3.14). The Cash-total selectivity trends remained stable regardless of temperature. At 50 – 110 °C a Cash-total of near 80 % was observed at 20 % conversion, which reduces to between 62 – 64 % at 80 % conversion, except at 110 °C where 61 % ( $\pm 4$ ) Cash-total was observed at 70 % conversion. At 110 °C, 80 % conversion was not observed due to reaction quenching. The reaction at 130 °C (Figure 3.14b) yielded lower Cash-total selectivity with 68 % observed at 20 % conversion, which reduced to 39 % at 68 % conversion. This was after a significant drop in selectivity after 60 % conversion, similar to the drop-off in selectivity observed in the reaction at 110 °C (Figure 3.5b). The drop off in Cash-total selectivity at higher temperatures could be linked to the more rapid quenching effect described above (Figure 3.12). If the reaction to oxidise THPMI into the desired products is slowed down at a greater rate than the reaction further oxidising the desired products, then this would result in greater rate of reduction in the Cash-total value.

A noticeable effect of varying the temperature of reaction on the Cashmeran to Cashmeran-alcohol ratio (CTA), which was shown to be proportional to temperature. Under any reaction conditions the CTA increased as the reaction proceeded as Cashmeran-alcohol was oxidised into Cashmeran. However, the disparity in the concentration of Cashmeran compared to the alcohol increases with temperature. At 20 % conversion a CTA of 0.37 was observed at 50 °C, 0.59 at 70 °C, 0.65 at 90 °C, 1 at 110 °C and 1.28 at 130 °C. At all temperatures the rate of change of the CTA seemed to be consistent, which suggests that the change in initial CTA is due to an increase in the relative rate of the reaction that converts THPMI-HP directly into Cashmeran (route 5, Scheme 3.2).

Another effect of the variation in temperature was its subtle effect on the concentration of THPMI-HP. All reactions performed with Co-bis(2-EH) present result in very low concentrations of THPMI-HP, however there is still an inversely proportional relationship between THPMI-HP concentration and reaction temperature. At 50 °C and 70 °C THPMI-HP selectivity of 1 – 6 % was observed throughout the reactions, at 90 °C this selectivity reduces to 0 – 4 %, at 110 °C it is 0 – 3 % and at 130 °C no THPMI-HP is observed at all. This effect could also impact the change in CTA ratio described above, as a greater temperature could result in THPMI-HP directly converting into Cashmeran at a greater relative rate. The levels of over-oxidation products (HC, HCA and CK) or THPMI-epoxide were not significantly different for reactions performed between

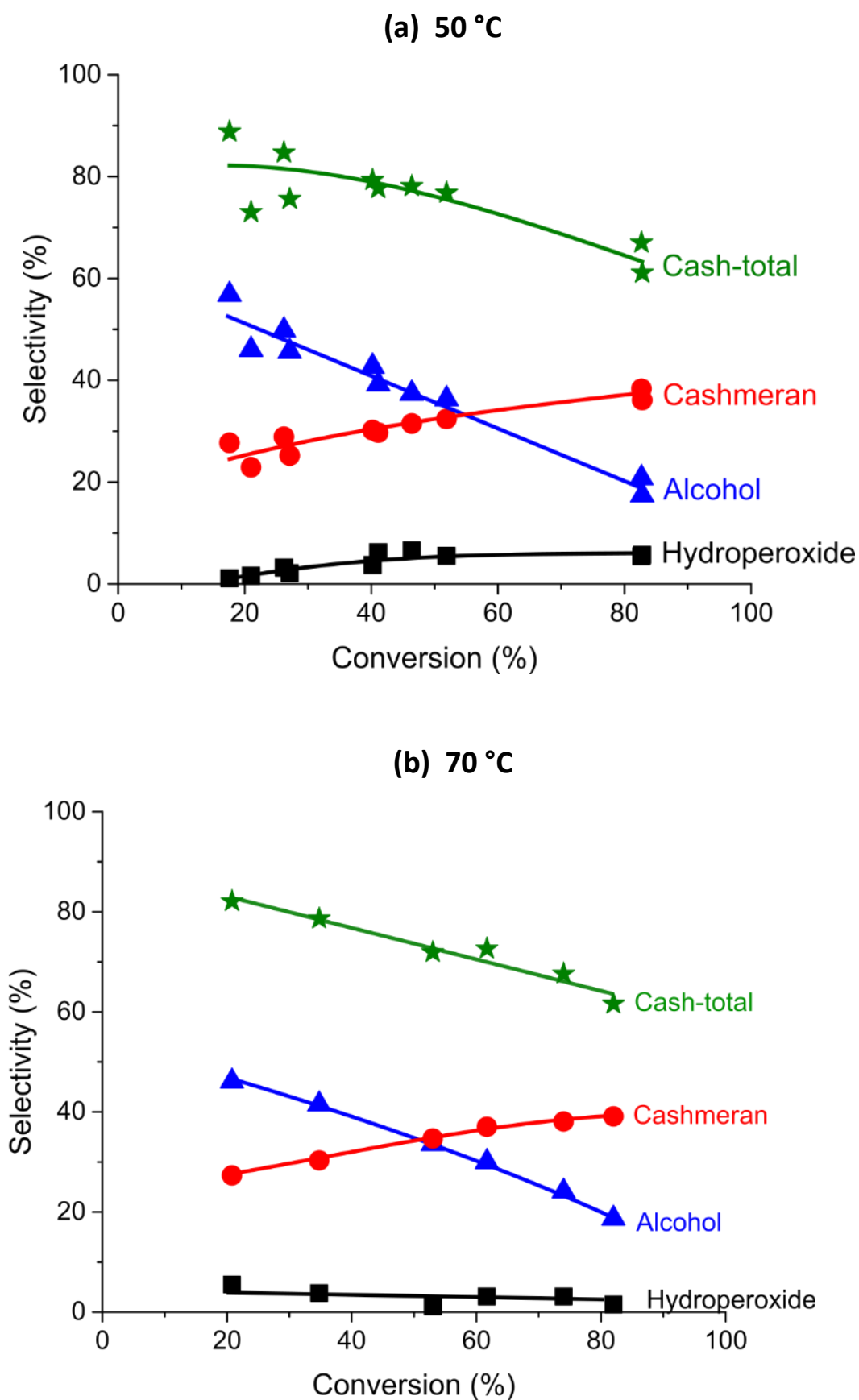


**Figure 3.13.** Selectivity against conversion for catalysed reactions at (a) 50 °C and (b) 70 °C. Conditions: THPMI (10 mL), hexadecane (1 mL), Co-bis(2-ethylhexanoate) (13 mg/0.15 wt%), 70 or 90 °C, 0.5 – 24 h, air residence time (0.11 min), 900 rpm. Data for 50 °C plot was taken from 2 separate reactions, data from the 70 °C plot was taken from 1 reaction.

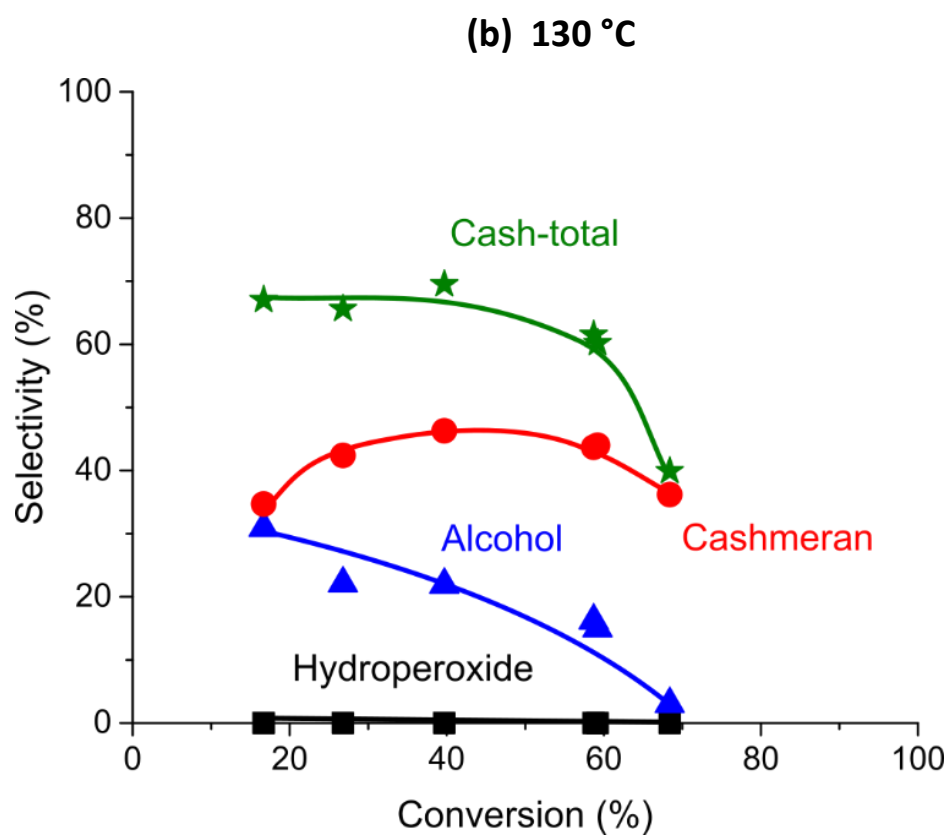
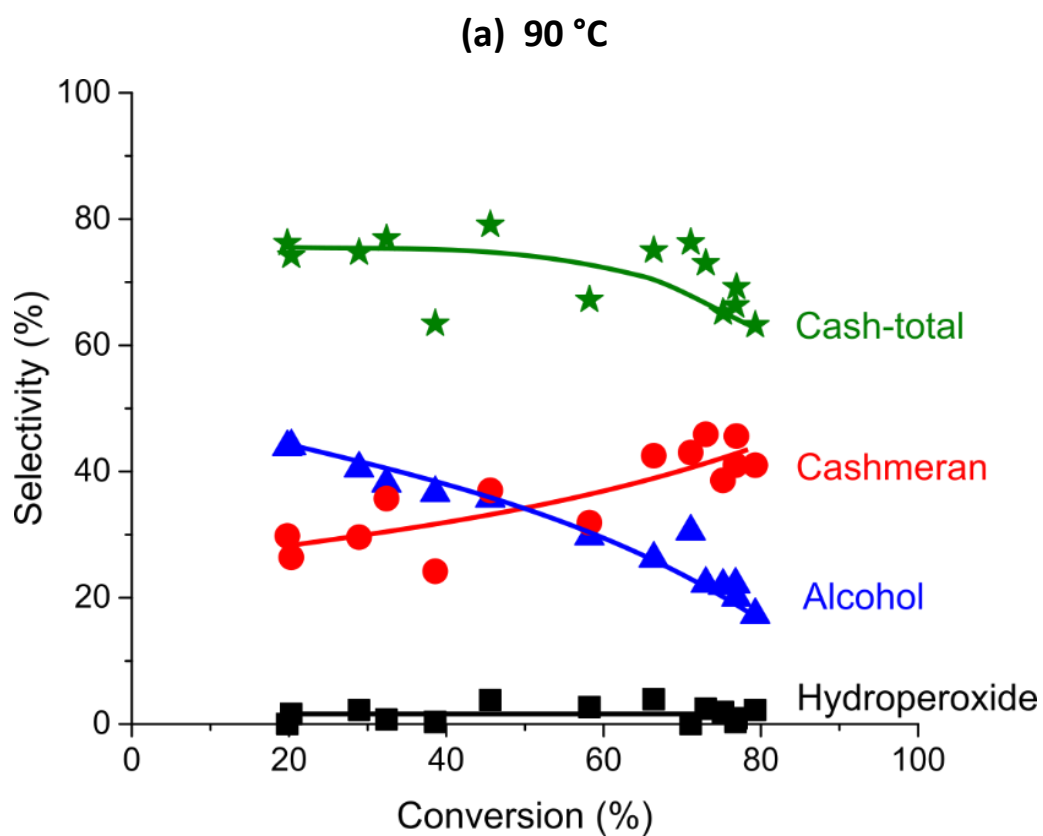


**Figure 3.14.** Selectivity against conversion for catalysed reactions at (a): 90 °C and (b): 130 °C. Conditions: THPMI (10 mL), hexadecane (1 mL), Co-bis(2-ethylhexanoate) (13 mg/0.15 wt%), 70 or 90 °C, 0.25 – 24 h, air residence time (0.11 min), 900 rpm. Data for the 90 °C plot was taken from 2 separate reactions and data for the 130 °C plot was taken from 1 reaction.

50 – 130 °C, compared to the reaction at carried out at 110 °C (Figure 3.6b). The effect of higher temperature reducing THPMI-HP concentration, whilst also increasing the rate of reaction adds evidence to the theory that a larger  $\text{Co}^{2+}$  to hydroperoxide ratio will result in radical termination of the reaction.<sup>28</sup>

To summarise, reducing reaction temperature does not improve the selectivity in either the blank or catalysed reactions. When Co-bis(2-EH) was present, an increase in temperature up to 90 °C benefits allylic oxidation and any further increase in temperature only increases the rate of THPMI oxidation. When Co-bis(2-EH) is present the overall Cash-total allylic selectivity is largely unaffected by temperature, however selectivity towards Cashmeran is increased with higher temperature. This suggests temperature has an impact on the oxidation of Cashmeran-alcohol into Cashmeran, or the direct conversion of THPMI-HP into Cashmeran. The rather marginal effects of temperature on selectivity are likely explained by the radical nature of the reaction. Due to radical reactions having an activation energy of close to 0  $\text{kJ mol}^{-1}$ ,<sup>38,39</sup> once the radical cascade mechanism has been initiated, temperature will play little role in the overall selectivity of the process. This means that decreasing the reaction temperature will not turn off any undesired radical reaction routes once activated.

### 3.6 Effect of Varying Co-bis(2-ethylhexanoate) Loading

The investigation into the effect of varying reaction temperature (section 3.5) demonstrated that the presence of Co-bis(2-EH) in the reaction was integral to the quenching phenomena. This was further investigated by studying the effect of altering the catalyst loading. For reactions at a constant 70 °C (Figure 3.15a), four catalyst loadings were tested: 50 ppm (0.005 wt%), 0.09 wt%, 0.15 wt% and 1.2 wt%. A catalyst loading of 50 ppm was selected as it was part of another study described later in the report (4.5). The lower two weight loadings did not result in any obvious reaction quenching, the reaction at 0.15 wt% slowed down slightly more rapidly than the equivalent reaction with 0.09 wt%, potentially suggesting some quenching, however the effect is too subtle to be confirmed. The increase in weight loading to 1.3 wt% caused the reaction to rapidly quench after only 2 h of reaction and reached only 45 % conversion. The same results were observed when a constant 110 °C reaction temperature was employed. The effect of decreasing from 1.5 wt% to 0.09 wt% results in a slightly delayed rate of quenching and increasing to a 1.2 wt% catalyst loading results in sudden, rapid quenching after only 1 hour of reaction and at 36 % conversion. These results confirm that both temperature and Co-bis(2-EH) concentration influence the presence and rate of reaction quenching for the oxidation of THPMI. The influence of cobalt concentration is to be expected as previous literature suggests that in

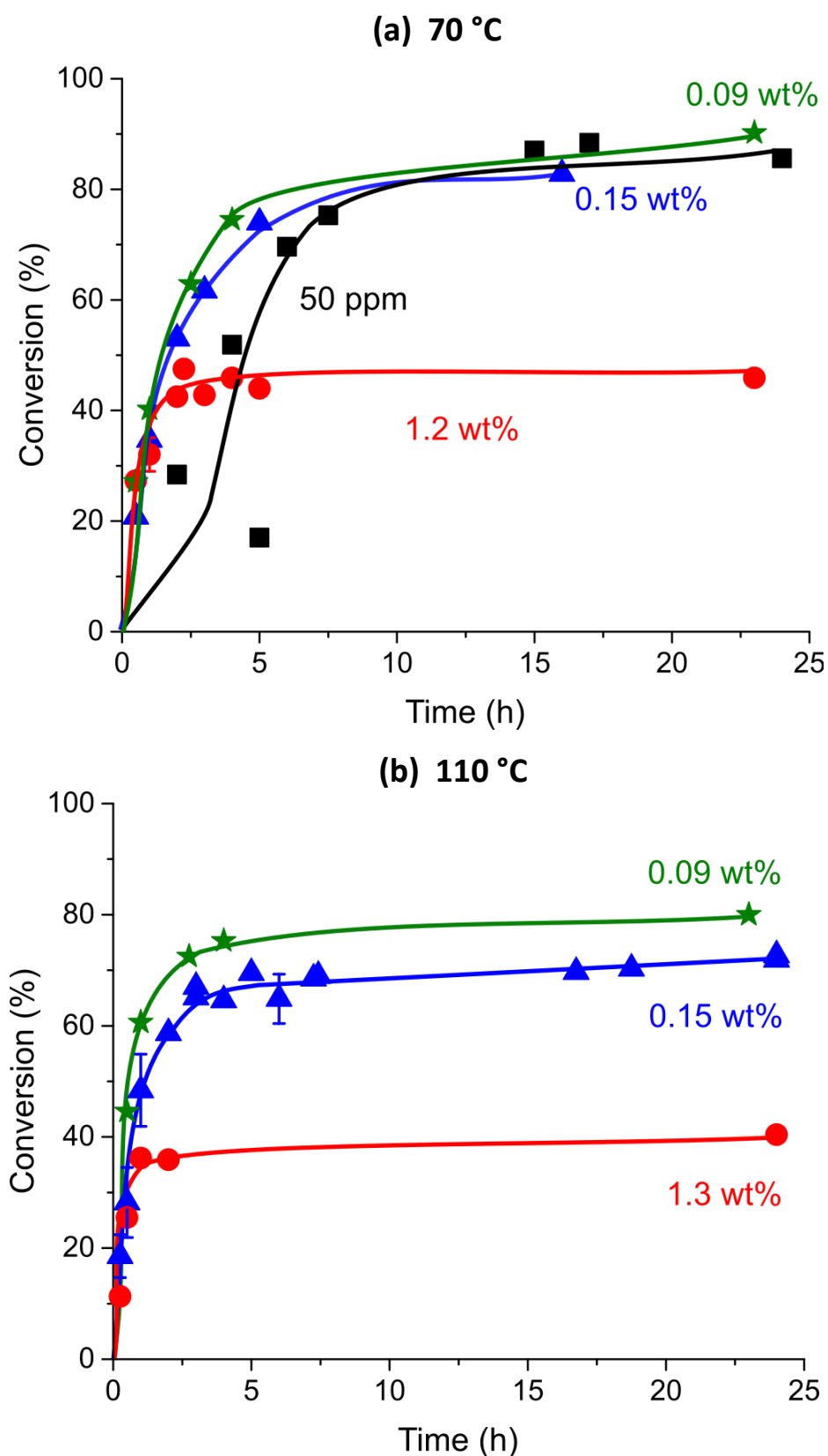


**Figure 3.15.** Conversion against time for reactions at (a): 70 °C and (b) 110 °C with varying catalyst loadings. Conditions: THPMI (10 mL), hexadecane (1 mL), Co-bis(2-ethylhexanoate) (0.005 – 1.2 wt%), 70 °C, 0.25 – 25 h, air residence time (0.11 min), 900 rpm. (a) 70 °C: Data from the 50 ppm plot was taken from 3 separate reactions, data for the 0.09 and 0.15 wt% plot was taken from 1 reactions and the data for the 1,2 wt% plot was taken from 2 separate reactions. (b) 110 °C: Data from the 0.09 and 1.3 wt% plots were from one reaction and the data from the 0.15 wt% plot was from 6 separate reactions.

solvent media of low polarity, when the concentration of  $\text{Co}^{2+}$  exceeds that of the hydroperoxide species an undesired termination step will occur and radical oxidation will cease.<sup>28</sup>

### 3.7 Effect of Radical Scavengers

From the work already conducted and the literature discussed in Chapter 1, radical mechanisms appear to control the aerobic oxidation of THPMI. To confirm this beyond doubt, butylated hydroxytoluene (BHT) was added to both blank and catalysed reactions, with the expected impact being near total shutdown of oxidation. BHT acts as a radical scavenger as it can donate its hydroxy proton to other radicals without becoming unstable, behaviour similar to that of vitamin E.<sup>40</sup> This scavenging reaction is favoured as the radical formed from BHT is relatively stable. BHT has been widely used as a radical scavenger for oxidation reactions in the literature.<sup>15,20,41</sup>

For both the blank (Figure 3.16a) and catalysed (Figure 3.16b) reactions, BHT was added in loadings of between 1 – 17 wt%. In both reactions as little as 1 wt% BHT was enough to suppress THPMI conversion significantly, although in all cases at least some conversion was observed. This demonstrated that most THPMI conversion in both the blank and catalysed reactions was a result of a radical mechanism. Unexpectedly, the degree of reaction quenching was not proportional to the weight loading of BHT added to the reaction, with and without catalyst present the reaction with 1 wt% BHT addition resulting in less conversion than the reactions with 17 wt% BHT.

The effects of BHT addition on selectivity of the catalysed and blank reactions are shown below (Figure 3.17). The blank reaction with 17 wt% BHT and the catalysed reaction with 1 wt% BHT are not shown as they yielded close to 0 % conversion. The low level of conversion (< 10 %) observed for the blank reaction with 1 wt% BHT (Figure 3.17a) demonstrates very low Cash-total selectivity between 31 – 55 %. This effect was exaggerated by the increased addition of 5 wt% BHT (Figure 3.17b), where observed Cash-total ranged from 3 – 5 % between 8 – 26 % conversion. The addition of 17 wt% BHT to the catalysed reaction (Figure 3.18) demonstrated greater selectivity, between 54 – 84 %, but at very low conversion of < 5 %, and then the Cash-total reduced to 15 % at 14 % conversion. These results demonstrate that the selectivity observed in both the blank and catalysed reactions is predominantly a result of radical reactions and if there are any non-radical routes present in the reaction, they will likely not yield the desired products and reduce selectivity. When low selectivity was observed it was not clear what products were being formed as products were determined by GC analysis, it is possible that

gaseous or very heavy products were being formed. It should also be noted that no evidence of BHT to THPMI/Cashmeran adducts was observed by GC-MS analysis as this may have been an explanation for low selectivity, particularly when large BHT loadings were employed.

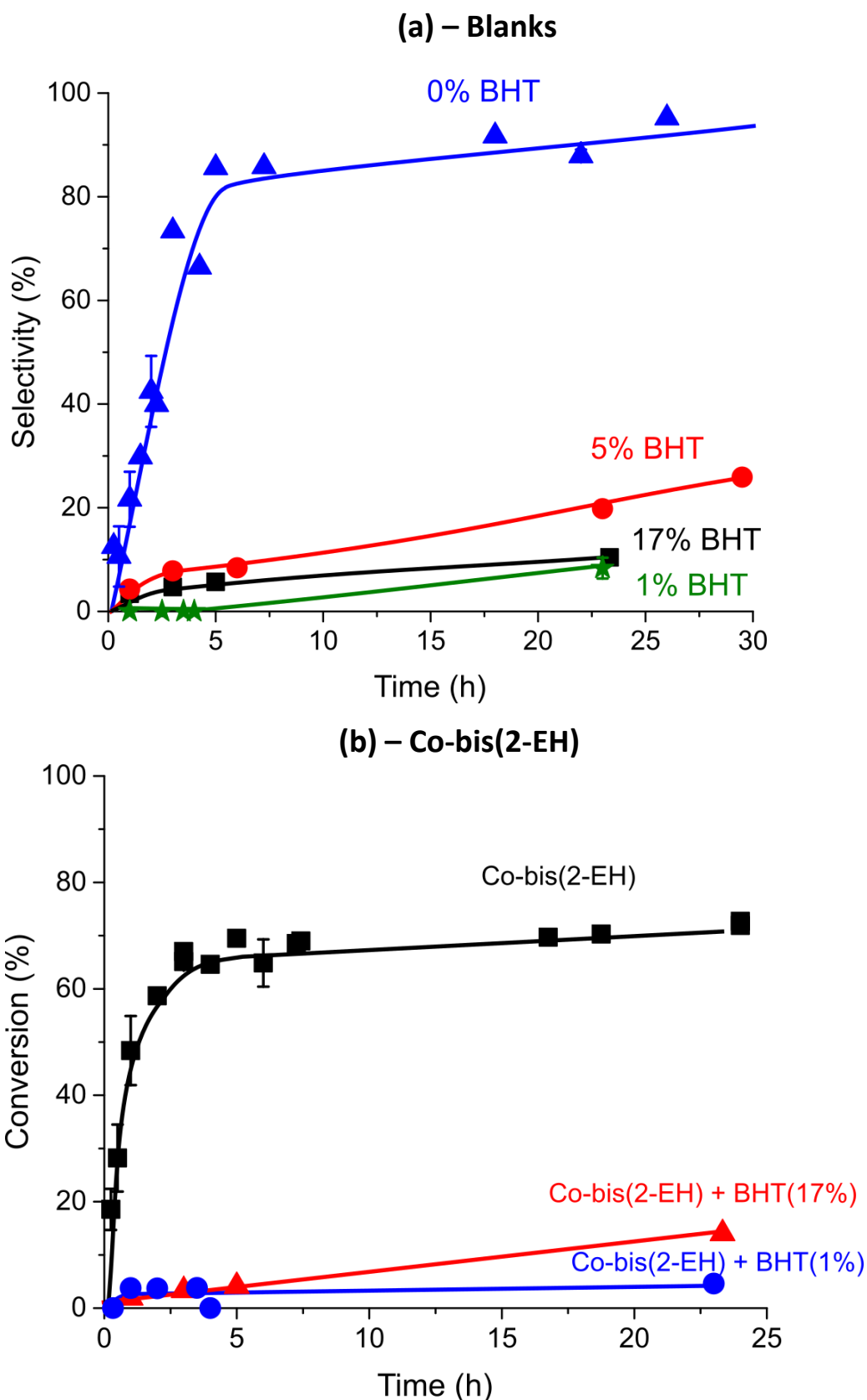
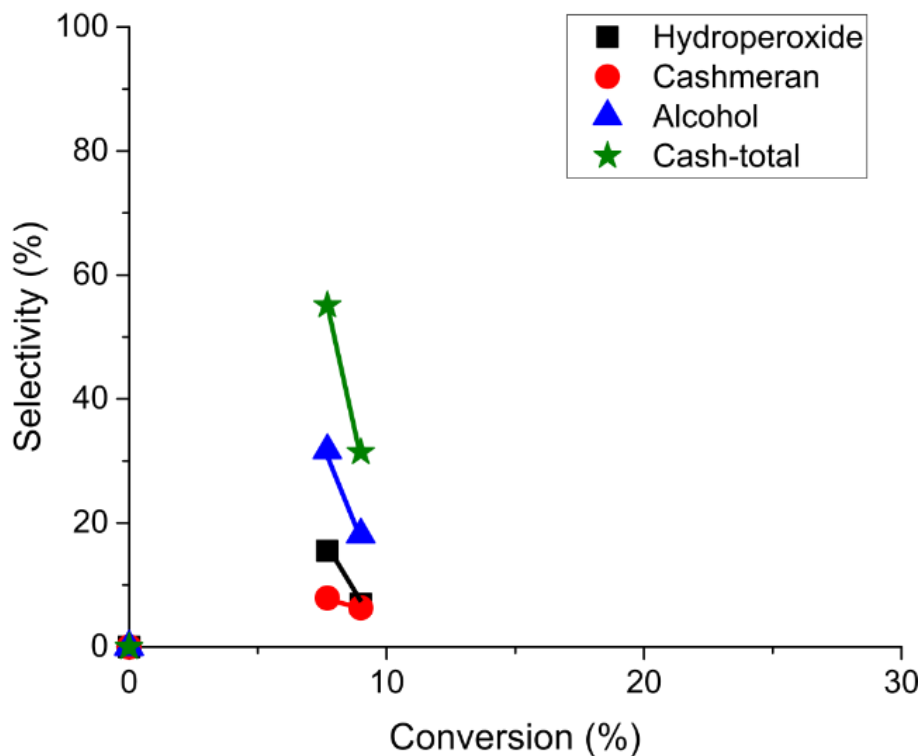


**Figure 3.16.** Conversion against time for reactions with BHT. (a): Blank reaction and (b): Reaction with Co-bis(2-ethylhexanoate). Conditions: THPMI (10 mL), hexadecane (1 mL), 110 °C, 0.5 -30 h, Co-bis(2-ethylhexanoate) (13 mg/0.15 wt%) (b only), BHT (0.06 – 1.51 g/0.7 wt % – 17.4 wt%), air residence time (0.11 min), 900 rpm. (a) Blanks: Data for the 0 % BHT plot was from 5 separate reactions, data for the 1 % BHT was from 2 separate reactions, and data from the 5 and 17 % BHT plots were from 1 reaction each. (b) Co-bis(2-EH): data for the 0% BHT plot was from 6 separate reactions, data from the 17 % BHT reaction was from 1 reaction, and data from the 1 % BHT plot was from 2 separate reactions.

(a) – Blank + 1 wt% BHT



(b) – Blank + 5 wt%

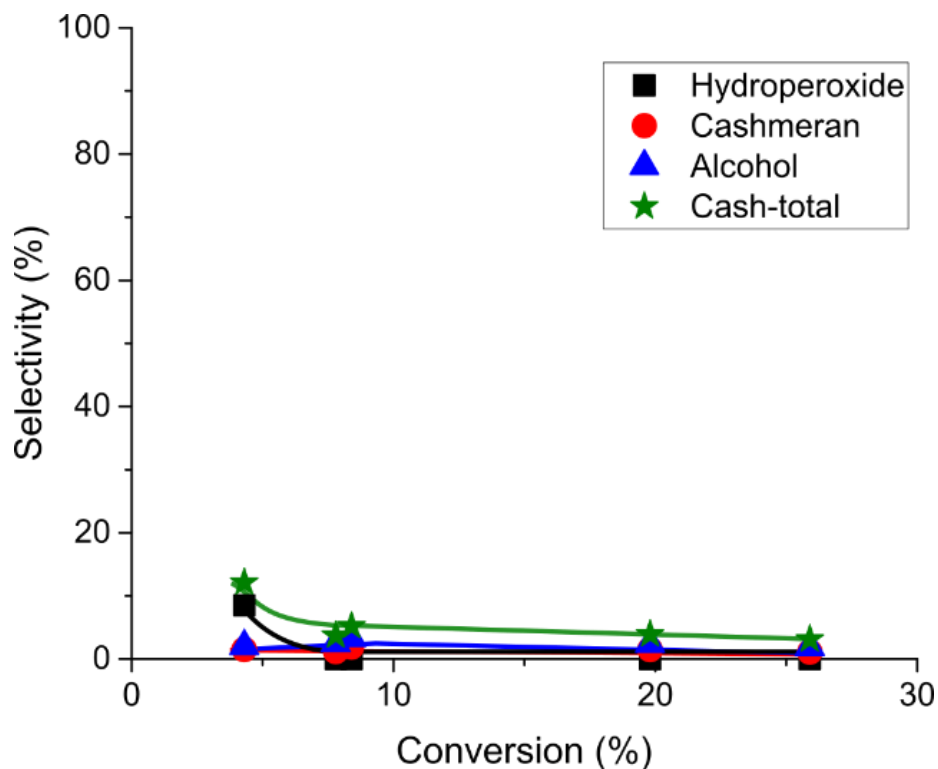


**Figure 3.17.** Selectivity against conversion for reactions with added BHT. (a): Blank with 1 wt% BHT. (b): Blank with 5 wt% BHT. (c): Co-bis(2-EH) with 17 % BHT. Conditions: THPMI (10 mL), hexadecane (1 mL), 110 °C, 1-30 h, Co-bis(2-ethylhexanoate) (13 mg/0.15 wt%), BHT (0.06 – 0.42 g/0.7 wt% – 4.8 wt%), air residence time (0.11 min), 900 rpm. (a) Blank + 1 wt% BHT: data taken from 2 separate reactions,. (b) Blank + 5 wt% BHT data taken from 1 reaction.

### (a) – Co-bis(2-EH) + 17 wt% BHT

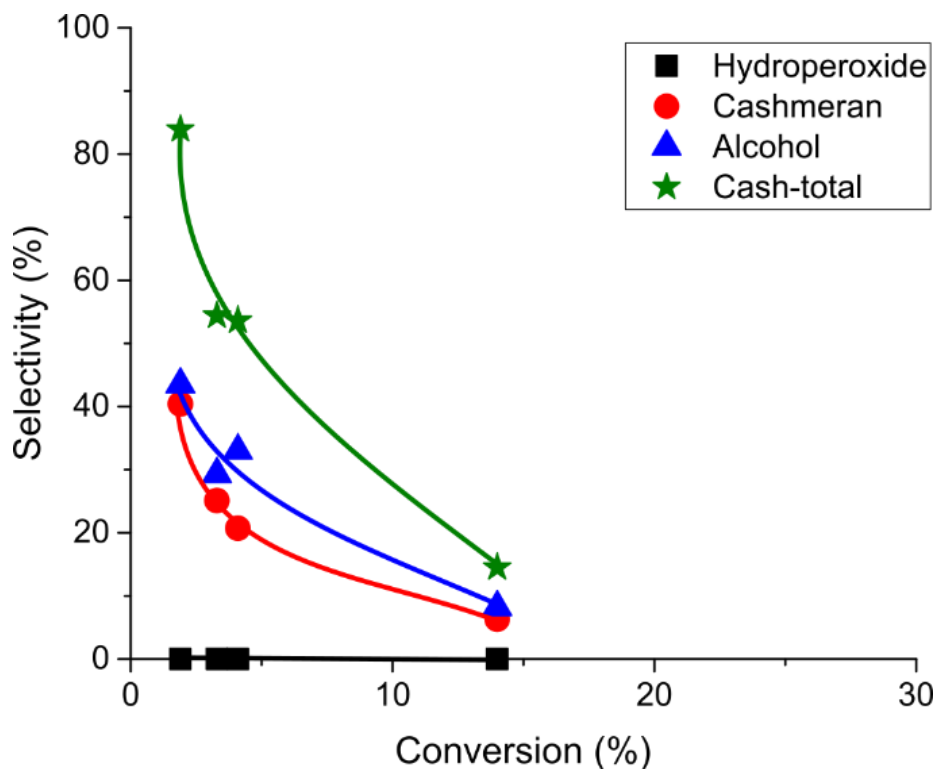


**Figure 3.18.** Selectivity against conversion for reaction catalysed by Co-bis(2-EH) with added BHT. Conditions: THPMI (10 mL), hexadecane (1 mL), 110 °C, 1-30 h, Co-bis(2-ethylhexanoate) (13 mg/0.15 wt%), BHT (1.51 g/17.4 wt%), air residence time (0.11 min), 900 rpm. Data taken from 1 reaction.

## 3.8 Separating Ligand Effects from Metal Effects in Co-bis(2-ethylhexanoate)

The solution of Co-bis(2-EH) utilised in this project was 51 % active material dissolved in naphtha (hydrogenated, heavy, 30 – 47 %) and 2-ethylhexanoic acid (3 – 10 %). It is known that pH will affect the reaction and so it is important to determine what effect the excess ligand (2-

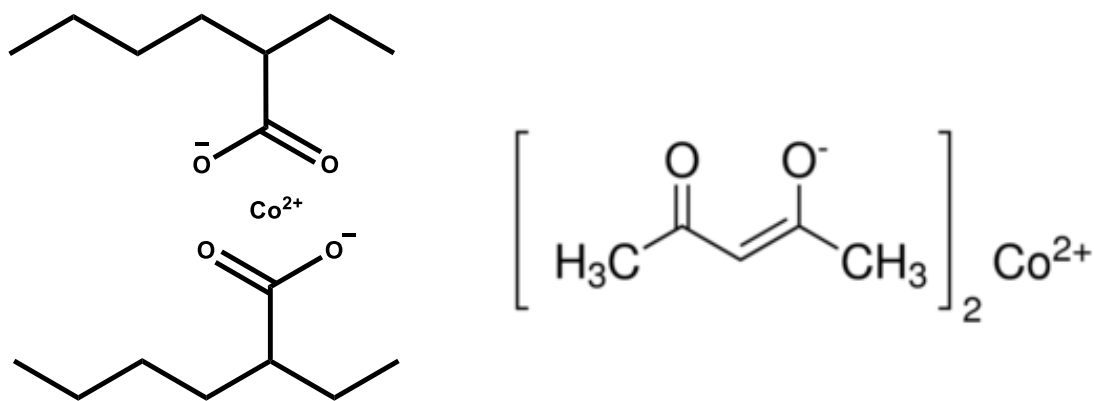


**Figure 3.19.** Left: Co-bis(2-ethylhexanoate) and right: Co(acac)<sub>2</sub>.

ethylhexanoic acid) plays in the reaction, if any. Two experiments were conducted to investigate the relative, individual effects that cobalt and 2-ethylhexanoic acid, have on the reaction. For the first reaction Co-bis(2-ethylhexanoate) was replaced by with cobalt(II) acetylacetonate ( $\text{Co}(\text{acac})_2$ ). This results in a reaction mixture where  $\text{Co}^{2+}$  ions were still present, however without the added effects from the excess 2-ethylhexanoic acid in the standard catalytic solution. In the second reaction Co-bis(2-ethylhexanoate) was replaced by 2-ethylhexanoic acid, to determine the individual effect the excess ligand has on the reaction.

By replacing Co-bis(2-EH) with  $\text{Co}(\text{acac})_2$ , the rate of reaction was not significantly affected, and the quenching effect was still observed (Figure 3.20). This is to be expected, as the  $\text{Co}^{2+}$  ions in  $\text{Co}(\text{acac})_2$  can initiate oxidation in the same way as Co-bis(2-EH). The result provided further evidence that cobalt ions play an integral role in the quenching of the reaction as discussed in section (3.6). When Co-bis(2-EH) is replaced with a low loading of 2-ethylhexanoic acid the conversion over time is more comparable to a blank reaction. The initial rate of reaction is faster with the acid, which suggests the acid is capable of initiating oxidation. However unlike the reactions with cobalt present, no reaching quenching is observed, again evidencing the role of cobalt in reaction quenching.

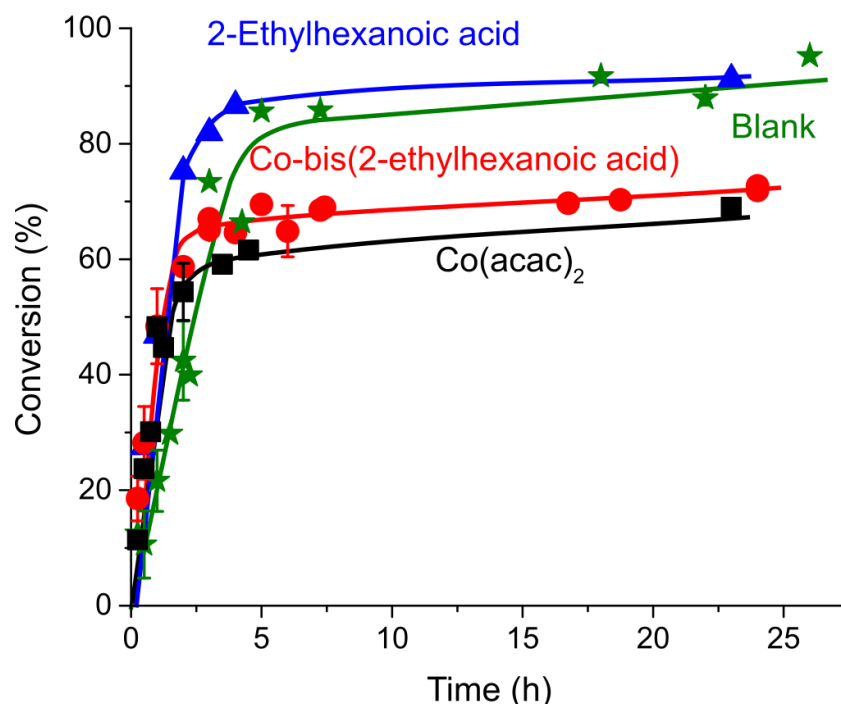


**Figure 3.20.** Conversion against time for reactions with 2-ethylhexanoic acid and  $\text{Co}(\text{acac})_2$  as the catalysts, compared to the standard blank and catalysed reactions. Conditions: THPMI (10 mL), hexadecane (1 mL), 110 °C, 0.25-30 h, Co-bis(2-ethylhexanoate) (13 mg/0.15 wt%) or  $\text{Co}(\text{acac})_2$  (17 mg/0.19 wt%) or 2-ethylhexanoic acid (11 mg/0.13 wt%) or no catalyst for blank, air residence time (0.11 min), 900 rpm. Data for the blank plot was taken from 5 separate reactions, data for the Co-bis(2-ethylhexanoic acid) plot was taken from 6 separate reactions, data for the 2-ethylhexanoic acid plot was taken from 1 reaction, and data for the  $\text{Co}(\text{acac})_2$  plot was taken from 2 separate reactions.

The effect of  $\text{Co}(\text{acac})_2$  on reaction selectivity (Figure 3.21) was minimal when compared to the standard catalysed reaction with  $\text{Co-bis}(2\text{-EH})$  (Figure 3.5b).  $\text{Co}(\text{acac})_2$  provided a similar overall Cash-total selectivity of 65 – 80 % at a conversion range of 20 – 60 %. The Cashmeran to Cashmeran-alcohol ratio was also similar, with a near 1:1 ratio that increased to 2:1 as the reaction proceeded to 60 % conversion. The level of THPMI-HP detected when using  $\text{Co}(\text{acac})_2$  was close to 0 % throughout the reaction, similar to the reaction with  $\text{Co-bis}(2\text{-EH})$ . These results suggest that the three main benefits of using  $\text{Co-bis}(2\text{-EH})$  (increase in overall selectivity, greater Cashmeran to Cashmeran-alcohol ratio and low levels of THPMI-HP) are a result of the cobalt in the catalyst. It should be noted however that  $\text{Co-bis}(2\text{-EH})$  is more soluble in THPMI than  $\text{Co}(\text{acac})_2$ , which is only soluble at elevated temperature.

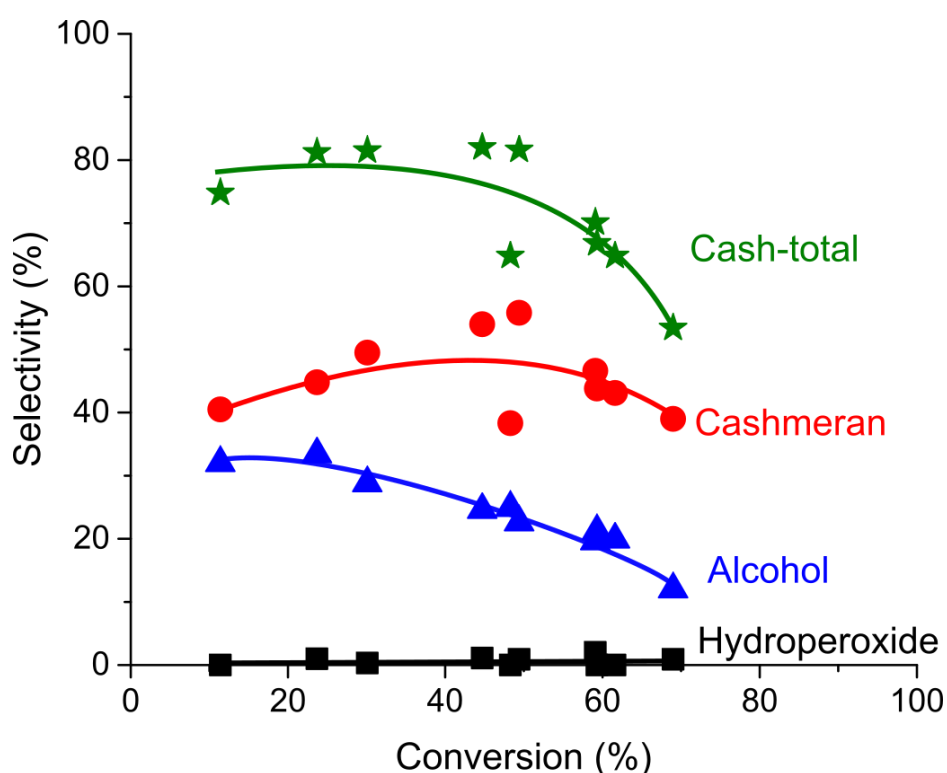


**Figure 3.21.** Selectivity against conversion for the oxidation of THPMI with  $\text{Co}(\text{acac})_2$ . Conditions: THPMI (10 ml), Hexadecane (1 ml), 110 °C, 0.5-24 h,  $\text{Co}(\text{acac})_2$  (17 mg/0.19 wt%), air residence time (0.11 min), 900 rpm. Data was taken from 2 separate reactions.

The similarities between the blank reaction and the reaction with 2-ethylhexanoic acid present were not as extensive as the similarities between the two cobalt catalysts described above. 2-ethylhexanoic acid demonstrated acid catalysed dehydration of THPMI-HP, which varied between 2 – 11 % throughout the reaction (Figure 3.21). This is a lower concentration compared to the blank reaction where between 30 - 55 % THPMI-HP was observed at below 50 % conversion (Figure 3.5a). The average Cash-total selectivity observed in both reactions is similar with approximately 60 % Cash-total observed at 50 % conversion, however the trends are different. In the blank reaction a steady decline from 70 to 45 % Cash-total was observed

from 10 to 75 % conversion, however with 2-ethylhexanoic acid a steady 55 – 60 % Cash-total was observed from 20 to 80 % conversion. In both reactions a sharp decline in Cash-total was observed after 75 % conversion, which is primarily a result of alcohol over-reaction. Cashmeran concentration rises in both reactions as THPMI-HP and alcohol molecules oxidise further.

This study demonstrated that both cobalt and 2-ethylhexanoic acid impact the oxidation of THPMI, with both species decomposing THPMI-HP, however the effect of 2-ethylhexanoic acid does not provide any increase in Cash-total selectivity. The effect of the presence of cobalt was more significant, with a more rapid decomposition of THPMI-HP, which improved the Cash-total selectivity by 10 – 20 %. Cobalt also increases the Cashmeran to Cashmeran-alcohol ratio, which does not occur with 2-ethylhexanoic acid. To conclude, although 2-ethylhexanoic acid does have noticeable effects on the reaction, these effects were dwarfed by the effects of cobalt and the impacts of the industrial catalyst on the reaction are a result of Co-bis(2-EH) and not the excess 2-ethylhexanoate.

### 3.9 Conclusions

The use of cobalt salts as catalysts and initiators for oxidation reactions has been known for decades. The effects of cobalt on the oxidation of alkanes are well documented, however its effects on alkene oxidation are less well known. This work has demonstrated that in the case of THPMI oxidation to Cashmeran and Cashmeran-alcohol, Co-bis(2-EH) benefits the process in three clear ways. Firstly, it initiates the reaction even at temperatures below those at which significant autoxidation take place. Secondly, it improves selectivity by increasing the Cash-total selectivity by 16 % at 50 % conversion (compared to the blank reaction), and by increasing the Cashmeran to Cashmeran-alcohol ratio substantially. This effect occurs whilst the level of THPMI-HP is suppressed to being close to 0 %. Thirdly, Co-bis(2-EH) will quench the reaction if a large enough catalyst loading is applied, this effect is also enhanced at higher reaction temperatures. The improvement in overall selectivity is likely linked to the suppression of THPMI-HP formation, as hydroperoxide molecules are susceptible to homolytic cleavage which could lead to the formation of undesired products. The effect of Co-bis(2-EH) directing the reaction towards Cashmeran as a product is due to an enhancement in the rate of one or more of the reaction routes **3**, **4** or **5** (Scheme 3.2). It is likely to be the oxidation of Cashmeran-alcohol (route **3**) as this is observed in the literature<sup>16,17</sup> and evidence is observed of oxidation of HCA into CA. However, it should not

be dismissed that dehydration of THPMI-HP or Russell termination (routes 4 and 5 respectively) have been enhanced also.

The selectivity of the reaction decreases with conversion, as expected kinetically. Thus far, only three over-oxidation products have been identified, HCA, HC and CK (Scheme 3.3), all containing two extra oxygen atoms, relative to THPMI. Co-bis(2-EH) seems to oxidise HCA into CK, further evidencing its role as an alcohol oxidation catalyst. However, the introduction of the catalyst does not seem to decrease the overall selectivity towards over-oxidation products. If the blank reaction is left to run for a prolonged period, these over-oxidation products start to react further. The majority of unwanted products are likely a result of over-oxidation and so to improve selectivity this must be suppressed. The other detected, undesired product is THPMI-epoxide, which is detected at very low concentrations in both reactions with and without Co-bis(2-EH) but approximately 1 % less when Co-bis(2-EH) is present, at 50 % conversion, accounting for a very small amount of the improvement observed when Co-bis(2-EH) is used.

Decreasing the temperature generally had little effect on the blank reaction apart from shutting off autoxidation at lower temperature. The selectivity of the blank reaction was slightly improved when the temperature was increased from 70 to 110 °C. The catalysed reaction was even less affected by a reduction in temperature. Co-bis(2-EH) is capable of initiating oxidation below autoxidation temperatures, but the overall Cash-total selectivity trend is the same regardless of temperature. However, as temperature was increased from 50 to 130 °C, the Cashmeran to Cashmeran-alcohol ratio increased, which is expected to be caused by more rapid Cashmeran-alcohol oxidation into Cashmeran. The effects of temperature were subtle, likely due to products resulting from radical mechanisms that are not particularly temperature sensitive.

For reactions at both 70 and 110 °C altering the Co-bis(2-EH) affected the quenching of the reaction. Increasing the Co-bis(2-EH) loading from 0.15 to 1.2 or 1.3 wt% caused the reaction to quench much more rapidly and at a much lower conversion. When the loadings were reduced to 0.09 wt%, the reaction lasted for slightly longer and so a marginally greater conversion was observed. These results confirm that cobalt is involved in the quenching mechanism and provide evidence for the theory that free  $\text{Co}^{2+}$  in the reaction medium can trigger a termination reaction if the concentration is large enough.<sup>28</sup>

Both blank and catalysed reactions were confirmed to be radical in nature as they were both quenched by small loadings of BHT. For the blank reaction any conversion that was observed did not result in desired products and so selectivity was 0 %, and it is currently

unclear which products do form. In the case of the catalysed reaction selectivity was also suppressed significantly, but to a lesser extent than the blank reaction. These results suggest that suppressing the radical oxidation pathways directs oxidation away from desired allylic oxidation products.

When Co-bis(2-EH) was replaced with Co(acac)<sub>2</sub>, little change was observed in the reaction. The rate of reaction was still rapid, as was the rate of reaction quenching. The selectivity was not distinctly different either. This showed that even in the absence of the excess ligand, 2-ethylhexanoic acid, Co<sup>2+</sup> still performs the functions that make it a desirable catalyst for this reaction. It was noted that adding 2-ethylhexanoic acid does affect the reaction by increasing the rate of reaction and by decomposition of THPMI-HP, however at a lower rate than Co<sup>2+</sup>. This shows that 2-ethylhexanoic acid does influence the reaction, but these effects are masked by the more significant effects of Co<sup>2+</sup>.

The work conducted in this chapter has enhanced the understanding of the subtle, yet important, role Co-bis(2-EH) plays in the oxidation of THPMI into Cashmeran. By promoting the rapid decomposition of THPMI-HP into Cashmeran and Cashmeran-alcohol, higher selectivities are observed and a faster rate of reaction is achieved if mass transfer is not a limiting factor. Reaction quenching has been found to be proportional to cobalt loading and temperature. Reaction temperature was also found to have a subtle effect on the Cashmeran to Cashmeran-alcohol ratio and the effect of the excess ligand was found to be negligible compared to the effect of the presence of Co<sup>2+</sup>. To discover more effective catalysts, these features need to be understood, as do the limitations of the catalysts.

### 3.10 References

- 1 European Patent Office, EP2305628, 2011.
- 2 B. P. C. Hereijgers and B. M. Weckhuysen, *J. Catal.*, 2010, **270**, 16–25.
- 3 A. Ramanathan, M. S. Hamdy, R. Parton, T. Maschmeyer, J. C. Jansen and U. Hanefeld, *Appl. Catal. A Gen.*, 2009, **355**, 78–82.
- 4 E. J. Silke, W. J. Pitz, C. K. Westbrook and M. Ribaucour, *J. Phys. Chem.*, 2007, **111**, 3761–3775.
- 5 B. Modén, B. Zhan, J. Dakka, J. G. Santiesteban and E. Iglesia, *J. Catal.*, 2006, **239**, 390–

401.

- 6 I. Hermans, J. Peeters and P. A. Jacobs, *J. Phys. Chem.*, 2008, **112**, 1747–1753.
- 7 I. Hermans, P. A. Jacobs and J. Peeters, *Chem. - A Eur. J.*, 2007, **13**, 754–761.
- 8 I. Hermans, P. A. Jacobs and J. Peeters, *Chem. - A Eur. J.*, 2006, **12**, 4229–4240.
- 9 P. Bujak, P. Bartczak and J. Polanski, *J. Catal.*, 2012, **295**, 15–21.
- 10 M. S. Hamdy, *Microporous Mesoporous Mater.*, 2016, **220**, 81–87.
- 11 O. Rogers, S. Pattison, J. Macginley, S. H. Taylor and G. J. Hutchings, *Catalysts*, 2018, **8**, 311.
- 12 R. Zhang and R. Tang, *J. Mater. Sci.*, 2016, **51**, 5802–5810.
- 13 A. Reza, S. Mosazadeh and F. Ashouri, *J. Colloid Interface Sci.*, 2017, **506**, 10–26.
- 14 V. B. Golovko, D. S. Ovoshchnikov, B. G. Donoeva and B. E. Williamson, *Catal. Sci. Technol.*, 2014, **4**, 752–757.
- 15 I. M. Denekamp, M. Antens, T. K. Slot and G. Rothenberg, *ChemCatChem*, 2018, **10**, 1035–1041.
- 16 R. A. Sheldon and J. K. Kochi, in *Metal-catalyzed Oxidations of Organic Compounds*, Academic Press, 1981, pp. 353–356.
- 17 Great Britain Patent Office, GB1275699A, 1972.
- 18 United States Patent Office, 2869989, 1959.
- 19 R. A. Sheldon and J. K. Kochi, in *Metal-catalyzed Oxidations of Organic Compounds*, Academic Press, 1981, pp. 350–352.
- 20 U. N. Gupta, N. F. Dummer, S. Pattison, R. L. Jenkins, D. W. Knight, D. Bethell and G. J. Hutchings, *Catal. Letters*, 2015, **145**, 689–696.

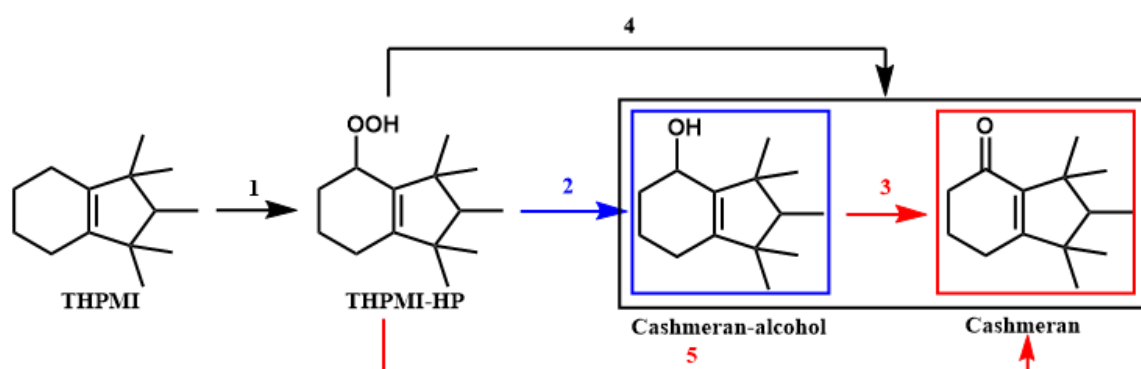
- 21 G. A. Russell, *J. Am. Chem. Soc.*, 1957, **79**, 3871–3872.
- 22 A. Onopchenko and J. G. D. Schulz, *J. Organic Chem.*, 1973, **38**, 3729–3733.
- 23 R. A. Sheldon and J. K. Kochi, in *Metal-catalyzed Oxidations of Organic Compounds*, Academic Press, 1981, p. 347.
- 24 Y. Kamiya and K. U. Ingold, *Can. J. Chem.*, 1964, **42**, 2424–2433.
- 25 Y. Kamiya, S. Beaton, A. Lafortune and U. Ingold, *Can. J. Chem.*, 1963, **41**, 2020–2033.
- 26 Y. Kamiya, S. Beaton, A. Lafortune and K. U. Ingold, *Can. J. Chem.*, 1963, **41**, 2034–2053.
- 27 Y. Kamiya and K. U. Ingold, *Can. J. Chem.*, 1963, **42**, 1027–1043.
- 28 J. F. Black, *J. Am. Chem. Soc.*, 1978, **100**, 527–535.
- 29 T. Sato, Y. Hamada, M. Sumikawa, S. Araki and H. Yamamoto, *Ind. Eng. Chem. Res.*, 2014, **53**, 19331–19337.
- 30 T. H. Ngo and A. Schumpe, *Int. J. Chem. Eng.*, 2012, **2012**, 1–7.
- 31 R. K. Jensen, S. Korcek, L. R. Mahoney and M. Zinbo, *J. Am. Chem. Soc.*, 1979, **101**, 7574–7584.
- 32 P. George and A. Robertson, *Trans. Faraday Soc.*, 1946, **42**, 217–224.
- 33 S. M. Mahajani, M. M. Sharma and T. Sridhar, *Chem. Eng. Sci.*, 1999, **54**, 3967–3976.
- 34 J. W. M. Stebman, S. Kaae and P. J. Hoftyzer, *Chem. Eng. Sci.*, 1961, **14**, 139–149.
- 35 R. A. Sheldon and J. K. Kochi, in *Metal-catalyzed Oxidations of Organic Compounds*, Academic Press, 1981, pp. 345–346.
- 36 A. Onopchenko and J. G. D. Schulz, *J. Organic Chem.*, 1973, **38**, 909–912.
- 37 Y. Duh, C. Kao, H. Hwang and W. W. Lee, *Process Saf. Environ. Prot.*, 1998, **76**, 271–276.
- 38 M. J. Pilling, *Pure Appl. Chem.*, 1992, **64**, 1473–1480.

- 39 A. I. Vitvitskii, *Theor. Exp. Chem.*, 1969, **5**, 276–278.
- 40 J. Clayden, N. Greeves and S. Warren, in *Organic Chemistry*, Oxford Univeristy Press, 2nd edn., 2012, pp. 974–975.
- 41 F. P. da Silva, R. V. Goncalves and L. M. Rossi, *J. Mol. Catal. A Chem.*, 2017, **426**, 534–541.

# 4 Investigating Alternative Catalysts for the Oxidation of THPMI

## 4.1 Introduction

The work in chapter 3 demonstrated how Co-bis(2-EH) improves the overall selectivity of the oxidation of THPMI to Cashmeran, compared to the equivalent reaction with no added catalyst. The catalyst rapidly converts the hydroperoxide intermediate (THPMI-HP) into the desired products (Cashmeran-alcohol and Cashmeran) (Scheme 4.1) improving the Cash-total selectivity. The overall process is, at least partially, radically mediated and so selectivity control is limited,<sup>1</sup> as discussed in section 1.5 and demonstrated in section 0. If Co-bis(2-EH) can be replaced with a catalyst which operates by a non-radical, heterolytic oxygen activation then perhaps more control can be attained over the selectivity of the reaction. Heterogeneous catalysts may also avoid the reaction quenching phenomena described in the previous chapter (3.5 and 3.6) and detailed in the literature (1.6). Previous works describing heterogeneous catalysts tested for the oxidation of cyclohexene have been described earlier in the report (1.7) and provide some basis for the catalysts tested here. This chapter describes the production and testing of several catalysts for the oxidation of THPMI including cobalt oxide supported on aminated silica (CoO/SiO<sub>2</sub>), bulk cobalt(II/III) oxide (Co<sub>3</sub>O<sub>4</sub>) and Molybdenum Blue. Studies on



**Scheme 4.1.** Reaction route for the oxidation of THPMI into the desired allylic oxidation products. Route 1 represents the formation of the initial intermediate, THPMI-HP, by the oxidation of the starting material, THPMI. Route 2 represents the breakdown of THPMI-HP into Cashmeran-alcohol. Route 3 represents the oxidation of Cashmeran-alcohol to Cashmeran. Route 4 represents a Russell termination where two THPMI-HP molecules form one Cashmeran-alcohol and one Cashmeran molecule. Route 5 represents the conversion of THPMI-HP to Cashmeran, directly.

the leaching of cobalt were also conducted and some acid catalysts were tested, which is described below.

## 4.2 Acid Catalysts

It is known that acids are capable of catalysing the decomposition of organic hydroperoxides<sup>2,3</sup> and so could provide a cheap way of directly decomposing THPMI-HP into Cashmeran *via* a dehydration reaction. Amberlyst-15 was first tested at 110 °C, with the aim that it would decompose the large amounts of THPMI-HP which are produced at this temperature, directly into Cashmeran, without the need for Co-bis(2-EH). Amberlyst-15 is a polystyrene based ion exchange resin with highly acidic sulfonic groups, and has previously been utilised in the decomposition of cumene hydroperoxide.<sup>4</sup>

Surprisingly, when tested, the solid acid had a significant effect on conversion as well as selectivity (Figure 4.1). Conversion was dampened, suggesting some radical scavenging or termination-catalysing properties of Amberlyst-15, however the selectivity at this conversion was also poor. The undesired products that were formed from the THPMI are currently unidentified as they do not appear on GC traces, suggesting these are either highly oxidised, heavy polymerised, or gaseous species.

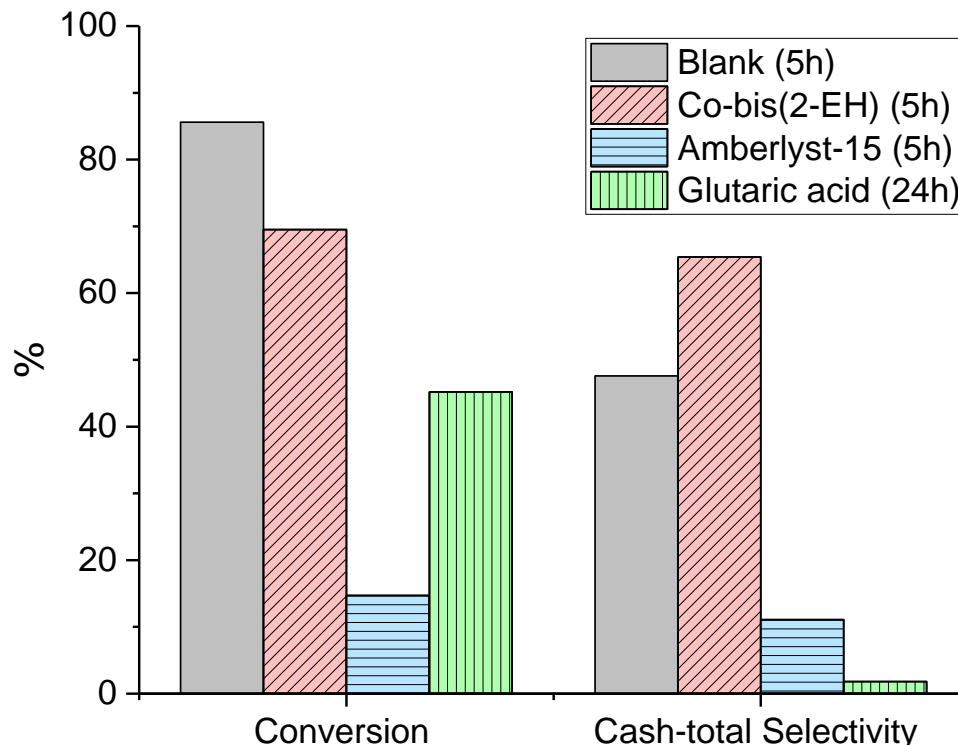


**Figure 4.1.** Conversion and selectivity for reactions with Amberlyst-15 and glutaric acid, compared to standard blank and catalysed reactions. Conditions: THPMI (10 ml), hexadecane (1 mL), Co-bis(2-ethylhexanoate) (13 mg/0.15 wt%) or Amberlyst-15 (150 mg/1.7 wt%) or Glutaric acid (772 mg/8.9 wt%) or no catalyst for blank, 110 °C, 5 or 24 h, air residence time (0.11 min), 900 rpm.

Following the poor results when using Amberlyst-15, a similar experiment was designed using glutaric acid as the catalyst. Glutaric acid was chosen as it is soluble in the THPMI reaction mixture. As with the Amberlyst-15 test, glutaric acid was added to the blank reaction at 110 °C to assess whether it would catalyse the decomposition of THPMI-HP into Cashmeran. The result was very similar to Amberlyst-15, where both conversion and selectivity were suppressed considerably relative to the blank reaction (Figure 4.1). The conversion observed was largely made up of unknown products, which remain uncharacterised. No hydroperoxide was detected in the test with glutaric acid, suggesting that it does catalyse the decomposition of THPMI-HP, however it also catalysed other reaction routes that direct away from the desired products. With evidence from two separate acid reactions, it can be suggested that the acid itself is suppressing THPMI oxidation.. It is possible that the acid species are acting as radical scavengers in a similar manner to the antioxidant, ascorbic acid.<sup>5</sup> It is also possible that although acid does catalyse the decomposition of THPMI, it does it in a way that terminates the chain radical mechanism and so drastically reduces the rate of reaction.

To confirm the theory that acid-catalysed condensation is occurring, a third experiment was conducted, where a post reaction solution was treated with butyric acid. Butyric acid was chosen for this reaction as, unlike glutaric acid, it can be observed by GC analysis. Under the standard oxidation conditions, a reaction was performed with  $\text{Co}_3\text{O}_4$  as the catalyst for 5 h, as it was known that this would produce a large amount of THPMI-HP (section 0). The reaction was cooled to room temperature after 5 h of reaction and the air flow was replaced with a nitrogen flow to avoid further oxidation. An excess of butyric acid (11:2 ratio relative to THPMI-HP) was added to the solution and stirred for 15 minutes. Almost half of the THPMI-HP was converted into Cashmeran-alcohol, and the level of Cashmeran and all other products was unaffected (Figure 4.2). This demonstrates that a low pH environment will decompose THPMI-HP, however into

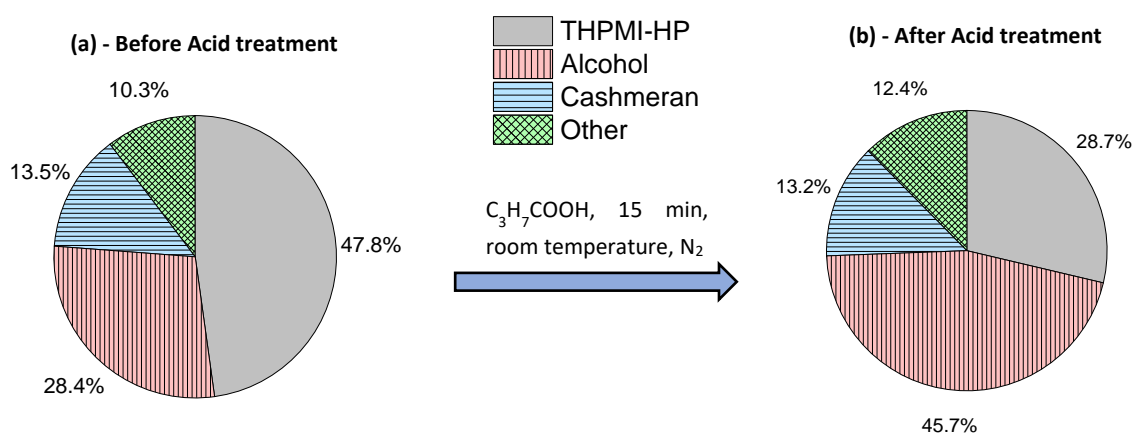


**Figure 4.2.** Before and after the addition of butyric acid to the post reaction mixture. Reaction conditions to produce sample (a): THPMI (10 ml), hexadecane (1 ml), 70 °C, 5 h,  $\text{Co}_3\text{O}_4$  (100 mg/1.15 wt%), air residence time (0.11 min), 900 rpm. Acid treatment conditions to convert (a) to (b): reaction mixture (a), butyric acid (5.87 g), 15 min, flowing  $\text{N}_2$ , room temperature.

Cashmeran-alcohol and not Cashmeran. This transformation is supported in the literature, where it has been suggested that, for the decomposition of cyclohexane hydroperoxide (CHHP), acids can catalyse the transformation of a CHHP molecule into cyclohexanol, with cyclohexanone acting as a co-catalyst *via* a radical mechanism.<sup>3</sup>

The fourth acid test was conducted with 2-ethylhexanoic acid (2-EHA), which was introduced in section 3.8 as it is the excess ligand present in the industrial catalyst. The study concluded that a very low loading of acid will cause decomposition of THPMI-HP, but will not affect Cash-total selectivity relative to the blank reaction. In this study greater loadings of 2-ethylhexanoic acid were used. When only 10 mg of 2-EHA was used, no quenching was observed, and conversion of THPMI follows a similar trend to the blank reaction (3.4). When larger loadings of 110 and 770 mg were used, the initial rate of reaction was similar, however the reaction seemed to quench after approximately 4 h (Figure 4.3). Similar selectivity trends were observed for all three loadings of 2-EHA; 0 – 10 % THPMI-HP was observed throughout the reaction and a Cash-total of 60 – 70 % was consistent until 70 – 80 % conversion, where selectivity dropped off significantly. Selectivity to Cashmeran was initially low and then increased as the reaction proceeded with the opposite trend being true for the alcohol (Figure 4.5, Figure 4.4, and Figure 4.6). The effect of 2-EHA was significantly milder than the effect observed with Amberlyst-15 or glutaric acid. It is proposed that this is due to 2-EHA acid being a weaker acid and so reducing

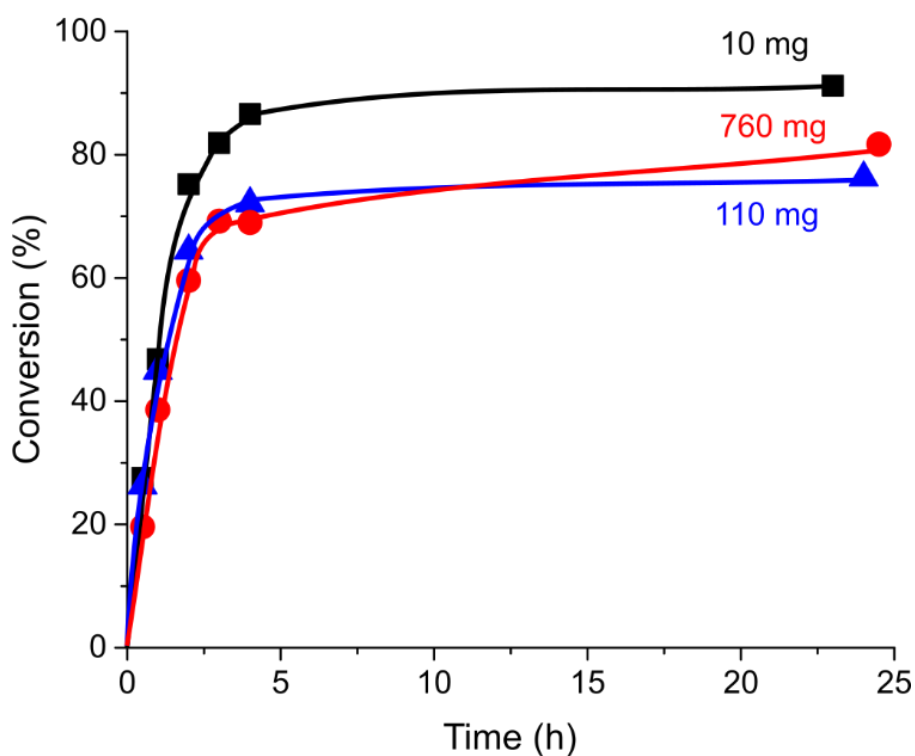


**Figure 4.3.** Conversion against time for reactions with 2-ethylhexanoic acid as the catalyst. Conditions: THPMI (10 ml), hexadecane (1 ml), 110 °C, 0.5 - 24.5 h, 2-ethylhexanoic acid (10 - 760 mg/0.12 - 8.77 wt%), air residence time (0.11 min), 900 rpm. All data plots were taken from 1 reaction each.

the pH of the reaction less significantly. However, the pH of these reactions were not monitored and so this would need to be confirmed.

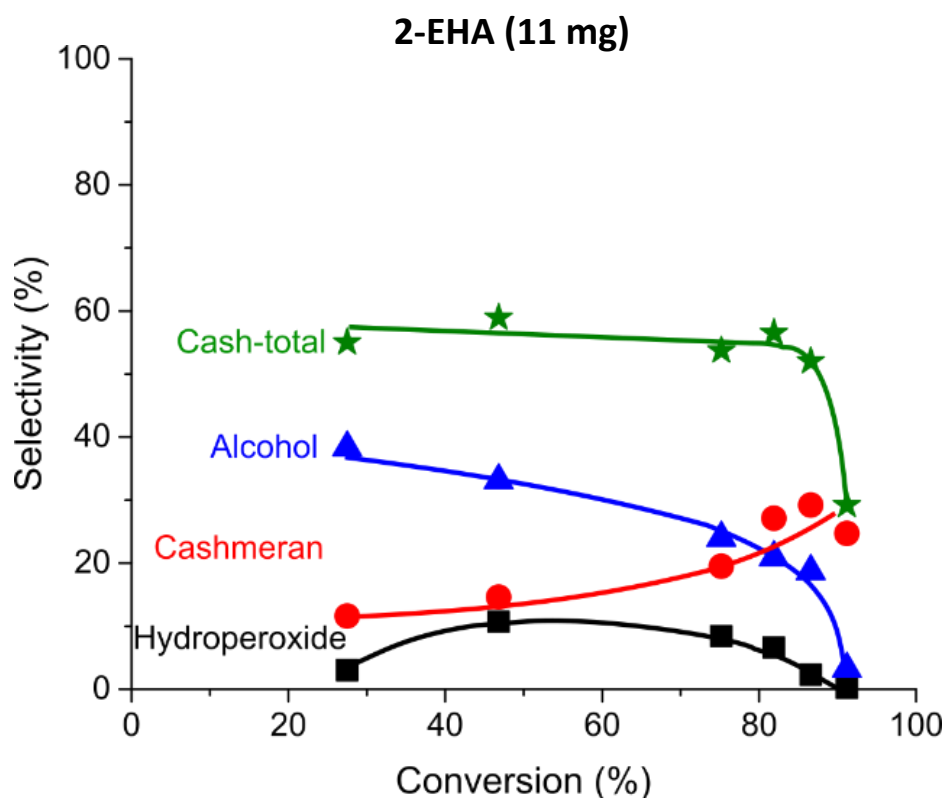


**Figure 4.4.** Selectivity against conversion for a reaction with 2-ethylhexanoic acid as the catalyst. Conditions: THPMI (10 ml), hexadecane (1 ml), 110 °C, 0.5 - 23 h, 2-ethylhexanoic acid (11 mg/0.13 wt%), air residence time (0.11 min), 900 rpm. Data was taken from 1 reaction.

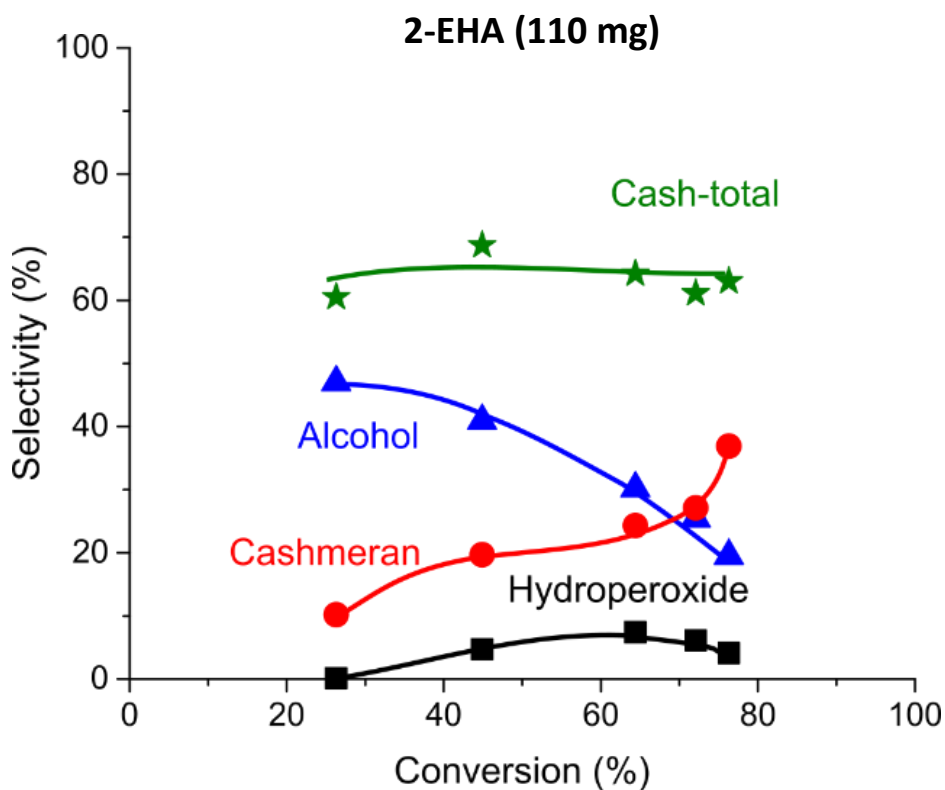


**Figure 4.5.** Selectivity against conversion for a reaction with 2-ethylhexanoic acid as the catalyst. Conditions: THPMI (10 ml), hexadecane (1 ml), 110 °C, 0.5 - 24 h, 2-ethylhexanoic acid (110 mg/1.26 wt%), air residence time (0.11 min), 900 rpm. Data was taken from 1 reaction.

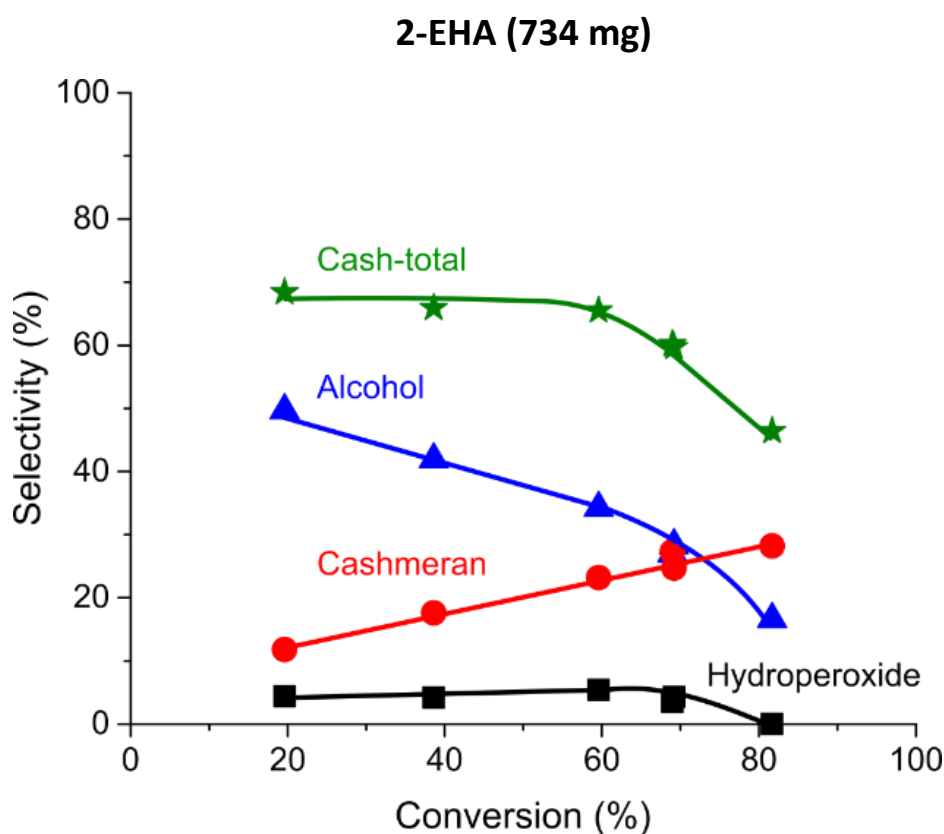


**Figure 4.6.** Selectivity against conversion for a reaction with 2-ethylhexanoic acid as the catalyst. Conditions: THPMI (10 ml), hexadecane (1 ml), 110 °C, 0.5 - 24.5 h, 2-ethylhexanoic acid (734 mg/8.46 wt%), air residence time (0.11 min), 900 rpm. Data was taken from 1 reaction.

Acids had varied effects on the oxidation of THPMI into Cashmeran and a more detailed study on the effect of pH on the reaction is required. When Amberlyst-15 or glutaric acid were added to the reaction, conversion was suppressed, and selectivity dropped significantly. If butyric acid is added to a post reaction solution, then THPMI-HP will react to form Cashmeran-alcohol at room temperature. When 2-ethylhexanoic acid was added to the reaction more subtle effects were observed, with levels of THPMI-HP reducing to <10 %, but with a largely similar selectivity to that achieved in a blank reaction. A moderate quenching effect was also observed when the 2-ethylhexanoic loading was greater than 1 wt%. These results suggest that when a relatively strong acid is in solution during the reaction, it will cause termination of the radical oxidation reaction and slow the rate of reaction dramatically. This change also results in undesired products forming, possibly through acid catalysed reactions of the desired products. When a milder acid is added to the reaction it can react with THPMI-HP, however this does not result in an improvement in selectivity to allylic oxidation products. The addition of acid to a post reaction solution promotes the conversion of THPMI-HP to Cashmeran alcohol as described in literature where ketone molecules act as co-catalysts to convert hydroperoxide to alcohol.<sup>3</sup>

## 4.3 CoO/SiO<sub>2</sub> as a Catalyst for THPMI Oxidation

Cobalt supported on silica was tested as a catalyst due to favourable results in a study by Silva *et al.*,<sup>6</sup> where cobalt nanoparticles supported on silica-coated ferrite were found to catalyse the aerobic oxidation of cyclohexene, with allylic selectivities of up to 90 %. A greater discussion of this literature is available in section 1.7.3. The catalyst (herein referred to as CoO/SiO<sub>2</sub>) was synthesised by first functionalising commercial SiO<sub>2</sub> gel with amine groups *via* treatment with (3-aminopropyl)triethoxysilane (APTES). The aminated silica was then treated with cobalt nitrate to impregnate cobalt onto the support surface, and subsequently treated with sodium hydroxide to form the CoO active site (2.3.1).

### 4.3.1 Characterisation of CoO/SiO<sub>2</sub>

#### 4.3.1.1 Microwave Plasma Atomic Emission Spectroscopy (MP-AES)

MP-AES was used to quantify the metal loadings of CoO/SiO<sub>2</sub> (Table 4.1). A cobalt metal loading of 0.8 wt% was determined, which suggests that 16 % of all cobalt in the solution was deposited onto the silica. Complete deposition of cobalt would have resulted in a loading of 4.9 wt%. A 0.2 wt% of sodium was also observed which is likely to be residual from the sodium hydroxide used in the formation of the CoO active sites.

**Table 4.1.** Metal loading data from MP-AES for CoO/SiO<sub>2</sub>.

Metal	Maximum Possible Loading (wt%)*	Actual Loading (wt%)
Cobalt	4.9	0.8
Sodium	-	0.2

#### 4.3.1.2 X-Ray Photoelectron Spectroscopy (XPS)

XPS is a surface sensitive technique used to determine the elements present on the surface of CoO/SiO<sub>2</sub> and their oxidation states. Two peaks were observed for cobalt, the Co 2p<sup>3/2</sup> peak appeared at 781.1 eV with a satellite at 786.5 eV, and the Co 2p<sup>1/2</sup> peak appeared at 797.3 eV with a satellite at 803.0 eV (Figure 4.7). The presence of these peaks does not determine whether cobalt is part of a CoO or Co<sub>3</sub>O<sub>4</sub> phase, however their separation and relative satellite

strength does. The energy gap between  $\text{Co } 2p^{3/2}$  and  $\text{Co } 2p^{1/2}$  was 16.2 eV, which was close to the literature value of 15.8<sup>6</sup> or 15.9<sup>7</sup> eV for CoO. A gap of 14.9 eV would be observed for  $\text{Co}_3\text{O}_4$ .<sup>7</sup> The intensity ratio between the  $\text{Co } 2p^{1/2}$  satellite/main peak was 0.79, which was closer to literature values of 0.66,<sup>6</sup> 0.77 and 0.9<sup>7</sup> for CoO, than it was to literature values for  $\text{Co}_3\text{O}_4$  of 0.41 and 0.32.<sup>7</sup> It should be noted that it is difficult to distinguish between CoO and  $\text{Co}(\text{OH})_2$  phases from XPS spectra;<sup>8</sup> although it is clear from XPS analysis that this sample consists primarily of cobalt in its 2+ oxidation state.

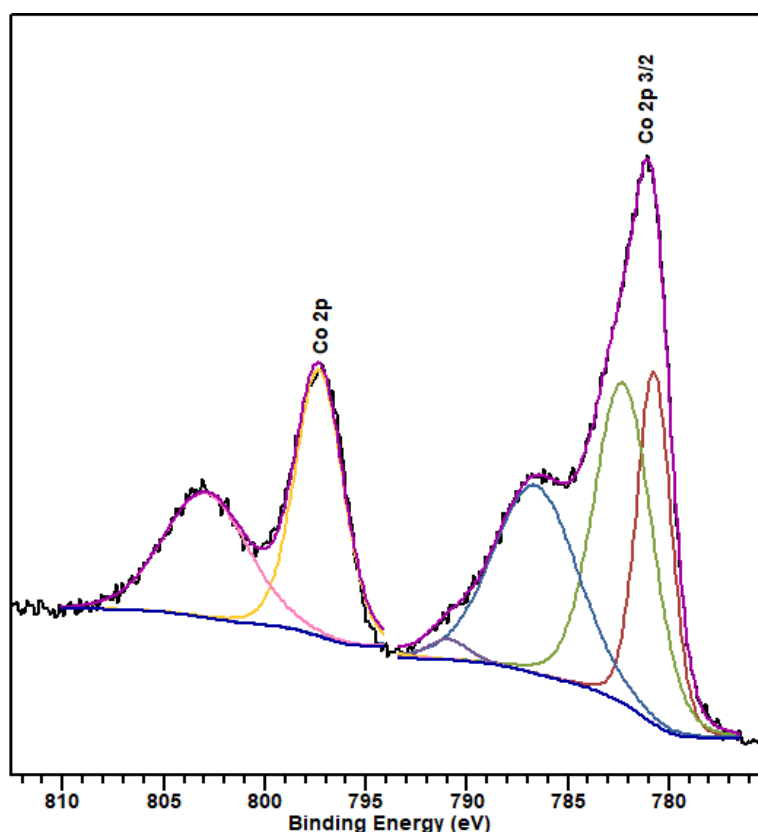


Figure 4.7. XPS spectrum for  $\text{CoO}/\text{SiO}_2$ , cobalt energy region.

XPS was also used to quantify the relative ratios of the elements present on the surface of  $\text{CoO}/\text{SiO}_2$  (Table 4.2). As expected, cobalt was concentrated on the surface of the catalyst and so a 19.2 wt% was observed. This was much larger than the total 0.8 wt% of the bulk catalyst or the nominal bulk maximum of 4.9% (Table 4.1), and so suggests that the area examined by XPS was particularly cobalt rich. 2.3 wt% nitrogen was observed, which demonstrates the amino functionalisation step was successful. Although a low sodium loading of 0.2 wt% was detected by MP-AES (Table 4.1), no sodium was detected by XPS.

**Table 4.2.** Surface concentrations for CoO/SiO<sub>2</sub> from XPS analysis.

Element	Mol %	Weight %
Co	7.6	19.2
Si	31.8	38.4
O	58.3	40.1
N	2.3	2.3
Na	0	0

#### 4.3.1.3 Scanning Electron Microscopy (SEM) and Energy Dispersive X-ray Spectroscopy (EDX)

SEM was used in conjunction with EDX to investigate the morphology and dispersion of the expected cobalt oxide nanoparticles on the surface of CoO/SiO<sub>2</sub>. Images produced from SEM did not reveal any CoO particles larger than 2 nm; however with the resolution of the machine it is possible that particles < 2 nm are present, but not observable, or that CoO is present as a thin film over the support (Figure 4.8). Higher resolution microscopy would be needed to confirm this. It is already known from MP-AES (4.3.1.1) and XPS (4.3.1.2) analysis that cobalt is present on the catalyst, so EDX analysis was used to confirm this. EDX analysis demonstrated a uniform dispersion of cobalt over the surface of the catalyst (Figure 4.9), and a cobalt loading of 2.7 (± 0.5) wt% was detected over the two regions targeted (Table 4.3). This value is much lower than the surface loading detected by XPS which was 19.2 wt% (Table 4.2), it is thought that this is partially due to XPS being a particularly surface sensitive technique,<sup>9</sup> whereas EDX penetrates further into the sample,<sup>10</sup> and so surface atoms will make up a relatively smaller percentage of the sample quantified. It is also possible that the XPS was targeting an area of the sample that was particularly rich in cobalt.

**Table 4.3.** Surface coverage of CoO/SiO<sub>2</sub> from EDX analysis.

Element	Mol %	Weight %
Co	0.9 (± 0.2)	2.7 (± 0.5)
Si	32.1 (± 0.7)	44.4 (± 0.9)
O	67.0 (± 0.6)	52.8 (± 0.5)

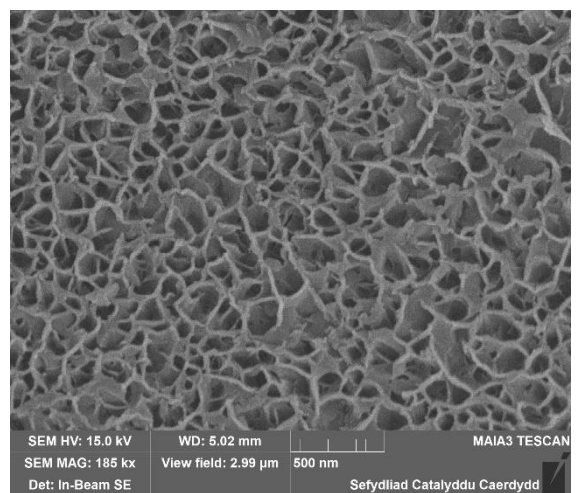
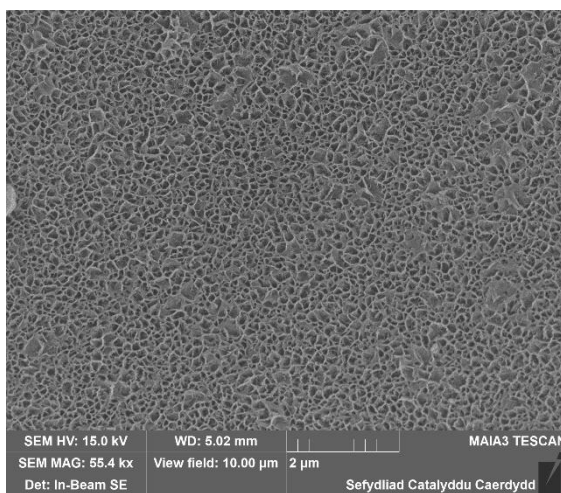
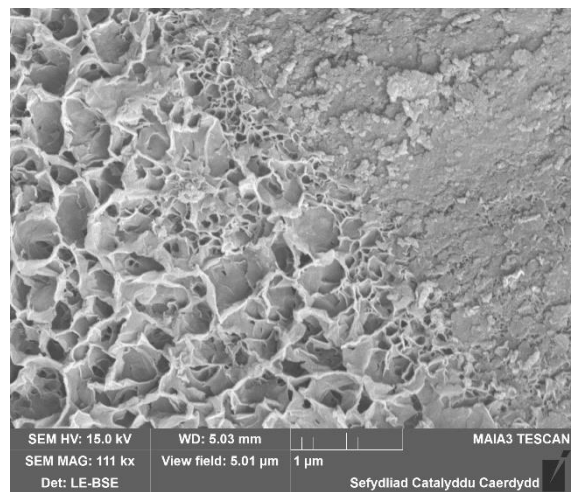
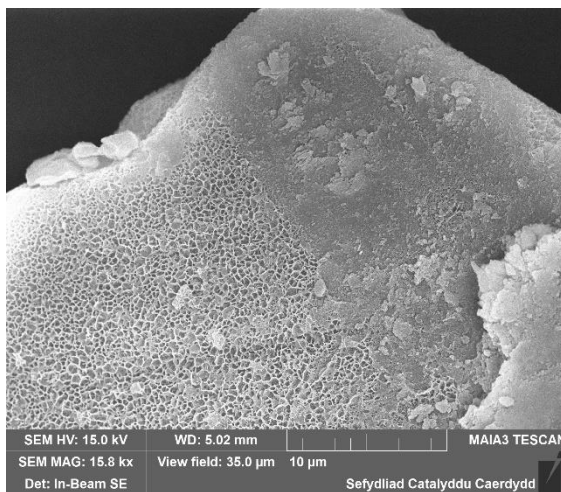
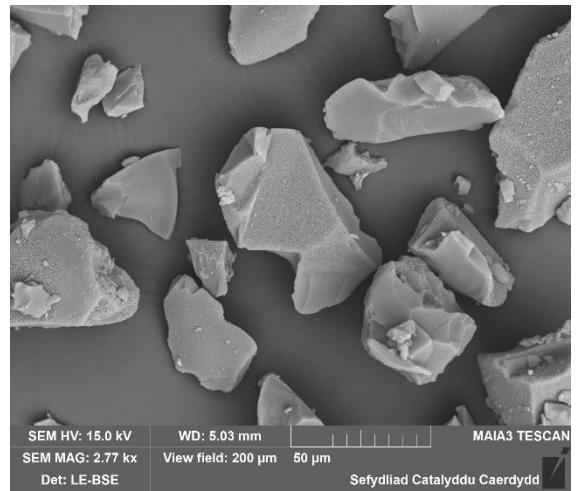
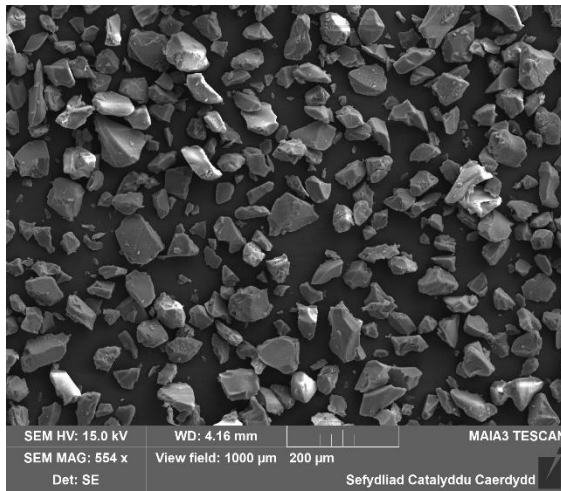
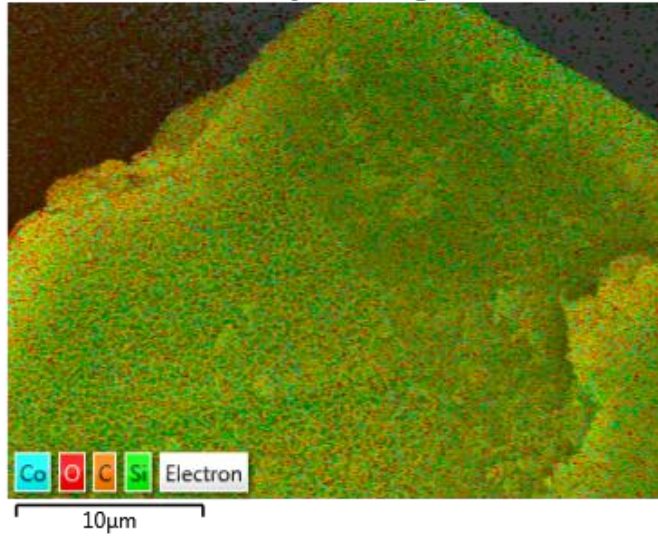
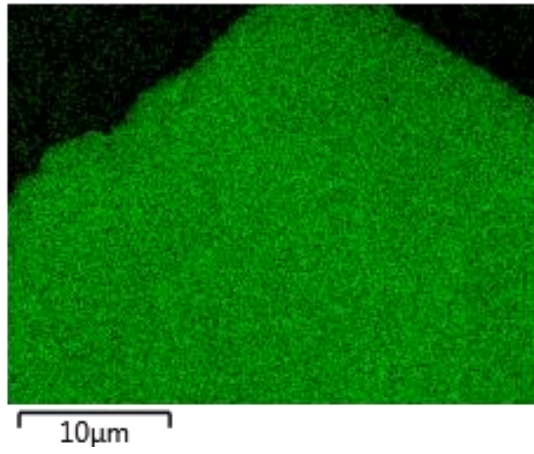


**Figure 4.8.** Images from SEM of CoO/SiO<sub>2</sub>.

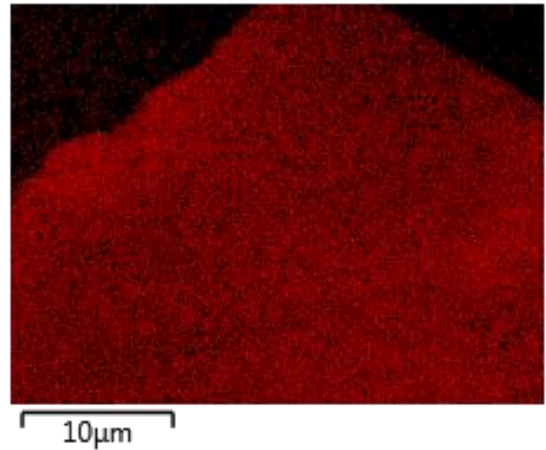
EDS Layered Image 1



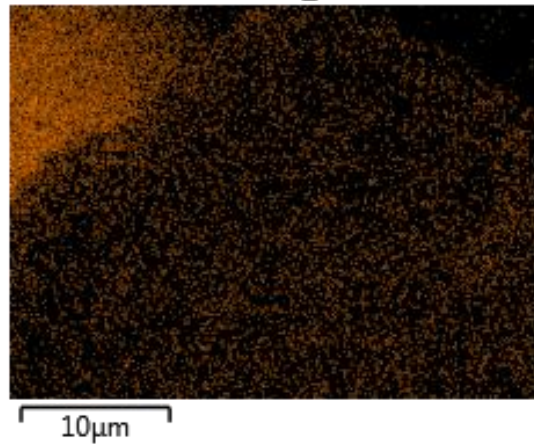
Si Kα1



O Kα1



C Kα1\_2



Co Kα1

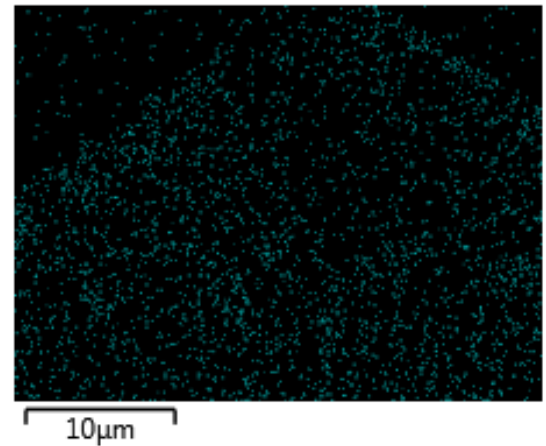


Figure 4.9. EDX mapping of CoO/SiO<sub>2</sub>.

#### 4.3.1.4 Infra-red Spectroscopy (IR)

The success of the amination step in the preparation of CoO/SiO<sub>2</sub> has already been demonstrated by the detection of nitrogen on the catalyst surface by XPS (4.3.1.2). IR spectroscopy was used as a secondary tool to confirm this. IR spectra were recorded for both the original silica and the silica post-treatment with APTES, herein referred to as 'aminated silica'. The two spectra are largely similar, however there is a key absorption at 1558 cm<sup>-1</sup>, which corresponds to an N-H stretching vibration.<sup>11</sup> The overall shape of these spectra match very well with aminated silica in the literature, when compared with their respective untreated silicas.<sup>11</sup>

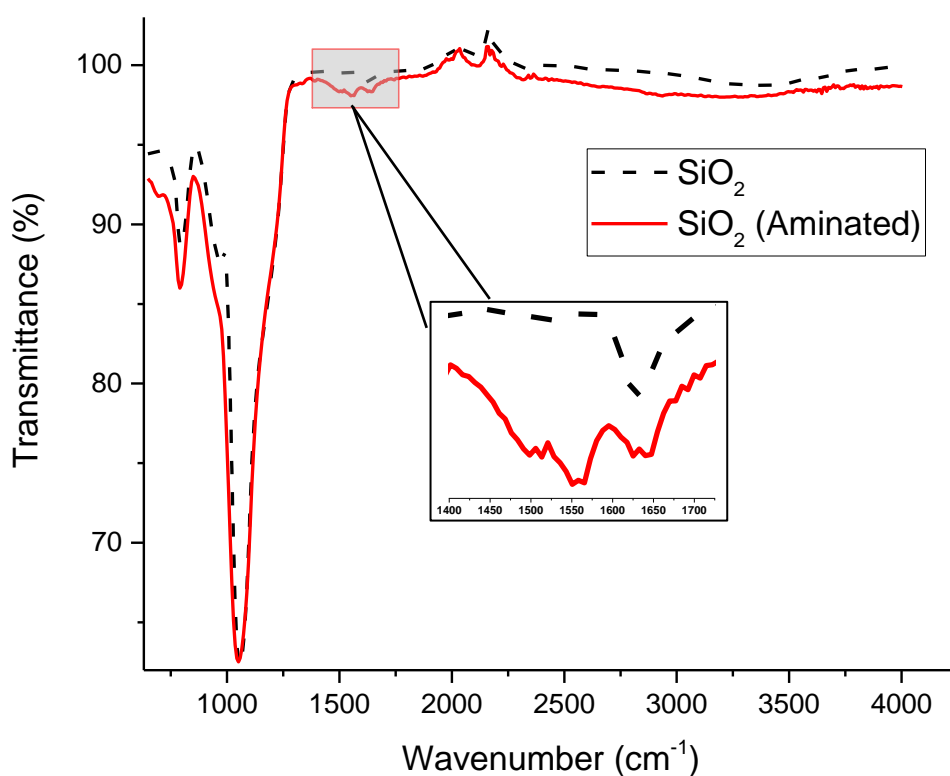
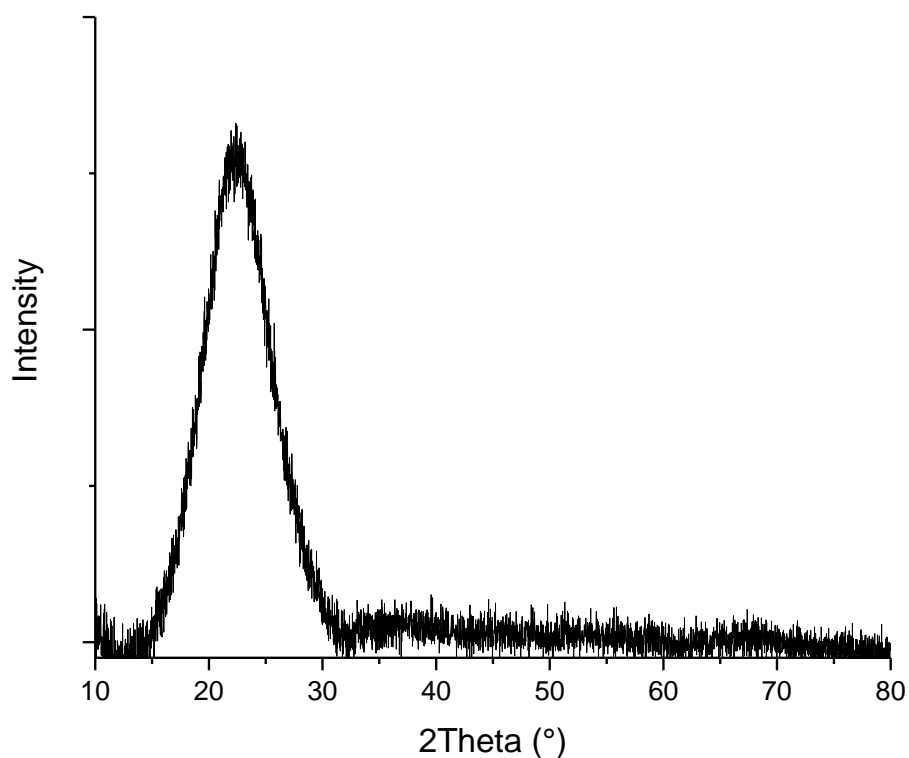


Figure 4.10. IR spectra for untreated silica and aminated silica.

#### 4.3.1.5 Powder X-ray Diffraction (XRD)

XRD was used as a tool to further characterise the CoO phase that is present on CoO/SiO<sub>2</sub>. The XRD pattern for CoO/SiO<sub>2</sub> shows one broad, major feature at 22.3° corresponding to the silica gel used for the catalyst support.<sup>12</sup> No reflections were observed corresponding to a CoO phase,<sup>13</sup> however it is known that cobalt atoms are present on the catalyst from MP-AES (4.3.1.1) and EDX analysis (4.3.1.3). Furthermore, it is known CoO is present on the surface from XPS (4.3.1.2), however a CoO phase was not detected by XRD analysis..



**Figure 4.11.** XRD pattern obtained for CoO/SiO<sub>2</sub>.

#### 4.3.1.6 Brunauer-Emmet-Teller Surface Area Analysis (BET)

The surface area of CoO/SiO<sub>2</sub> was analysed by nitrogen gas adsorption and using BET analysis. A relative pressure ( $P/P_0$ ) range of 0.05 to 0.3 was measured in a five-point analysis. This is the typical range where a linear isotherm will be observed and so the BET equation remains valid.<sup>14</sup> The result was a surface area of 202 m<sup>2</sup>g<sup>-1</sup> (Table 4.4, Figure 4.12), which was less than the expected 480 m<sup>2</sup>g<sup>-1</sup> for the commercial SiO<sub>2</sub> used in the catalyst preparation. The reduction in surface area is possibly due to the amine and cobalt functionalisation blocking the mesopores.

**Table 4.4.** Surface area for CoO/SiO<sub>2</sub>.

Catalyst	Surface Area (m <sup>2</sup> /g)
CoO/SiO <sub>2</sub>	202

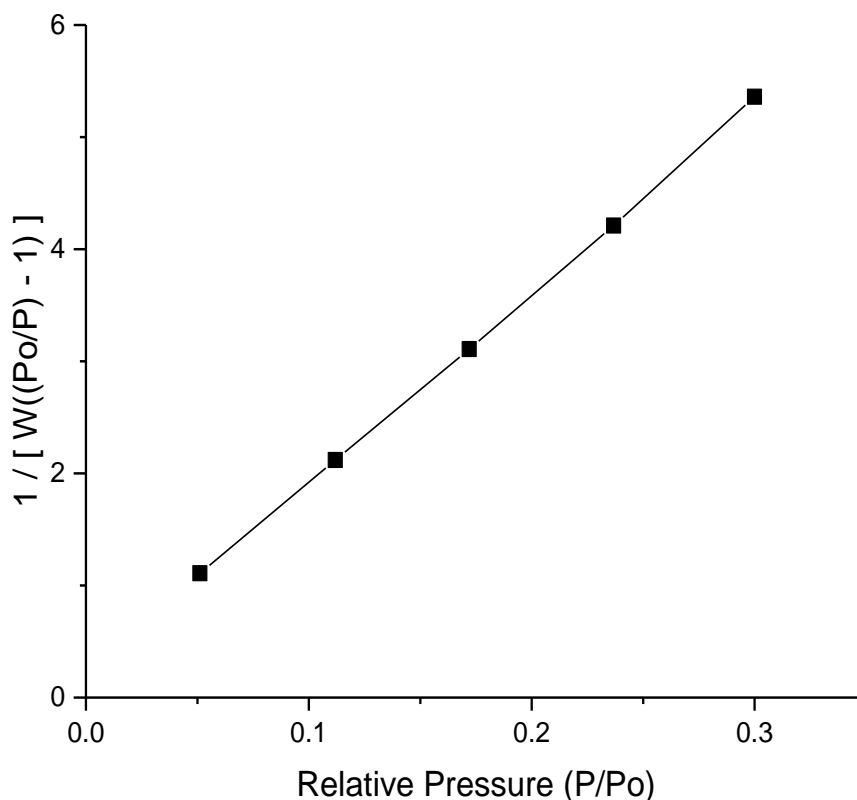


**Figure 4.12.** Surface area analysis of CoO/SiO<sub>2</sub> from N<sub>2</sub> adsorption

### 4.3.2 Catalytic Testing of CoO/SiO<sub>2</sub>

Catalytic testing of CoO/SiO<sub>2</sub> for the oxidation of THPMI was performed at 70 °C as this is a high enough temperature to observe reasonable activity within a short timeframe, whilst also being low enough to avoid significant autoxidation of THPMI. CoO/SiO<sub>2</sub> did act as a catalyst at 70 °C, which is shown as the rate of reaction was significantly greater than the blank reaction at the same temperature (Figure 4.13). The rate of reaction was, however, much less than when using Co-bis(2-EH), which was more active at the same temperature. This was somewhat expected as with oxidations using homogenous transition metals such as Co or Mn, induction periods are generally not present.<sup>15</sup> The rate of reaction observed with the heterogenous CoO/SiO<sub>2</sub> did demonstrate an induction effect, where the rate of reaction increased over time. This could be a result of leaching effects which is discussed more in section 4.5, although it is common to observe induction effects with heterogeneous oxidation catalysts when no initiator is deliberately added.<sup>16,17</sup> There was also no quenching effect when CoO/SiO<sub>2</sub> was used as the catalyst, adding credence to the theory that quenching is a result of dissolved cobalt ions,<sup>18</sup> as discussed in sections 3.5 and 3.6.

The selectivity observed when using CoO/SiO<sub>2</sub> (Figure 4.14b) was compared with Co-bis(2-EH) at the same temperature (Figure 4.14a). The Cash-total selectivity was lower when using

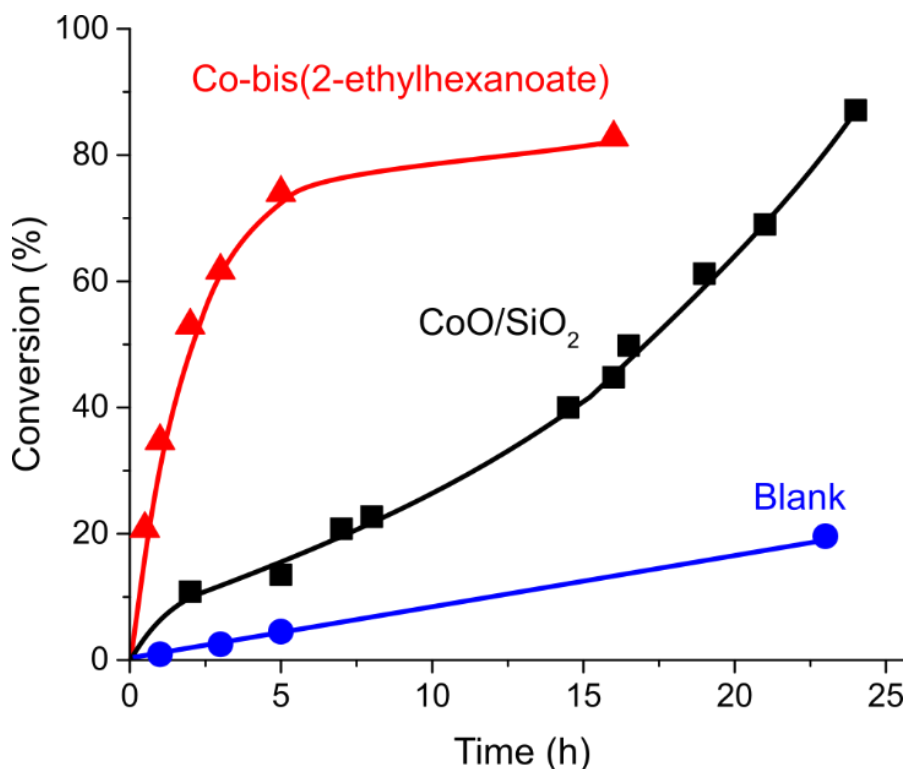


**Figure 4.13.** Conversion against time for the reaction catalysed by CoO/SiO<sub>2</sub>, compared to the industrial catalyst and blank reaction all at 70 °C. Conditions: THPMI (10 ml), hexadecane (1 ml), 70 °C, 0.5 - 24 h, CoO/SiO<sub>2</sub>-NH<sub>2</sub> (200 mg/4.6 wt%), Air residence time (0.5 min), 900 rpm. Data for the Co-bis(2-ethylhexanoate) and blank plots were taken from 1 reaction and data from the CoO/SiO<sub>2</sub> plot was taken from 4 separate reactions.

CoO/SiO<sub>2</sub>, compared with Co-bis(2-EH), a drop from 78 % Cash-total to 70 % was observed at 50 % conversion. A more significant disparity in the two reactions was observed in the makeup of this Cash-total selectivity. When using CoO/SiO<sub>2</sub>, a much higher proportion of product was the hydroperoxide (THPMI-HP), between 30 – 50 % at conversions up to 60 %. As conversion increases beyond 60 % the concentration of THPMI-HP drops significantly. This was very different to Co-bis(2-EH) where at any conversion at 70 °C, THPMI-HP makes up <10 % of products. This suggests that although CoO/SiO<sub>2</sub> catalyses the oxidation of THPMI into THPMI-HP, it is not efficient at breaking down THPMI-HP at a rate close to that of Co-bis(2-EH). When Co-bis(2-EH) was used, a much higher proportion of the products were Cashmeran and Cashmeran-alcohol, where the level of Cashmeran increased with conversion, as Cashmeran-alcohol concentration reduced. When CoO/SiO<sub>2</sub> was used, the concentration of Cashmeran and Cashmeran-alcohol were consistently close to or below 20 %, which did not alter until very high conversion, where Cashmeran concentration started to increase. The consistent, approximate 1:1 ratio of Cashmeran to Cashmeran-alcohol in the reaction catalysed by CoO/SiO<sub>2</sub> may suggest that these products are formed primarily from a non-catalysed Russell termination.<sup>19,20</sup> This is a termination reaction where two peroxide radicals react to form one ketone and one alcohol molecule. This would further explain the slow rate of reaction as unlike other routes to form

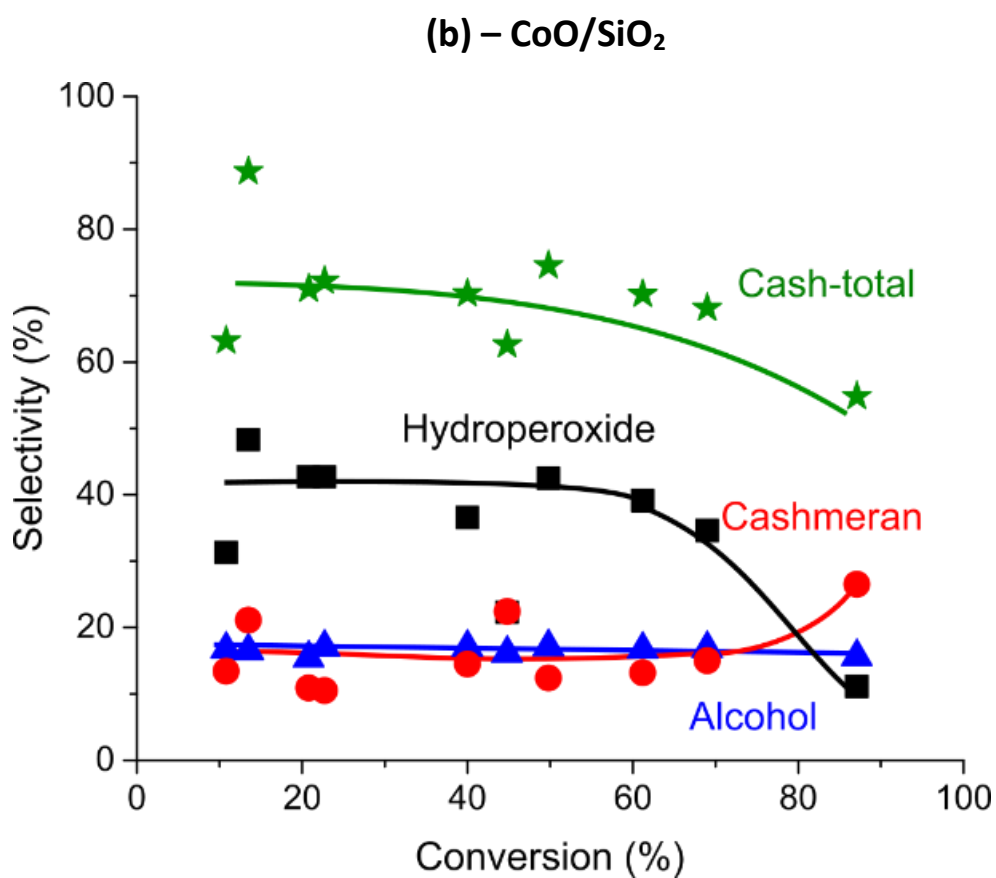
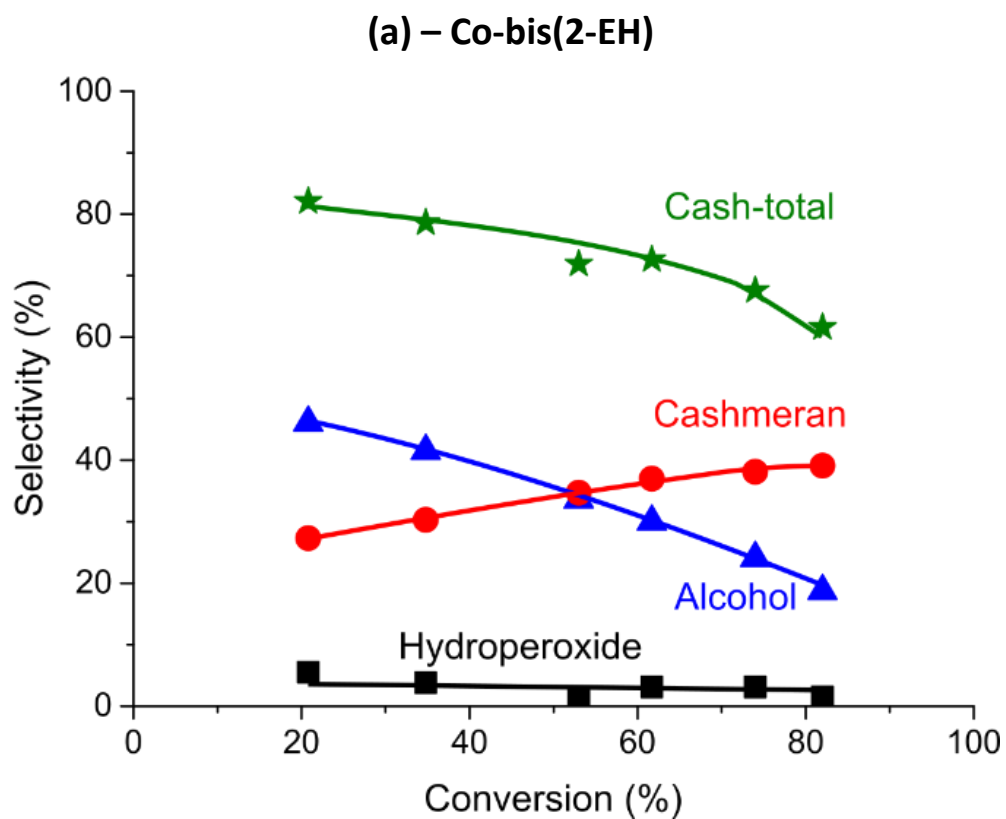


**Figure 4.14.** Selectivity against conversion for the reaction catalysed by (b) - CoO/SiO<sub>2</sub>, compared to (a) - Co-bis(2-ethylhexanoate). Conditions: THPMI (10 ml), hexadecane (1 ml), 70 °C, 2 - 24 h, CoO/SiO<sub>2</sub>-NH<sub>2</sub> (200 mg/4.6 wt%), Air residence time (0.5 min), 900 rpm. (a) Co-bis(2-EH): data was taken from one reaction. (b) CoO/SiO<sub>2</sub>: data was taken from 4 separate reactions.

allylic oxidation products, such as homolytic cleavage of the O—O peroxide bond, a Russell termination would not propagate further radical activation of THPMI.<sup>1</sup> If the route to forming products from THPMI-HP is based on a non-catalytic Russell termination, then it is likely that the property of CoO/SiO<sub>2</sub> to catalyse the formation of THPMI-HP is a result of oxygen activation on the catalyst surface. This would be similar to the oxidation of CO to CO<sub>2</sub> by CoO, where oxygen first reacts with CoO to form a Co<sub>3</sub>O<sub>4</sub> active site.<sup>21</sup> Although this is only a possibility and currently there is not enough evidence to make definitive claims on mechanistic routes, it is also possible that CoO/SiO<sub>2</sub> is catalysing the decomposition of THPMI-HP into radical species, or the oxidation of Cashmeran alcohol into Cashmeran. It should also be stated here that the support, aminated silica, alone did not demonstrate any catalytic activity.

The results demonstrate that although CoO/SiO<sub>2</sub> is active as a catalyst for the oxidation of THPMI, it is not effective at directing selectivity towards the desired allylic oxidation products. Where Co-bis(2-EH) rapidly breaks down THPMI-HP into the desired products, CoO/SiO<sub>2</sub> does not. There is also no definitive evidence that CoO/SiO<sub>2</sub> is acting as a catalyst to oxidise the alcohol into Cashmeran. The property of CoO/SiO<sub>2</sub> to form THPMI-HP and not break it down may provide function as part of a dual-catalytic system where CoO/SiO<sub>2</sub> forms THPMI-HP and another catalyst breaks THPMI-HP down into Cashmeran. However, for this system to constitute an improvement on the current processes the first catalyst (in this case CoO/SiO<sub>2</sub>) would need to be far more selective towards THPMI-HP as currently Cash-total selectivity with this catalyst is too low (only 70 % Cash-total at 50 % conversion).

#### 4.4 Co<sub>3</sub>O<sub>4</sub> as a Catalyst for THPMI Oxidation

Due to the ability of CoO/SiO<sub>2</sub> to catalyse the oxidation of THPMI into THPMI-HP but not to further oxidise THPMI-HP into the desired products, it was hypothesised that any bulk oxidation catalyst would display similar properties. To test this hypothesis, Co<sub>3</sub>O<sub>4</sub> was prepared by precipitation from cobalt nitrate with sodium carbonate and tested as a catalyst. It has previously been demonstrated that Co<sub>3</sub>O<sub>4</sub> can be used as a cheap and easy to produce catalyst for the total oxidation of propane,<sup>22–25</sup> isopropanol,<sup>24</sup> and propene<sup>24</sup>. It is thought that Co<sub>3</sub>O<sub>4</sub> would show similar catalytic properties to CoO/SiO<sub>2</sub> for the oxidation of THPMI as Co<sub>3</sub>O<sub>4</sub> will act as a non-selective oxidation catalyst.

#### 4.4.1 Thermogravimetric Analysis (TGA) of Cobalt Carbonate

The co-precipitation of cobalt nitrate with sodium carbonate results in formation of a cobalt carbonate phase, which is then calcined to produce  $\text{Co}_3\text{O}_4$ .<sup>25,26</sup> The temperature of this calcination was determined by TGA. A significant reduction in mass was observed between 200 – 275 °C, where approximately 20 % of the mass was lost (Figure 4.15). This was due to the loss of carbon dioxide from the carbonate to form  $\text{Co}_3\text{O}_4$ . The total weight loss of 24.8 % includes both water and carbon dioxide and is in line with literature for this type of procedure.<sup>27,28</sup> A calcination temperature of 300 °C, under aerobic conditions, was selected to ensure full decomposition of the carbonate phase into  $\text{Co}_3\text{O}_4$ .

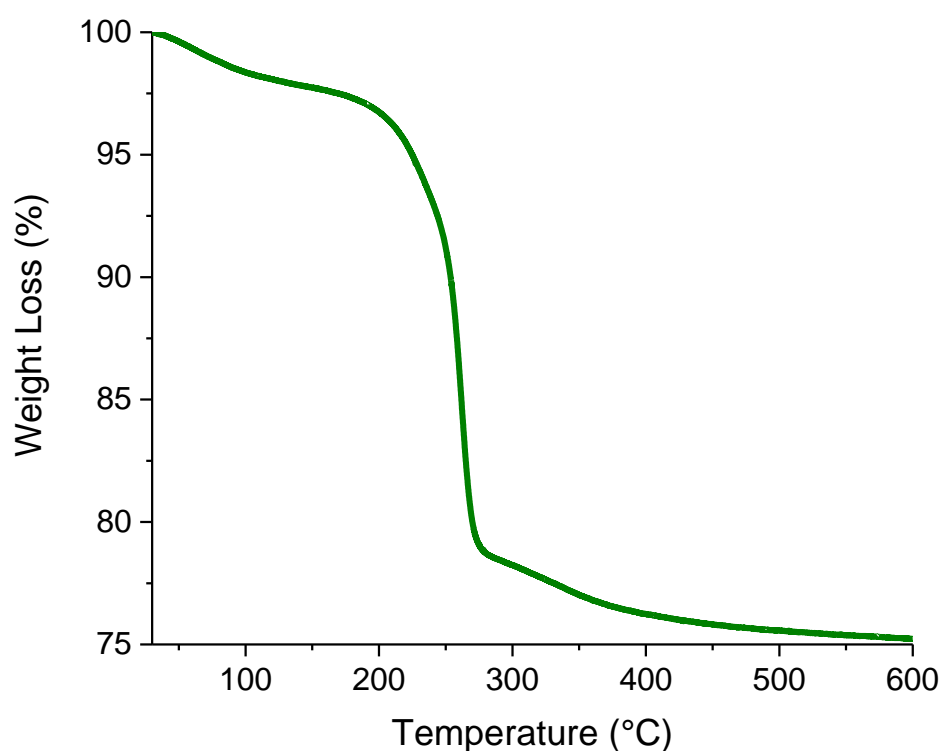


**Figure 4.15.** Thermogravimetric analysis of the precursor to  $\text{Co}_3\text{O}_4$ . See section 2.6.2 for heating regimen.

#### 4.4.2 Characterisation of $\text{Co}_3\text{O}_4$

##### 4.4.2.1 Microwave Plasma Atomic Emission Spectroscopy (MP-AES)

MP-AES was used to quantify the metal loadings of  $\text{Co}_3\text{O}_4$  (Table 4.5). For pure  $\text{Co}_3\text{O}_4$  a cobalt weight loading of 73.4 % would be expected, however in the prepared catalyst a loading of 65.1 % was observed. Additionally, 0.5 wt% of sodium was also observed, which is a result of the sodium carbonate used in the co-precipitation technique. It is possible that there was some

cobalt carbonate phase present from the precursor, which would account for the deficit of cobalt in the final catalyst.

**Table 4.5.** Metal loading data from MP-AES for  $\text{Co}_3\text{O}_4$ .

Metal	Nominal Loading (wt%)	Actual Loading (wt%)
Cobalt	73.4	65.1
Sodium	-	0.5

#### 4.4.2.2 Powder X-ray Diffraction (XRD)

The XRD pattern shown for  $\text{Co}_3\text{O}_4$  (Figure 4.16) matched with literature in terms of both reflection position and relative intensity.<sup>23</sup> Reflections are observed at: 19.0 (220), 31.4 (311), 36.8 (400), 45.1 (511) and 59.5 (440) and 65.5 (440) degrees. No reflections for a CoO phase were observed, where a reflection at 42.4 ° would be expected.<sup>13</sup>

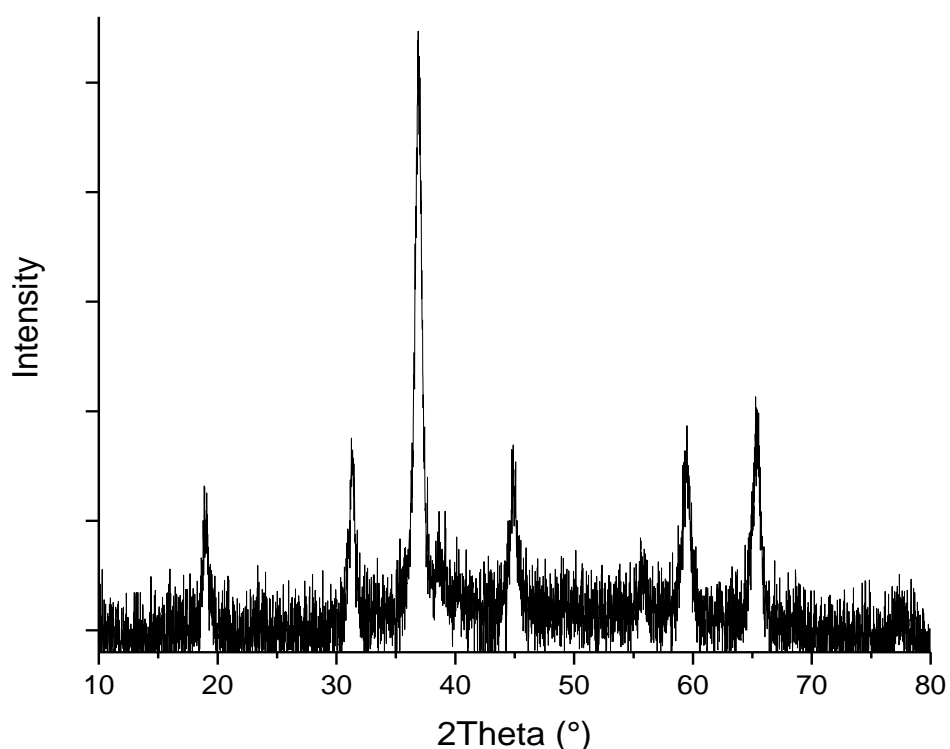


**Figure 4.16.** XRD pattern for  $\text{Co}_3\text{O}_4$ .

#### 4.4.2.3 X-Ray Photoelectron Spectroscopy (XPS)

As expected, the XPS spectra of  $\text{Co}_3\text{O}_4$  demonstrated typical Co 2p peaks for  $\text{Co}_3\text{O}_4$  (Figure 4.17). As with CoO/SiO<sub>2</sub>, the presence of the Co 2p<sub>3/2</sub> and 1/2 peaks does not confirm either a CoO or  $\text{Co}_3\text{O}_4$  phase, however the nature of these peaks does. The peak separation between Co

2p 3/2 and 1/2 was 14.7 eV, which is a good match to the literature value of 14.9 eV.<sup>7</sup> A CoO phase would result in a separation of 15.8,<sup>6</sup> 15.9<sup>7</sup> or 16.3 eV, as observed earlier (4.3.1.2). The Co 2p1/2 satellite/main peak ratio was 0.30, which is closer to the literature values for Co<sub>3</sub>O<sub>4</sub> of 0.41 and 0.32,<sup>7</sup> than it is for the values of CoO of 0.66,<sup>6</sup> 0.77, 0.9<sup>7</sup> or 0.85 (4.3.1.2). The Co 2p3/2 satellite peak are slightly more intense than expected for pure Co<sub>3</sub>O<sub>4</sub><sup>8</sup> and so it is suspected that some cobalt(II) oxide or hydroxide phase is present on the surface. Having said this, the XPS analysis demonstrates clearly that the surface of the catalyst is primarily made up of a Co<sub>3</sub>O<sub>4</sub> phase.

Two peaks were observed for carbon in the XPS analysis of Co<sub>3</sub>O<sub>4</sub> (Figure 4.18), the largest being the C1s peak at 284.7 eV assigned to adventitious carbon. The second, smaller peak was observed at 288.6 eV and is proposed to result from a cobalt carbonate phase, not fully broken down during the heat treatment. The binding energy of this peak is in good alignment with literature for carbonate phases where a carbonate peak at close to 289.5 eV is expected<sup>29</sup>.

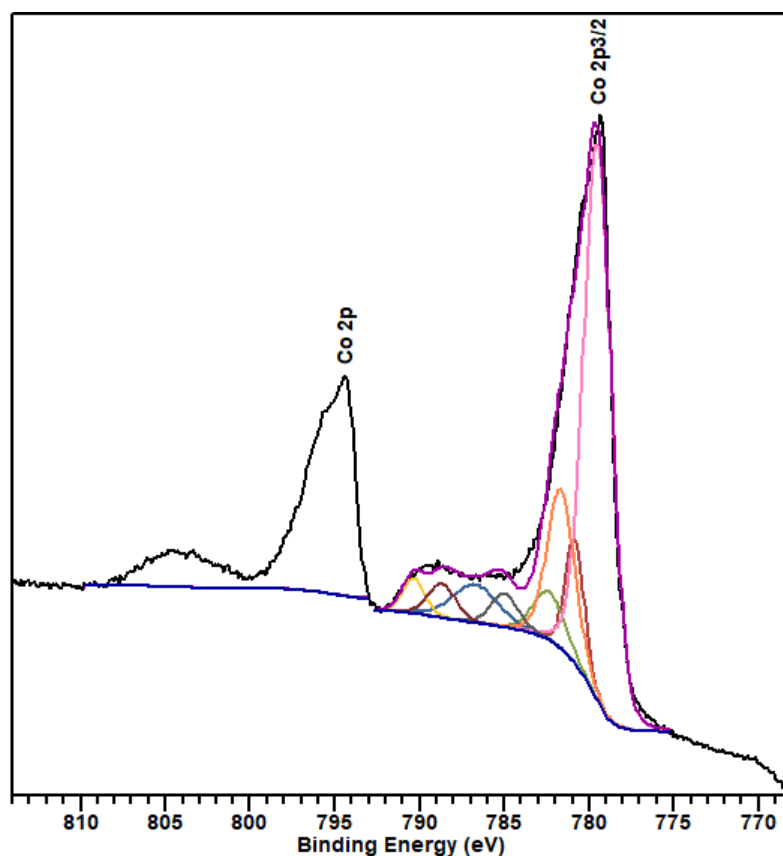


**Figure 4.17.** XPS spectrum for Co<sub>3</sub>O<sub>4</sub>, cobalt region.

The surface concentrations detected from XPS showed 68.7 wt% cobalt, which is close to the figure of 65.1 wt% stated by MP-AES (Table 4.6) and the expected figure for pure Co<sub>3</sub>O<sub>4</sub> of 73.4 wt%. 1.7 wt% sodium was also detected, which is expected to be residual from the sodium

carbonate used in the co-precipitation procedure. Carbon was also detected by XPS, with only the carbonate peak at 288.6 eV being quantified, which accounted for only 0.7 wt%.

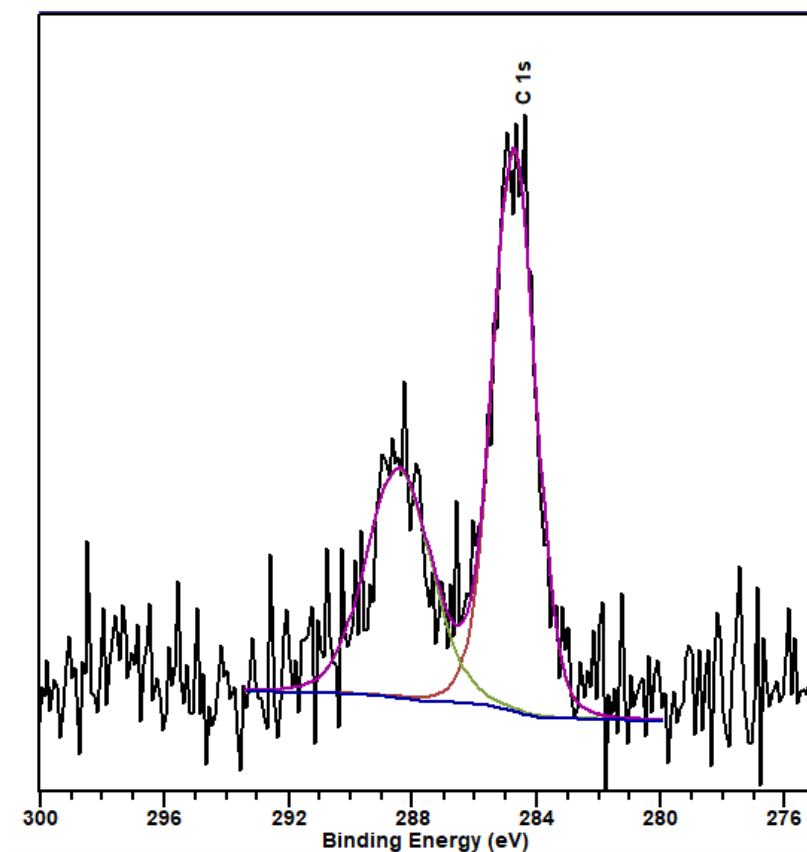


Figure 4.18. XPS analysis of carbon energy region for  $\text{Co}_3\text{O}_4$ .

Table 4.6. Surface concentrations for  $\text{Co}_3\text{O}_4$  from XPS analysis.

Element	Mol %	Weight %
Co	37.7	68.7
O	59.9	29.6
Na	2.4	1.7
C	1.8	0.7

#### 4.4.2.4 Brunauer-Emmett-Teller Surface Area Analysis (BET)

The surface area of  $\text{Co}_3\text{O}_4$  was analysed by using nitrogen gas adsorption and using the Brunauer-Emmett-Teller theory (BET). As with  $\text{Co/SiO}_2$  (4.3.1.6), a relative pressure ( $P/P_0$ ) range of 0.05 – 0.3 was applied as this is the range where the isotherm is linear and so the BET equation is valid.<sup>14</sup> The result was a surface area of  $83 \text{ m}^2\text{g}^{-1}$  (Table 4.7, Figure 4.19). This is far greater

than commercial  $\text{Co}_3\text{O}_4$  where the surface area can be as low as  $2 - 4 \text{ m}^2\text{g}^{-1}$ , and is in a similar range to prepared  $\text{Co}_3\text{O}_4$  catalysts in the literature of between  $14 - 160 \text{ m}^2\text{g}^{-1}$ .<sup>22,23</sup> These values vary significantly depending on the method of preparation of the material.

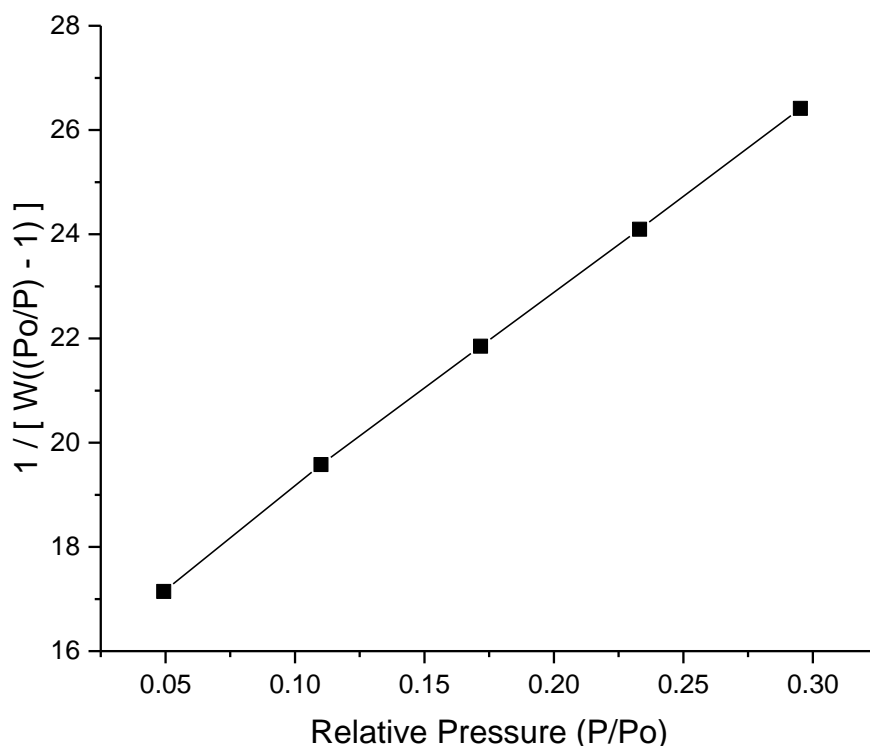


Figure 4.19. Surface area analysis of  $\text{Co}_3\text{O}_4$ .

Table 4.7. Surface area of  $\text{Co}_3\text{O}_4$ .

Catalyst	Surface Area ( $\text{m}^2\text{g}^{-1}$ )
$\text{Co}_3\text{O}_4$	83

#### 4.4.3 Catalyst Testing of $\text{Co}_3\text{O}_4$

As with the testing of  $\text{CoO/SiO}_2$  (4.3.2), the testing of  $\text{Co}_3\text{O}_4$  took place at  $70^\circ\text{C}$  as this is a temperature where activity is relatively high, without any significant autoxidation taking place. The rate of oxidation when using  $\text{Co}_3\text{O}_4$  was significantly higher than when no catalyst was used, which demonstrates that  $\text{Co}_3\text{O}_4$  was acting as a catalyst (Figure 4.20). However, this rate was also much slower than that observed when using Co-bis(2-EH), and no induction effect was observed as with  $\text{CoO/SiO}_2$  (4.3.2). No quenching effect was observed unlike for  $\text{CoO/SiO}_2$ , this may be due to the much larger loading of cobalt in the reaction with  $\text{Co}_3\text{O}_4$ . Double the weight loading of  $\text{CoO/SiO}_2$  was used in the reactions; however, 41 times more cobalt was present in the reactions with  $\text{Co}_3\text{O}_4$  based on MP-AES analysis (4.3.1.1 and 4.4.2.1). Although most of the

cobalt in  $\text{Co}_3\text{O}_4$  is part of the bulk and not surface of the catalyst, so when surface area and surface concentration are considered the level of potentially active and accessible cobalt in each reaction are more similar. The faster rate of reaction with Co-bis(2-EH) is likely due to an immediate decomposition of the THPMI-HP, initiating radical chain oxidation.  $\text{Co}_3\text{O}_4$  is more likely to catalyse oxidation by a heterolytic Mars and van Krevelen mechanism<sup>30</sup> resulting in a slower, more steady rate of reaction.

The effect that  $\text{Co}_3\text{O}_4$  had on selectivity (Figure 4.21b) was similar to that observed when using  $\text{CoO/SiO}_2$  (Figure 4.14). THPMI-HP was observed at 35 – 40 % consistently up until 75 % conversion, after which the concentration dropped rapidly. A high Cash-total selectivity was observed using  $\text{Co}_3\text{O}_4$ , with 75 % selectivity at 50 % conversion, a drop of 8 % relative to Co-bis(2-EH). Cashmeran concentration was consistently low throughout the reaction, varying between 10 – 16 %. Cashmeran-alcohol concentration accounted for an initial 35 % at low conversion, which gradually decreased to 15 % as conversion increased. These selectivity values and trends were similar to  $\text{CoO/SiO}_2$ , however when using  $\text{Co}_3\text{O}_4$  there was relatively less THPMI-HP and relatively more Cashmeran-alcohol present. This suggests that  $\text{Co}_3\text{O}_4$  is more effective at breaking down THPMI-HP into the alcohol, possibly *via* homolytic cleavage of the O—O peroxide bond, similar to supported gold catalysts for the conversion of cyclohexane hydroperoxide to cyclohexanol.<sup>31</sup> In spite of this,  $\text{Co}_3\text{O}_4$  was still largely ineffective at breaking down THPMI-HP into the desired products, especially when compared with the industrial catalyst, Co-bis(2-EH). For both of the cobalt-based catalysts that have been tested it is necessary to determine if any, or all, of the activity observed is a result of metal leaching, which is discussed in the next section.

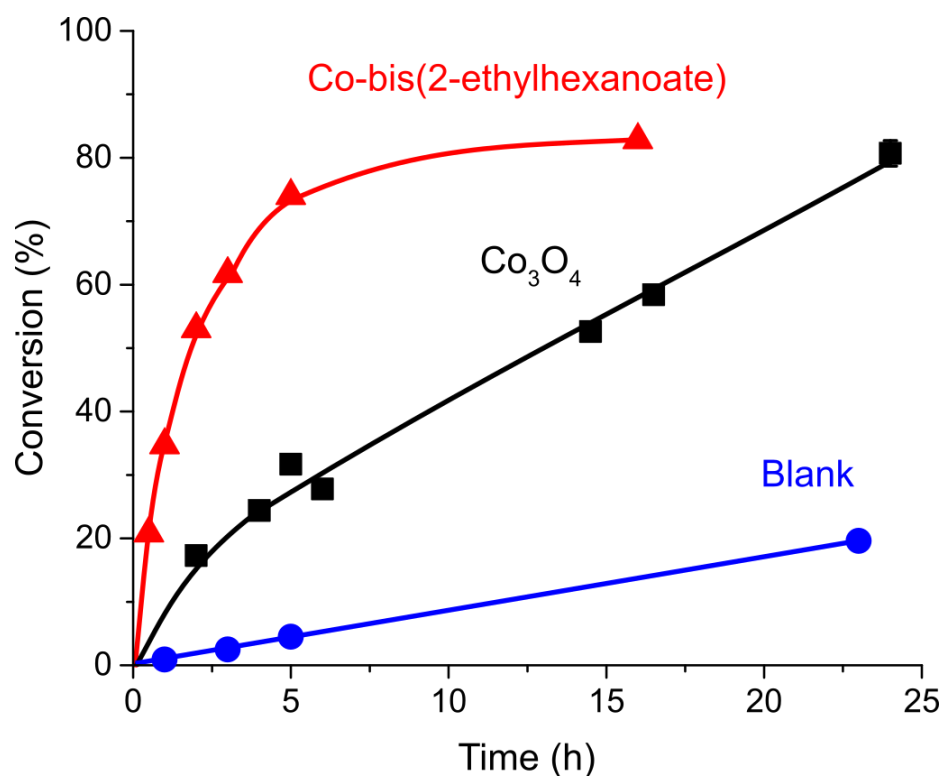
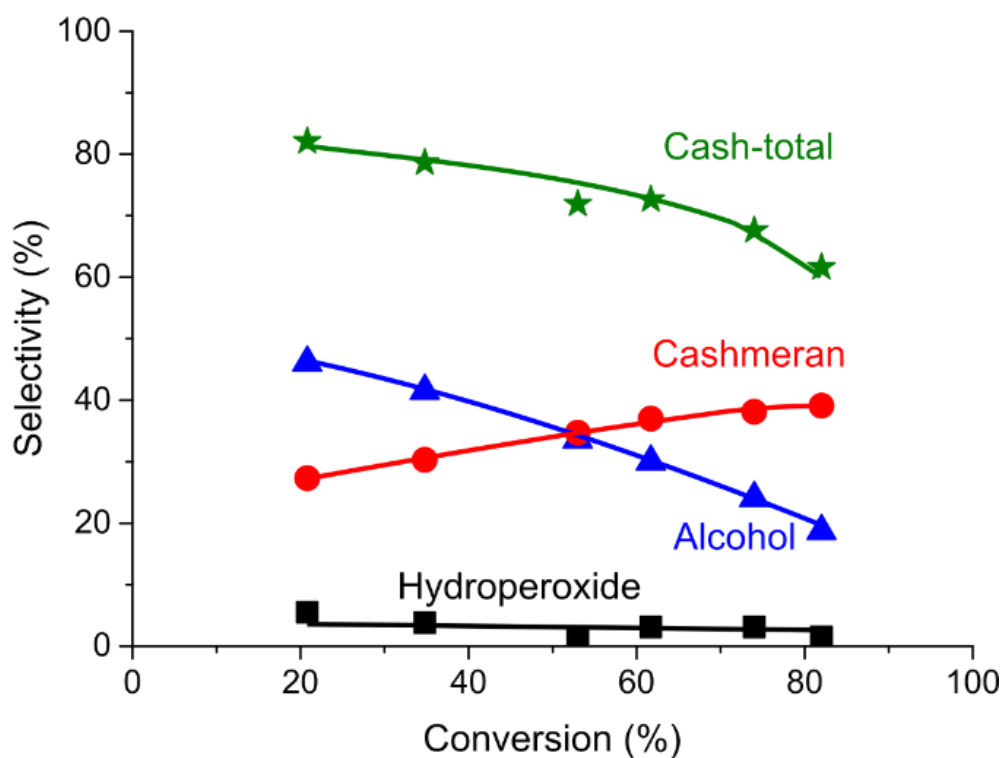


**Figure 4.20.** Conversion against time for reactions catalysed by  $\text{Co}_3\text{O}_4$ , compared to the standard industrial catalyst and the blank reaction, all at 70 °C. Conditions: THPMI (10 ml), hexadecane (1 ml), 70 °C, 0.5 – 24 h,  $\text{Co}_3\text{O}_4$  (100 mg/1.15 wt%), Air residence time (0.5 min), 900 rpm. Data for the Co-bis(2-ethylhexanoate) and blank plots were taken from 1 reaction and data from the  $\text{Co}_3\text{O}_4$  plot was taken from 5 separate reactions.

(a) – Co-bis(2-EH)



(b) – Co<sub>3</sub>O<sub>4</sub>

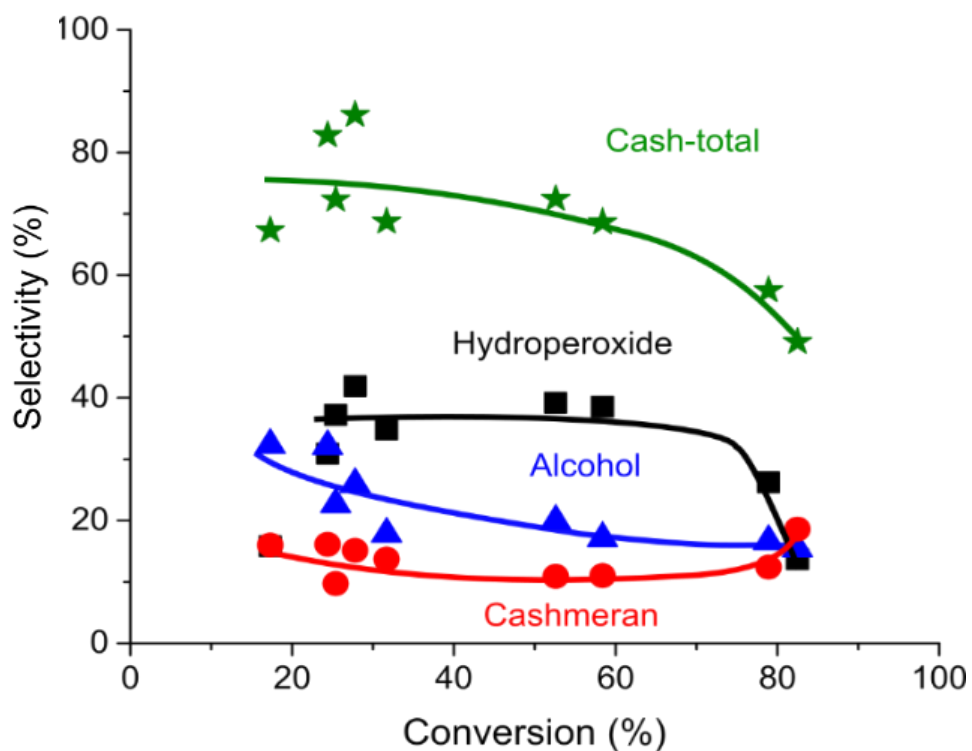


**Figure 4.21.** Selectivity against conversion for the reaction catalysed by (b) - CoO/SiO<sub>2</sub>, compared to (a) - Co-bis(2-ethylhexanoate). Conditions: THPMI (10 ml), hexadecane (1 ml), 70 °C, 0.5 - 24 h, Co<sub>3</sub>O<sub>4</sub> (100 mg/1.15 wt%), Air residence time (0.5 min), 900 rpm. (a) Co-bis(2-EH): data was taken from one reaction. (b) Co<sub>3</sub>O<sub>4</sub>: data was taken from 5 separate reactions.

## 4.5 Cobalt Leaching

When the two heterogeneous cobalt catalysts were tested, as described in previous sections (4.3.2 and 0), they both demonstrated catalytic activity. This may be due to the active sites on the catalysts; however, it is also possibly due to cobalt leaching from the surface of the catalysts into the reaction solution. As with the industrial catalyst, Co-bis(2-EH), low loadings of dissolved cobalt salt can be highly active catalysts for this reaction. It is for this reason that ICP-MS (inductively coupled plasma mass spectrometry) was performed on several reaction solutions after a reaction with a cobalt based heterogeneous catalyst (Table 4.8).

**Table 4.8.** Leaching data for reactions with  $\text{Co}_3\text{O}_4$  and  $\text{CoO}/\text{SiO}_2$ , from ICP-MS analysis.

Entry	Catalyst	Reaction Conditions				Co Leached (ppm)	Co Leached (%)
		Temperature (°C)	Time (h)	Cobalt loading (wt%)	Conversion (%)		
1	$\text{Co}_3\text{O}_4$	70 °C	5	0.75	32	2.4	Trace
2			24		83	4.2	0.1
3	$\text{CoO}/\text{SiO}_2$	50 °C	5	0.02	10	Trace	0.0
4			24		23	0.1	0.1
5		70 °C	0.04	5	13	2.6	1.8
6				16	45	0.7	0.5
7				24	90	3.9	2.7
8				24	76	0.9	1.2

Two samples of a reaction with  $\text{Co}_3\text{O}_4$  as the catalyst were analysed using ICP-MS, after 5 and 24 h of reaction. After 5 h and 32 % THPMI conversion 2.43 ppm (parts per million) cobalt was detected in solution, this increased to 4.18 ppm after 24 h and 83 % conversion. 2 – 4 ppm cobalt constitutes 0.04 -0.07 % of the total cobalt added to the reaction as  $\text{Co}_3\text{O}_4$ . These levels of leaching seem low, but may have an impact on the reaction, which will be discussed later in this section.

In the case of reactions catalysed with  $\text{CoO}/\text{SiO}_2$ , two 50 °C reactions were analysed. Even after 24 h only 0.05 ppm cobalt leaching was detected, which accounts for 0.07 % of all cobalt added to the reaction. For reactions at 70 °C more leaching is observed with between 0.69 – 3.86 ppm cobalt detected, accounting for 0.5 – 2.65 % of all cobalt added to the reaction.

The reaction at 50 °C only reached 23 % conversion after 24 h, whereas the reaction at 70 °C reached up to 90 %; both values significantly larger than their respective blank reactions (3.5.1). It is unclear from these data alone whether this increase in activity is caused by the additional leaching at 70 °C or an increased rate of heterogeneously-catalysed reaction, or a mix of the two.

To test the effect that ppm levels of cobalt have on the reaction, two experiments were performed where ppm levels of Co-bis(2-EH) were added to the reaction at 70 °C (Figure 4.22). When 3 ppm Co-bis(2-EH) was added, a very slow rate of reaction was observed; initially the same as the blank reaction. Eventually 35 % conversion was reached after 24 h, higher than the 20 % conversion for the blank after 23 h. This suggests 3 ppm Co-bis(2-EH) has a slight catalytic effect but only after a lengthy induction period. This was also a much slower rate of reaction when compared to the two heterogeneous cobalt catalysts which can leach up to 4 ppm of cobalt into solution. Although dissolved Co-bis(2-EH) will not be identical to the cobalt ions dissolved into solution from leaching, these results suggest that a significant amount of the catalyst activity is a result of the heterogeneous active sites. When 50 ppm Co-bis(2-EH) was added, the rate of reaction was significant and comparable to the standard Co-bis(2-EH) loading

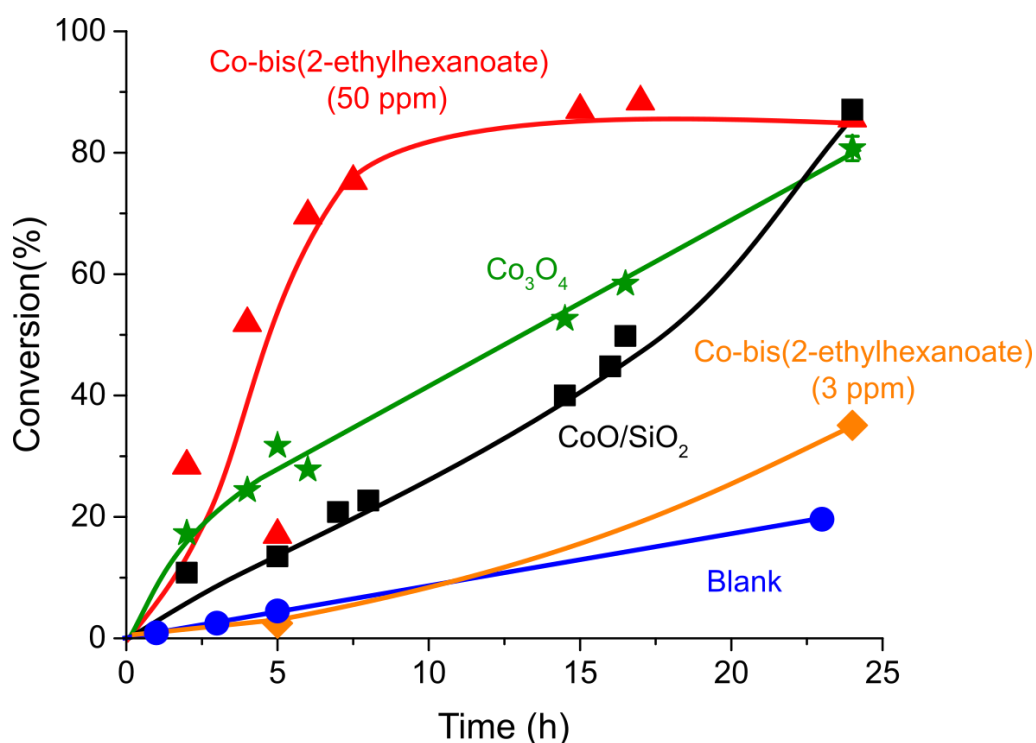


**Figure 4.22.** Conversion against time for reactions with ppm levels of Co-bis(2-ethylhexanoate), compared to a blank and reactions with Co<sub>3</sub>O<sub>4</sub> and CoO/SiO<sub>2</sub>. Conditions: THPMI (10 ml), hexadecane (1 ml), 70 °C, 1 - 24 h, Co<sub>3</sub>O<sub>4</sub> (100 mg/1.15 wt%) or CoO/SiO<sub>2</sub> (200 mg/4.6 wt%) or Co-naphthenate (3 or 50 ppm), air residence time (0.5 min), 900 rpm. Data from the 50 ppm plot was taken from 3 reactions, data from the blank and 3 ppm plots were taken from one reaction each, data for the Co<sub>3</sub>O<sub>4</sub> ploy was taken from 5 separate reactions, and data for the CoO/SiO<sub>2</sub> plot was taken from 4 separate reactions.

of 1.15 wt% (or 1200 ppm). This shows that only a very small loading of cobalt can have significant catalytic effects on the reactions, in particular the selectivity, something that is described below.

When a standard loading (1.15 wt% or 1200 ppm) of Co-bis(2-EH) was used in a reaction, very little hydroperoxide was observed and high Cash-total selectivities were observed throughout (Figure 4.21a), including close to 80 % selectivity at 50 % conversion. When the level of catalyst was reduced significantly to only 50 ppm (Figure 4.23), the level of Cash-total selectivity dropped from 80 to 70 % at 50 % conversion and much higher levels of hydroperoxide were observed, with initial levels of hydroperoxide dropping from 50 to 5 %. The overall selectivity trends when using 50 ppm of Co-bis(2-EH) were more similar to reactions with  $\text{Co}_3\text{O}_4$  (Figure 4.21b) and  $\text{CoO/SiO}_2$  (Figure 4.14b). The major difference being that when using 50 ppm of Co-bis(2-EH), THPMI-HP reduced in concentration more gradually when compared with the heterogeneous catalysts, where a more rapid drop off was observed above 70 % conversion. These results demonstrate an interesting duality in the function of Co-bis(2-EH); only ppm levels of the catalyst are required to oxidise THPMI into THPMI-HP rapidly. However, relatively much higher loadings are required to break down THPMI-HP into the desired products and thus

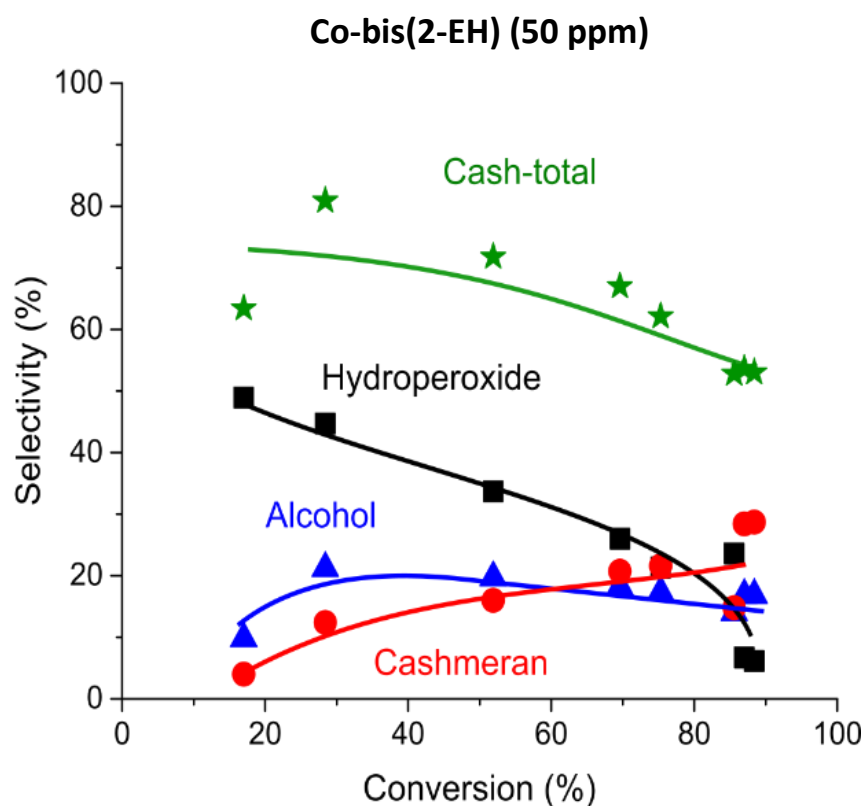


**Figure 4.23.** Selectivity against conversion for reaction with ppm levels of Co-bis(2-ethylhexanoate). Conditions: THPMI (10 ml), hexadecane (1 ml), 70 °C, 1 - 24 h, Co-bis(2-ethylhexanoate) (50 ppm), Air residence time (0.5 min), 900 rpm. Data was taken from 3 separate reactions.

improve Cash-total selectivity. It is likely that ppm levels of Co-bis(2-EH) were acting as a catalytic initiator for radical oxidation, but then did not play a significant role in the formation of desired products. Alternatively, 0.15 wt% Co-bis(2-EH) was acting as both a catalytic initiator and as a catalyst to direct selectivity towards Cashmeran. It should also be noted that these tests were conducted at 70 °C, where autoxidation is not significant, and the initiating property of Co-bis(2-EH) becomes less important at industrial temperature (110 °C) where autoxidation is significant.

## 4.6 Molybdenum Blue as a Catalyst for THPMI Oxidation

The results of testing  $\text{Co}_3\text{O}_4$  and  $\text{CoO/SiO}_2$  demonstrated that these catalysts could activate catalytic oxidation of THPMI, but were not effective at breaking down the first oxidation product, THPMI-HP. To demonstrate similar, or improved, activity to Co-bis(2-EH), a catalyst must be utilised which is capable of breaking down THPMI-HP into Cashmeran and Cashmeran-alcohol rapidly and selectively.

Molybdenum Blue is commonly used in quantification assays of phosphate ions<sup>32</sup> and reducing sugars.<sup>33</sup> For a long time the structure was unknown, however characterisation performed in the 1990s unveiled Molybdenum Blue to be made of  $[\text{Mo}^{6+}_{126}\text{Mo}^{5+}_{28}\text{O}_{462}\text{H}_{14+}(\text{H}_2\text{O})_{70}]^{14-}$  anions, with a supramolecular arrangement of nano-wheels of approximately 2 nm in diameter.<sup>34–36</sup> The structure of Molybdenum Blue was recently imaged using scanning transmission electron microscopy.<sup>37</sup> Molybdenum Blue has demonstrated activity as a selective catalyst for cyclohexane oxidation even in the presence of a radical scavenger, a property which was not replicated in cobalt naphthenate in the same study.<sup>37</sup> The selectivity of cyclohexane oxidation has also shown to be tuneable towards adipic acid production with thermal treatment of Molybdenum Blue.<sup>36</sup> Most importantly, it has been suggested that Molybdenum Blue will bond to cyclohexane-hydroperoxide and catalyse its subsequent non-radical breakdown into cyclohexanol.<sup>36</sup> If Molybdenum Blue can demonstrate similar catalytic properties with THPMI-HP as the substrate, then this may provide a route for efficient and selective decomposition into Cashmeran and Cashmeran-alcohol.

## 4.6.1 Characterisation of Molybdenum Blue

### 4.6.1.1 Microwave Plasma Atomic Emission Spectroscopy (MP-AES)

MP-AES was used to quantify the metal content of Molybdenum Blue. Molybdenum makes up 51.2 % of the mass of the catalyst, lower than the 63.0 % for a pure  $[\text{Mo}^{6+}_{126}\text{Mo}^{5+}_{28}\text{O}_{462}\text{H}_{14+}(\text{H}_2\text{O})_{70}]^{14-}$  phase.

**Table 4.9.** MP-AES analysis for Molybdenum Blue.

Element	Nomial Loading (wt%)	Actual Loading (wt%)
Mo	63.0	51.2

### 4.6.1.2 X-ray Photoelectron Spectroscopy (XPS)

The XPS spectrum for Molybdenum Blue was similar to previous examples in the literature.<sup>37–39</sup> The peak at 233.2 eV with a satellite at 236.5 eV can be assigned to  $\text{Mo}^{6+}$  and the peak at 231.9 eV with a satellite at 235.1 eV can be assigned to  $\text{Mo}^{5+}$ .<sup>37,38</sup> The relative ratio of  $\text{Mo}^{6+}$  to  $\text{Mo}^{5+}$  from XPS was 3 : 1, which is not far from the 4 : 1 ratio observed in the literature from XPS<sup>37</sup> and previously from titration.<sup>40</sup>

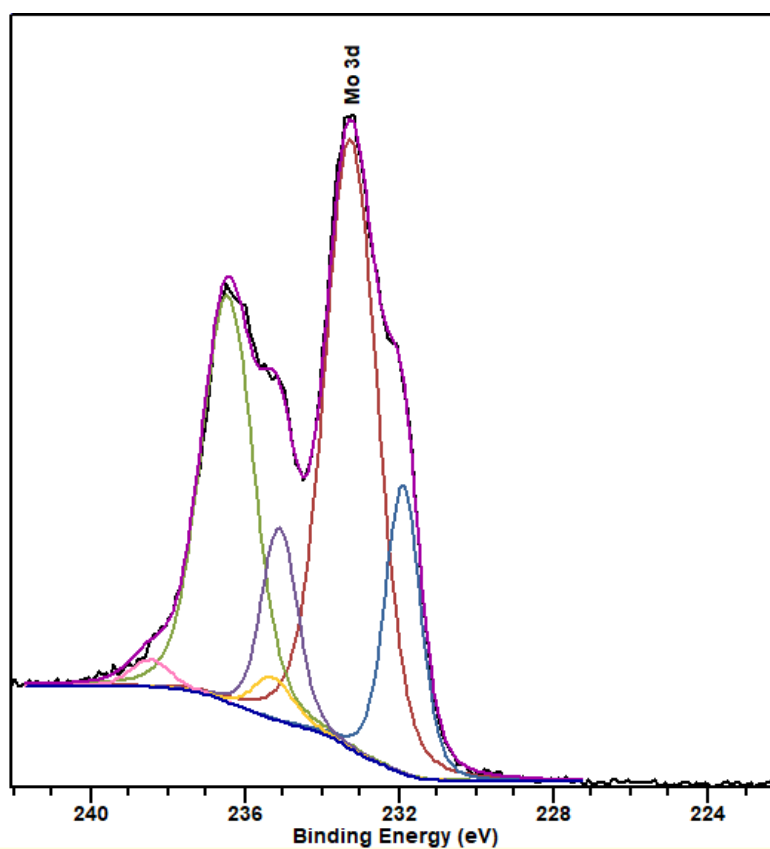


**Figure 4.24.** XPS spectra for Molybdenum Blue.

Quantification of the surface from XPS gave a molybdenum weight content of 70.2 %, greater than 63 %, which would be expected from a pure  $[\text{Mo}^{6+}_{126}\text{Mo}^{5+}_{28}\text{O}_{462}\text{H}_{14+}(\text{H}_2\text{O})_{70}]^{14-}$  phase. This may be due to the presence of some  $\text{MoO}_2$  phase on the surface, which would have a molybdenum concentration 75 %, if pure.

**Table 4.10.** Surface concentration of molybdenum blue from XPS.

Metal	Mol %	Weight %
Mo	28.3	70.2
O	71.7	29.8

#### 4.6.1.3 Powder X-ray Diffraction (XRD)

The broad reflections centred at  $28^\circ$  and  $52^\circ$  correspond well with literature for Molybdenum Blue<sup>39</sup> (Figure 4.25). If a  $\text{MoO}_2$  phase was present in this catalyst, a reflection at  $37^\circ$  would be observed, and for  $\text{MoO}_3$  a reflection at  $39^\circ$ ,<sup>39</sup> neither of which were observed and so no significant  $\text{MoO}_2$  or  $\text{MoO}_3$  phases are present in the bulk of the catalyst. It should be noted that other more intense reflections observed for  $\text{MoO}_2$  and  $\text{MoO}_3$  would be disguised by the strong Molybdenum Blue reflections.

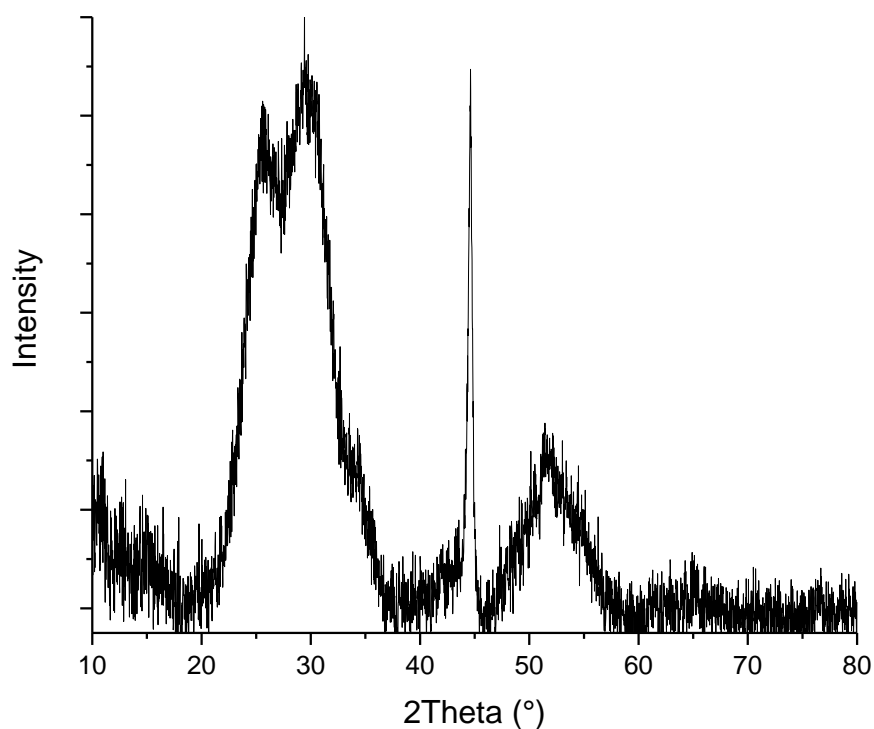


**Figure 4.25.** XRD pattern for Molybdenum Blue.

#### 4.6.1.4 Scanning Electron Microscopy (SEM) and Energy Dispersive X-ray Spectroscopy (EDX)

SEM imaging of the solid Molybdenum Blue sample showed very large crystalline particles in the micro-meter size range (Figure 4.26). EDX analysis of two separate regions demonstrated a molybdenum weight percentage of 76.4 % ( $\pm 2.1$ ) (Table 4.11). This suggests the presence a  $\text{MoO}_2$  phase, where the molybdenum weight percentage would be 75 %. The images from EDX mapping suggest regions of more concentrated oxygen content (Figure 4.27). Areas of higher oxygen content may suggest a more pure Molybdenum Blue phase, as the oxygen to molybdenum ratio of Molybdenum Blue is 3.5 : 1.

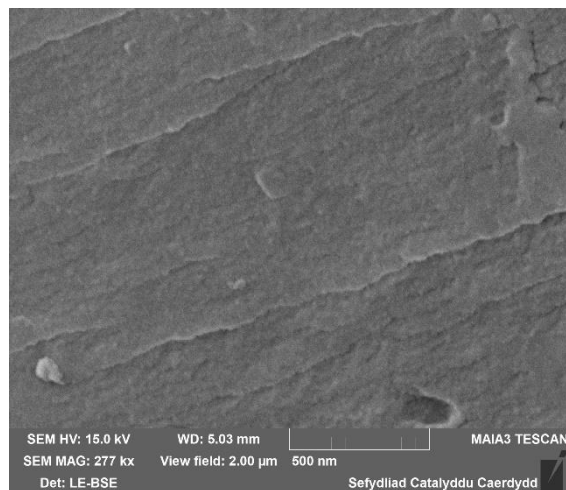
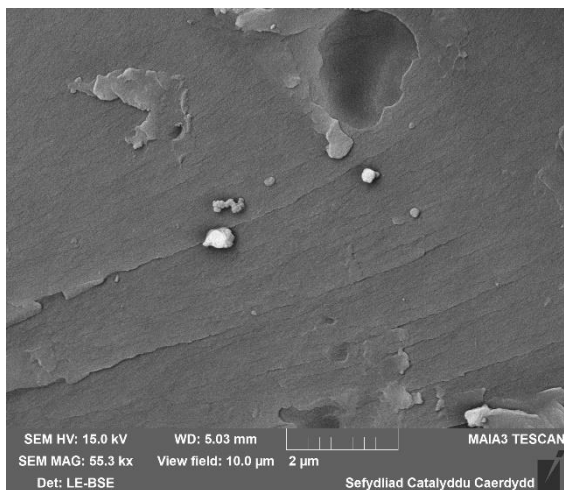
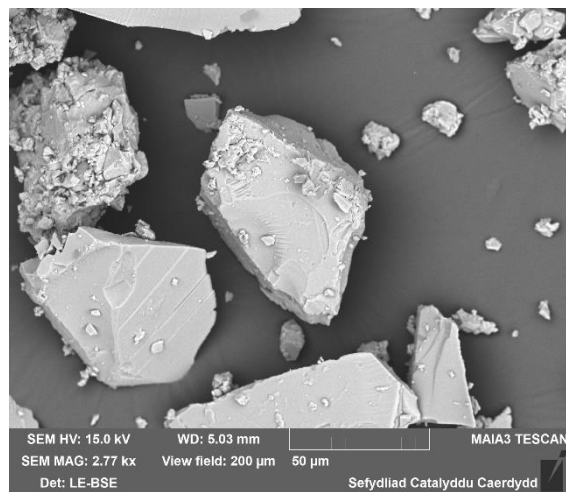
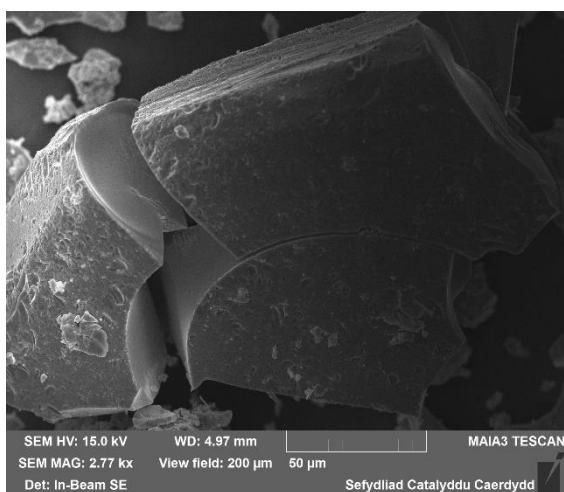
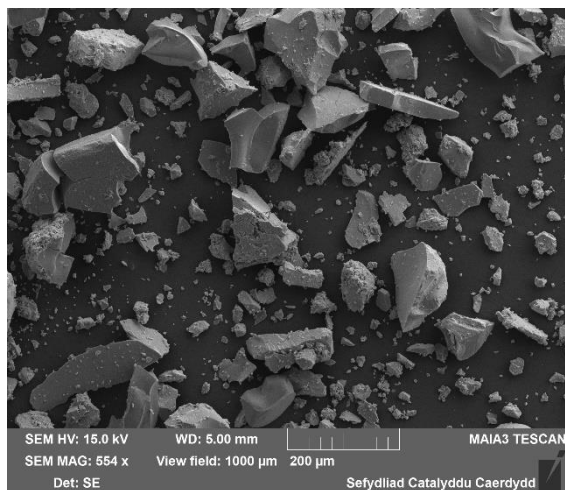
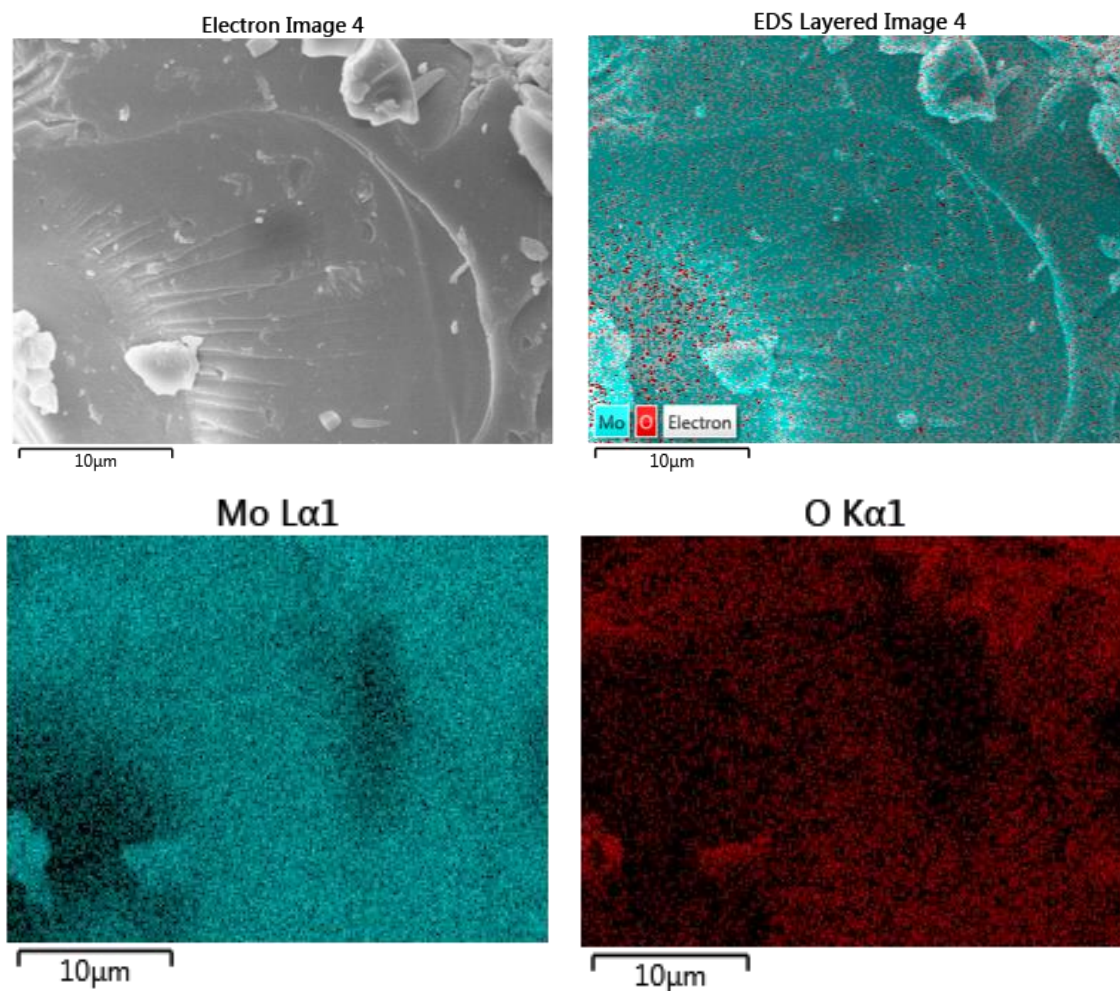


Figure 4.26. Images from SEM for molybdenum blue.

**Table 4.11.** Surface coverage of Molybdenum Blue from EDX analysis.

Element	Mol %	Weight %
Mo	35.1 ( $\pm$ 2.7)	76.4 ( $\pm$ 2.1)
O	64.9 ( $\pm$ 2.7)	23.6 ( $\pm$ 2.1)



**Figure 4.27.** EDX mapping of Molybdenum Blue.

## 4.6.2 Catalytic Testing of Molybdenum Blue

Molybdenum Blue was initially tested at 70 °C, as with the two cobalt catalysts in the previous sections (4.3.2 and 0). However, the activity of the catalyst was so poor at this temperature that even the blank reaction saw a greater rate of conversion (Figure 4.28). The temperature of the reaction was increased from 70 to 110 °C and although the rate of reaction did increase, it was still much slower than reactions with Co-bis(2-EH),  $\text{Co}_3\text{O}_4$  (Figure 4.13) or  $\text{CoO/SiO}_2$  (Figure 4.20), with only 25 % conversion being reached after 24 h. At both 70 and 110 °C the rate of reaction was slower than their respective blank reactions with no catalyst present, which suggests that Molybdenum Blue was in some way inhibiting the reaction, possibly by acting as a radical scavenger.

A graph depicting the selectivity when using Molybdenum Blue as the catalyst is not shown as the selectivity was zero or very close to zero for all the major products (Cashmeran, Cashmeran-alcohol and THPMI-HP) in all reaction samples taken. It is currently unknown what the THPMI is being converted into, but it was not detectable by GC or GC-MS.

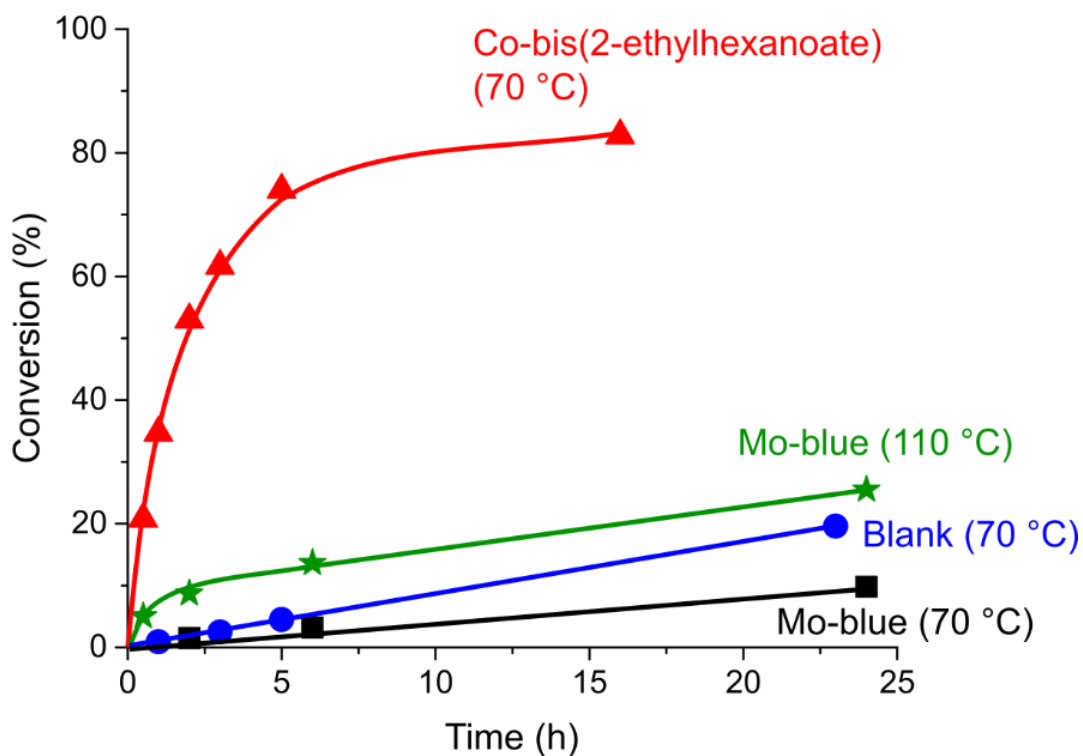


**Figure 4.28.** Conversion against time for reactions with molybdenum blue as the catalyst, compared to the standard industrial catalyst and the blank reaction all at 70 °C. Conditions THPMI (10 ml), hexadecane (1 ml), 70 or 110 °C, 0.5- 23 h, molybdenum blue (100 mg/1.15 wt%), air residence time (0.5 min), 900 rpm. All data plots were taken from 1 reaction each.

There is evidence in the literature of  $\text{MoO}_3$  nanoparticles having anti-oxidant and radical scavenging properties,<sup>41,42</sup> and molybdenum based polyoxometalates have been observed to

possess radical scavenging capabilities.<sup>43</sup> It is possible that if even low levels of these species are present in the prepared Molybdenum Blue, it would prevent further oxidation, as was observed.

## 4.7 Conclusions

Several alternative catalysts were tested with the aim of improving the selectivity achieved in the current industrial process of converting THPMI into Cashmeran, currently catalysed by Co-bis(2-EH). Acid catalysts were tested with the aim of catalysing the direct decomposition of THPMI-HP into Cashmeran, circumventing the formation of the more reactive Cashmeran-alcohol. Amberlyst-15 and glutaric acid were both tested as catalysts individually and both resulted in suppression of conversion of THPMI and product selectivity. These results suggest that these acids in the reaction are either acting as radical scavengers, possibly in a similar manner to ascorbic acid,<sup>5</sup> or are catalysing alternative reaction routes which do not lead to radical propagation and the desired products. Butyric acid was added to a post reaction mixture; it was found that even after only 15 minutes of reaction much of the THPMI-HP had been converted into Cashmeran-alcohol. This supports the theory that acid catalysis can be used to decompose THPMI-HP, however not to Cashmeran as intended. This result supports literature that suggests that organic hydroperoxides can be converted into alcohols *via* acid catalysis, with a ketone being used as a co-catalyst.<sup>3</sup> More subtle effects were observed when using 2-ethylhexanoic acid as the catalyst. Decomposition of THPMI-HP was observed, but no change in Cash-total selectivity relative to the blank reaction. A slight quenching effect was observed with a larger loading of 2-ethylhexanoic acid. Overall, acid catalysts did not offer any improvement on the current process for oxidation of THPMI and in many cases prevented the reaction from occurring. Acids can clearly decompose THPMI-HP under certain reaction conditions and so a more detailed study into the effect of pH on the reaction should be undertaken; it may be the case that acidic products are forming in the reactions, altering the pH and so affecting selectivity.

CoO/SiO<sub>2</sub> was prepared first by amination of the silica support and then by deposition of the cobalt active phase. Amination and the presence of a CoO phase were determined by IR and XPS, with CoO either being made up of very small < 2 nm size particles or as a thin film on the surface of the catalyst. The catalyst was tested at 70 °C and was found to be catalytically active, but less active than Co-bis(2-EH). Cash-total selectivity was lower than for the industrial benchmark and was directed mainly towards THPMI-HP, demonstrating CoO/SiO<sub>2</sub> is capable of oxidising THPMI, but not breaking down the primary hydroperoxide product.

Bulk  $\text{Co}_3\text{O}_4$  was produced by co-precipitation from cobalt nitrate and sodium carbonate followed by a heat treatment. The resulting material was expected to show similar reaction selectivity to  $\text{CoO}/\text{SiO}_2$  as  $\text{Co}_3\text{O}_4$  is typically a non-selective total oxidation catalyst.<sup>22–24</sup>  $\text{Co}_3\text{O}_4$  was initially more active than  $\text{CoO}/\text{SiO}_2$ , but still less active than Co-bis(2-EH). Selectivity when using  $\text{Co}_3\text{O}_4$  was largely similar to  $\text{CoO}/\text{SiO}_2$ , however less THPMI-HP and more alcohol was observed in the reaction with  $\text{Co}_3\text{O}_4$ . The reduction in activity by switching from the homogeneous Co-bis(2-EH) to the heterogeneous cobalt catalysts may infer information about the mechanism of activation. The homogeneous catalyst will initiate a radical cascade mechanism with a rapid rate of reaction due to the very low activation energy. The heterogeneous catalysts possibly operate *via* a non-radical Mars and Van Krevelen mechanism,<sup>21,30</sup> which has a higher activation energy and so results in a slower rate of reaction.

For the various reactions of THPMI oxidation with heterogeneous cobalt catalysts, leaching was analysed using ICP-MS. It was discovered that up to 4 ppm cobalt can leach into the reaction mixture, depending on the reaction conditions. To test the effect this may have on the reaction, reactions were run with 3 and 50 ppm Co-bis(2-EH). With 3 ppm Co-bis(2-EH) conversion only increased slightly above the blank reaction, and only towards the end of the reaction. This suggests that the cobalt leaching observed with  $\text{CoO}/\text{SiO}_2$  and  $\text{Co}_3\text{O}_4$  will have little effect on the selectivity and conversion and if so, it will be towards the end of the reaction, perhaps promoting the decomposition of THPMI-HP. When 50 ppm Co-bis(2-EH) was added as catalyst, high activity was observed but selectivity was largely similar to reactions with  $\text{CoO}/\text{SiO}_2$  and  $\text{Co}_3\text{O}_4$ . This result demonstrated that only ppm levels of homogeneous cobalt are required to initiate and promote the oxidation of THPMI, but much larger loadings are required to direct selectivity towards Cashmeran and Cashmeran-alcohol.

Due to neither heterogeneous cobalt-based catalyst being selective towards the Cash-total products, Molybdenum Blue was prepared and tested as it has previously demonstrated hydroperoxide decomposing traits.<sup>36,37</sup> Molybdenum Blue was produced in a simple procedure reacting molybdenum metal with hydrogen peroxide. The dark blue solid was tested as a catalyst at both 70 and 110 °C and at both temperatures conversion and selectivity were severely suppressed. It is likely that either Molybdenum Blue, an impurity formed during its preparation, or a species that forms from it *in situ* is a radical scavenging species, as observed for other molybdenum species.<sup>41–43</sup>

Clearly the oxidation of THPMI is a vastly complicated process with many competing pathways to form desired and undesired products. The results described in this chapter demonstrate that for a catalyst to match the selectivity achieved by 0.15 wt% Co-bis(2-EH), it must break down THPMI-HP in a rapid and controlled way so as to avoid uncontrolled radical

pathways. CoO/SiO<sub>2</sub>, Co<sub>3</sub>O<sub>4</sub>, and 50 ppm Co-bis(2-EH) seem to promote the formation of THPMI-HP but not its decomposition, therefore leading to limited Cash-total selectivity. Some ideas to overcome this limitation are presented in chapter 5.

## 4.8 References

- 1 X. Liu, Y. Ryabenkova and M. Conte, *Phys. Chem. Chem. Phys.*, 2015, **17**, 715–731.
- 2 M. S. Kharasch and J. G. Burt, *J. Org. Chem.*, 1950, **16**, 150–160.
- 3 L. V. Petrov, T. I. Drozdova, L. Y. Lyuta and V. M. Solyanikov, *Bull. Acad. Sci. USSR, Div. Chem. Sci.*, 1990, **39**, 226–232.
- 4 C. Iditoiu, E. Segal and B. C. Gates, *J. Catal.*, 1978, **54**, 442–445.
- 5 E. Niki, *Am. J. Clin. Nutr.*, 1991, **54**, 1119–1124.
- 6 F. P. Silva, M. J. Jacinto, R. Landers and L. M. Rossi, *Catal. Letters*, 2011, **141**, 432–437.
- 7 G. A. Carson, M. H. Nassir, M. A. Langell, G. A. Carson, M. H. Nassir and M. A. Langell, *J. Vac. Sci. Technol.*, 1996, **14**, 1637–1642.
- 8 M. C. Biesinger, B. P. Payne, A. P. Grosvenord, L. W. M. Laua, A. R. Gersonb and R. S. C. Smart, *Appl. Surf. Sci.*, 2011, **257**, 2717–2730.
- 9 J. W. Niemantsverdriet, in *Spectroscopy in Catalysis: An Introduction*, Weinheim, 3rd edn., 2007, pp. 41–44.
- 10 J. I. Goldstein, D. E. Newbury, J. R. Michael, N. W. M. Ritchie, J. H. J. Scott and D. C. Joy, in *Microscopy and X-Ray Microanalysis*, Springer, 4th edn., 2018, p. X.
- 11 S. Azarshin, J. Moghadasi and Z. A Aboosadi, *Energy Explor. Exploit.*, 2017, **35**, 685–697.
- 12 R. Ranjbar-Karimi, A. K. Khezri and M. Anary-Abbasinejad, *Heterocycl. Lett.*, 2014, **2**, 301–310.
- 13 S. Deka and K. Deori, *CrystEngComm*, 2013, **15**, 8465–8474.
- 14 C. Weidenthaler, *Nanoscale*, 2011, **3**, 792–810.
- 15 R. A. Sheldon and J. K. Kochi, in *Metal-catalyzed Oxidations of Organic Compounds*, Academic Press, 1981, p. 274.
- 16 S. Pattisson, O. Rogers, K. Whiston, S. H. Taylor and G. J. Hutchings, *Catal. Today*, 2020,

- 357, 3–7.
- 17 R. A. Sheldon and J. K. Kochi, in *Metal-catalyzed Oxidations of Organic Compounds*, Academic Press, 1981, p. 45.
- 18 J. F. Black, *J. Am. Chem. Soc.*, 1978, **100**, 527–535.
- 19 G. A. Russell, *J. Am. Chem. Soc.*, 1957, **79**, 3871–3872.
- 20 U. N. Gupta, N. F. Dummer, S. Patisson, R. L. Jenkins, D. W. Knight, D. Bethell and G. J. Hutchings, *Catal. Letters*, 2015, **145**, 689–696.
- 21 G. A. El-Shobaky, M. M. Selim and I. F. Hewaidy, *Surf. Technol.*, 1980, **10**, 55–63.
- 22 B. Solsona, T. Garcia, T. E. Davies, A. Dejoz and S. H. Taylor, *Catal. Letters*, 2007, **84**, 176–18.
- 23 B. Solsona, A. Dejoz, T. E. Davies, T. Garcia, I. Va and S. H. Taylor, *Appl. Catal. B Environ.*, 2008, **84**, 176–184.
- 24 G. Busca, M. Daturi, E. Finocchio, V. Lorenzelli, G. Ramis and R. J. Willey, *Catal. Today*, 1997, **33**, 239–249.
- 25 B. Solsona, T. García, G. J. Hutchings, S. H. Taylor and M. Makkee, *Appl. Catal. A Gen.*, 2009, **365**, 222–230.
- 26 Q. Liu, L. C. Wang, M. Chen, Y. Cao, H. Y. He and K. N. Fan, *J. Catal.*, 2009, **263**, 104–113.
- 27 R. K. Pinnell, PhD Thesis, Cardiff University, 2014.
- 28 P. Porta, R. Dragone, G. Fierro, M. Inversi, M. Lo Jacono and G. Moretti, *J. Chem. Soc. Faraday Trans.*, 1992, **88**, 311–319.
- 29 J. Stoch, 1991, **17**, 165–167.
- 30 P. Mars and D. W. van Krevelen, *Chem. Eng. Sci.*, 1954, **3**, 41–59.
- 31 M. Conte, X. Liu, D. M. Murphy and G. J. Hutchings, *Phys. Chem. Chem. Phys.*, 2012, **14**, 16279–16285.
- 32 Z. He and C. W. Honeycutt, *Commun. Soil Sci. Plant Anal.*, 2007, **36**, 1373–1383.
- 33 S. P. Deng and M. A. Tabatabai, *Soil Biol. Biochem.*, 1994, **26**, 473–477.
- 34 C. Serain, *Acc. Chem. Res.*, 2000, **33**, 2–10.
- 35 A. Müller, J. Meyer, E. Krickemeyer and E. Diemann, *Angew. Chemie - Int. Ed.*, 1996, **35**,

1206–1208.

- 36 M. Conte, X. Liu, D. M. Murphy, S. H. Taylor, K. Whiston and G. J. Hutchings, *Catal. Letters*, 2016, **146**, 126–135.
- 37 X. Liu, M. Conte, W. Weng, Q. He, R. L. Jenkins, M. Watanabe, D. J. Morgan, D. W. Knight, D. M. Murphy, K. Whiston, C. J. Kiely and G. J. Hutchings, *Catal. Sci. Technol.*, 2015, **5**, 217–227.
- 38 N. Gavrilova, V. Dyakonov, M. Myachina, V. Nazarov and V. Skudin, *Nanomaterials*, 2020, **10**.
- 39 O. Koyun, S. Gorduk, M. B. Arvas and Y. Sahin, *Synth. Met.*, 2017, **233**, 111–118.
- 40 C. M. Callahan, S. C. Foti and J. R. Lai, *Anal. Chem.*, 1960, **32**, 635–637.
- 41 A. Fakhri and P. Afshar, *J. Photochem. Photobiol. B Biol.*, 2016, **159**, 211–217.
- 42 M. Marimuthu, B. P. Kumar, L. M. Salomi, M. Veerapandian and K. Balamurugan, *Appl. Mater. Interfaces*, 2018, **10**, 43429–43438.
- 43 D. Ni, D. Jiang, C. J. Kutyreff, J. Lai, Y. Yan, T. E. Barnhart, H. Im, L. Kang, S. Y. Cho, Z. Liu, P. Huang, J. W. Engle, W. Cai and B. Yu, *Nat. Commun.*, 2018, **9**, 5421.

# 5 Conclusions & Future Work

## 5.1 Conclusions

The industrial production of Cashmeran is of great importance due to its unique odour properties that no other widely produced fragrant molecules possess.<sup>1,2</sup> Currently the process to produce Cashmeran from THPMI is limited because of decreasing selectivity with increasing conversion. The work conducted in chapter 3 of this thesis describes the effect Co-bis(2-ethylhexanoate) has on the aerobic oxidation, along with other studies of the effects of various reaction conditions. Chapter 4 describes testing of alternative catalysts that was conducted for the aerobic oxidation of THPMI. Summaries of the findings in these chapters are given below.

### 5.1.1 The Effect of Co-bis(2-ethylhexanoate) on the Oxidation of THPMI

Reaction conditions were established for the laboratory-scale aerobic oxidation of THPMI, where air is bubbled through the reaction mixture. Stir speed and the air flow were maximised so as to avoid mass transfer limitations when assessing different reaction conditions and catalysts. Reaction products were identified including THPMI-HP, which is not usually quantified in industrial analysis, as well as three undesired overoxidation products, and suspected THPMI-epoxide. The over-oxidation products and THPMI-epoxide not being identified prior to this work.

The oxidation of THPMI with Co-bis(2-EH) under industrially replicated conditions was compared with the equivalent blank reaction with no catalyst at various temperatures. It was confirmed that both reactions proceed primarily *via* radical mechanisms as the addition of the radical scavenger, BHT, suppresses both conversion and selectivity significantly. The catalyst affects the reaction in three ways: firstly, by initiating and promoting the reaction even at temperatures below autoxidation; secondly by affecting selectivity in three ways, described below; and thirdly by causing reaction quenching if a high enough Co-bis(2-EH) loading is applied, this effect is also dependent on reaction temperature. The effect on selectivity is perhaps the most important feature when considering the benefits of using Co-bis(2-EH). There are three effects on selectivity: firstly, the improvement of the overall Cash-total selectivity by 16 % at 50 % conversion compared to the blank reaction with no catalyst; secondly by increasing

the Cashmeran to Cashmeran-alcohol ratio, which is also proportional to temperature; and thirdly by reducing the concentration of THPMI-HP in the reaction to close to 0 %. By catalysing the rapid reaction of THPMI-HP, large concentrations cannot build up and so the reactive hydroperoxide is less likely to undergo O—O bond cleavage, producing reactive radical species. By catalysing the oxidation of Cashmeran-alcohol into Cashmeran, the relatively more reactive (to oxidation) alcohol is also not in large concentrations. By suppressing the formation of the alcohol and hydroperoxide products and forming the relatively less reactive (to oxidation) ketone; this likely means that undesired reactions stemming from these products are occurring at lower rates than in the equivalent blank reaction, thus leading to the effect of greater overall Cash-total selectivity. This is similar to the use of cobalt to break down CHHP in cyclohexane oxidation to improve selectivity.<sup>3-8</sup>

For both blank and catalysed oxidations of THPMI the Cash-total selectivity decreases with conversion. Three over-oxidation products have been identified, HCA, HC and CK (section 3.3), which can account for up to 12 % of the products. There is currently no evidence that the improvement in selectivity in the catalysed reaction is due to fewer over-oxidised products, however there is some evidence of Co-bis(2-EH) catalysing the oxidation of the alcohol HCA into HC. THPMI-epoxide was found to form at very low (< 5%) concentration in the reactions, and around 1 % less in the reactions with Co-bis(2-EH). THPMI-epoxide and the over-oxidation products do not account for all of the undesired products as many are not observed by the GC analysis used in this thesis. It is expected that the over-oxidation products can react further as they reduce in concentration if the blank reaction is left to run for an extended period of time. It is currently thought that products not appearing by our GC analysis are either highly oxidised gaseous species or heavy polymerised products, as observed in the industrial reaction.

Altering the temperature of the catalysed oxidation of THPMI had a negligible effect on Cash-total selectivity, however it did affect the composition of the Cash-total. A rise in reaction temperature results in an increase in the Cashmeran to Cashmeran-alcohol ratio, suggesting higher temperatures facilitate more rapid alcohol oxidation. The very low activation energy in reactions with radicals<sup>9,10</sup> is likely the reason altering temperature did not have much effect on selectivity.

It was confirmed that the primary benefits of using Co-bis(2-EH), compared to adding no catalyst, are due to the Co<sup>2+</sup> metal centre rather than the excess ligand, 2-Ethylhexanoate, present in the catalyst mixture. When Co(acac)<sub>2</sub> was used as the catalyst, similar results were observed to the standard reaction with Co-bis(2-EH). 2-ethylhexanoic acid as a catalyst demonstrated ability to decompose THPMI-HP, but not as rapidly as Co-bis(2-EH), although this did not result in a Cash-total selectivity superior to the blank reaction.

The work conducted in chapter 3 has detailed many properties of the industrial oxidation of THPMI to Cashmeran, including reaction products, selectivity, mass transfer effects, temperature effects and most importantly the effect of the catalyst. The catalyst, Co-bis(2-EH) has a subtle yet significant effect on the reaction and its properties can be described as somewhere between a radical initiator and a catalyst. To improve on the current industrial process this work must be understood and expanded on; only by understanding the current process can future research attempt to improve it.

### 5.1.2 Investigating Alternative Catalysts for the Oxidation of THPMI

To improve the selectivity to Cash-total products observed in Chapter 3, several alternative catalysts were tested. Two acid catalysts, Amberlyst-15 and glutaric acid, were tested and caused suppression of conversion and selectivity despite being tested at 110 °C, well above autoxidation, suggesting that the acids here are acting as radical inhibitors. A post reaction mixture, in which THPMI-HP was the major product, was treated with butyric acid under nitrogen. This resulted in the decomposition of much of the THPMI-HP into Cashmeran-alcohol. 2-Ethylhexanoic acid was tested as a catalyst and demonstrated some ability to decompose THPMI-HP into desired products but at no improvement to Cash-total selectivity. Acids demonstrated ability to decompose THPMI-HP over several reactions, however this did not improve Cash-total selectivity and in some cases reduced it, along with suppressing the rate of reaction. More work needs to be undertaken to understand the effect of pH on the oxidation of THPMI.

Two heterogeneous catalysts, CoO/SiO<sub>2</sub> and Co<sub>3</sub>O<sub>4</sub>, were tested at 70 °C, below significant autoxidation. Both catalysts were active for oxidation, although did not improve Cash-total selectivity compared to the blank reaction. Both catalysts demonstrated ability to form THPMI-HP, but not to break it down, with Co<sub>3</sub>O<sub>4</sub> being slightly more active for both THPMI oxidation and THPMI-HP decomposition into Cashmeran-alcohol. Up to 4 ppm of cobalt was found to leach into the liquid phase of the reaction mixture when using these catalysts. Testing equivalent ppm concentrations of Co-bis(2-EH) as catalysts demonstrated that this low level of leaching has little effect on the reaction, and if it does, it will be observed several hours into the reaction. When a larger 50 ppm loading of Co-bis(2-EH) was used as the catalyst, a much more significant effect was observed. The rate of THPMI oxidation was increased significantly, although not to the rate observed with a standard loading of 0.15 wt%, and large concentrations of THPMI-HP were detected. This demonstrated that only 50 ppm Co-bis(2-EH) is required to initiate THPMI

oxidation and produce a fairly rapid rate of reaction. However, much more Co-bis(2-EH) is required to affect the selectivity and improve Cashmeran yield.

Molybdenum Blue was the final heterogeneous catalyst to be tested and it resulted in extremely low conversions and close to 0 % selectivity to desired products. This low reactivity occurred even at 110 °C, well above autoxidation, suggesting that either Molybdenum Blue, a component of it, or a species which forms in the reaction mixture is acting as a radical scavenger; there is precedent for this in the literature.<sup>11-13</sup>

Although none of the alternative catalysts tested improved on the activity or selectivity achieved using Co-bis(2-EH), much was learned from the experiments. For a catalyst to be selective for the formation of Cashmeran from THPMI, it must breakdown THPMI-HP rapidly and not just catalyse its formation by activating oxygen. A very specific catalyst must be designed that does not just initiate radical oxidation but genuinely catalyses the formation of Cashmeran, without catalysing its over-oxidation. Some proposals for experiments to achieve these goals are provided in the next section.

## 5.2 Future Work

The work covered in chapter 3 of this thesis demonstrates the presence of three over-oxidation products and the possible presence of THPMI-epoxide from the oxidation of THPMI. However, more products in this reaction are currently uncharacterised; some appear on GC analysis, and some do not. It is possible that if over-oxidation continues to occur then gaseous products such as CO<sub>2</sub> may form, as with gold-catalysed cyclohexene oxidation in polar solvents.<sup>14</sup> It is also possible that oligomerisation or polymerisation reactions are occurring in small amounts as suggested by the industrial reactions, and demonstrated in the oxidation of methylstyrene.<sup>15</sup> A comprehensive study of all of the products of oxidation, including gaseous products and polymerised products, is required to fully understand which reaction pathways need to be avoided to improve selectivity.

It has been demonstrated that pH has some impact on the reaction, however it is currently unclear how this is manifested. A comprehensive study of the pH of the reaction over time may provide insights into a link between pH variation and effects on selectivity. Controlling the pH of the reaction medium may be the key to controlling the selectivity.

It is clear that, with or without Co-bis(2-EH) as the catalyst, the main driver of the reaction is the radical autoxidation mechanism that initially forms THPMI-HP. Once this mechanism is initiated it is extremely hard to control;<sup>16</sup> in this case Co-bis(2-EH) can only direct selectivity

rather than control it. To completely control selectivity, it may be necessary to avoid this radical mechanism altogether and use a catalyst that can catalyse oxidation by a non-radical route. This would require a capable catalyst and the reaction to be run at a low enough temperature for THPMI-HP to be stable, or the addition of radical scavengers. Molybdenum Blue was theorised to be an example of a catalyst capable of oxidation *via* a non-radical route,<sup>17</sup> however in this work it proved itself to act as a radical scavenger. Denekamp *et al.*<sup>18</sup> demonstrated a copper catalyst supported on porous, nitrogen-doped carbon that was active for the oxidation of cyclohexene. More importantly it was active in the presence of the radical scavenger, BHT. It was theorised that the bulky BHT molecules were too large to enter the pores, and so the copper active site could catalyse the oxidation of cyclohexene, and the subsequent decomposition of cyclohexene hydroperoxide, without the release of radical species into the solution. Although this exact catalyst would be unsuitable for THPMI, as the pores would be too small for THPMI to enter, an adapted catalyst could be produced that could control reaction selectivity more effectively than the current system. Rucinska *et al.*<sup>19</sup> demonstrated supported gold-palladium catalysts are capable of directing oxidation of cinnamyl alcohol away from autoxidation products and towards catalysed oxidation products, without the need for added scavengers. Although this system is for alcohol oxidation and not alkene oxidation, it demonstrates the potential in good catalyst design to control selectivity of oxidation reactions when radical routes are operative.

Another tactic to control the radical-mediated mechanism is to quench specific radical species in solution, with the aim to shut off undesired radical reaction routes. Dialkyl nitroxides have been used to specifically trap carbon-centred radicals,<sup>20</sup> galvinoxyl has been used to specifically trap oxygen-centred radicals,<sup>16,21</sup> and a selective spin trap for hydroxy radicals has been demonstrated.<sup>22</sup> A comprehensive study of the effects of these various radical scavengers or spin trappers may reveal which types of radical are causing unwanted reactions. If unwanted radical reaction routes can be quenched, without preventing desired routes of radical autoxidation, then improvements to Cash-total selectivity may be observed.

A more significant change from the current process would be to explore replacing the current semi-batch process with a continuous flow process. This may offer several benefits over the current process including improved mixing, mass transfer, and safety with the implementation of pure, or less dilute, O<sub>2</sub> possible safely.<sup>23,24</sup> It was demonstrated in the aerobic oxidation of 2-benzylpyridine that conversion can be controlled in a continuous flow system by altering flow rate, temperature or other conditions.<sup>25</sup> This is relevant for the oxidation of THPMI as currently conversion is limited to near 50 % conversion as selectivity drops at higher conversions. In a flow system, conditions could be applied where products are extracted at 50 %

conversion or lower, continuously. This could also occur with a much shorter reaction time with improved mass transfer, and a more efficient use of reactor space as the head space in the current batch reactor is eliminated. Continuous flow systems can be scaled from laboratory scale by running processes for longer, by increasing flow, by increasing the number of units, or by increasing volume in the reactor.<sup>26</sup> Flow systems generally scale up more effectively than for batch reactors, where it is often very difficult to replicate laboratory to industrial scale.<sup>23</sup>

## 5.3 References

- 1 I. Felker, G. Pupo, P. Kraft and B. List, *Angew. Commun.*, 2015, **54**, 1960–1964.
- 2 P. Kraft, V. Di Cristofaro and S. Jordi, *Chem. Biodivers.*, 2014, **11**, 1567–1596.
- 3 E. J. Silke, W. J. Pitz, C. K. Westbrook and M. Ribaucour, *J. Phys. Chem.*, 2007, **111**, 3761–3775.
- 4 A. Ramanathan, M. S. Hamdy, R. Parton, T. Maschmeyer, J. C. Jansen and U. Hanefeld, *Appl. Catal. A Gen.*, 2009, **355**, 78–82.
- 5 B. Modén, B. Zhan, J. Dakka, J. G. Santiesteban and E. Iglesia, *J. Catal.*, 2006, **239**, 390–401.
- 6 I. Hermans, J. Peeters and P. A. Jacobs, *J. Phys. Chem.*, 2008, **112**, 1747–1753.
- 7 I. Hermans, P. A. Jacobs and J. Peeters, *Chem. - A Eur. J.*, 2007, **13**, 754–761.
- 8 I. Hermans, P. A. Jacobs and J. Peeters, *Chem. - A Eur. J.*, 2006, **12**, 4229–4240.
- 9 M. J. Pilling, *Pure Appl. Chem.*, 1992, **64**, 1473–1480.
- 10 A. I. Vitvitskii, *Theor. Exp. Chem.*, 1969, **5**, 276–278.
- 11 D. Ni, D. Jiang, C. J. Kutyreff, J. Lai, Y. Yan, T. E. Barnhart, H. Im, L. Kang, S. Y. Cho, Z. Liu, P. Huang, J. W. Engle, W. Cai and B. Yu, *Nat. Commun.*, 2018, **9**, 5421.
- 12 M. Marimuthu, B. P. Kumar, L. M. Salomi, M. Veerapandian and K. Balamurugan, *Appl. Mater. Interfaces*, 2018, **10**, 43429–43438.
- 13 A. Fakhri and P. Afshar, *J. Photochem. Photobiol. B Biol.*, 2016, **159**, 211–217.
- 14 M. D. Hughes, Y. Xu, P. Jenkins, P. McMorn, P. Landon, D. I. Enache, A. F. Carley, G. A. Attard, G. J. Hutchings, F. King, E. H. Stitt, P. Johnston, K. Griffin and C. J. Kiely, *Nature*, 2005, **437**, 1132–1135.

- 15 Y. H. Lin, I. D. Williams and P. Li, *Appl. Catal. A Gen.*, 1997, **150**, 221–229.
- 16 X. Liu, Y. Ryabenkova and M. Conte, *Phys. Chem. Chem. Phys.*, 2015, **17**, 715–731.
- 17 X. Liu, M. Conte, W. Weng, Q. He, R. L. Jenkins, M. Watanabe, D. J. Morgan, D. W. Knight, D. M. Murphy, K. Whiston, C. J. Kiely and G. J. Hutchings, *Catal. Sci. Technol.*, 2015, **5**, 217–227.
- 18 I. M. Denekamp, M. Antens, T. K. Slot and G. Rothenberg, *ChemCatChem*, 2018, **10**, 1035–1041.
- 19 E. Rucinska, P. J. Miedziak, S. Pattison, G. L. Brett, S. Iqbal, D. J. Morgan, M. Sankar and G. J. Hutchings, *Catal. Sci. Technol.*, 2018, **8**, 2987–2997.
- 20 J. Chateaufneuf, J. Lusztyk and K. U. Ingold, *J. Organic Chem.*, 1988, **53**, 1629–1632.
- 21 M. Ochiai and T. Sueda, *Tetrahedron Lett.*, 2004, **45**, 3557–3559.
- 22 T. Rosenau, A. Potthast, P. Kosma and R. Möslinger, *J. Wood Chem. Technol.*, 2006, **26**, 53–63.
- 23 C. A. Hone and C. O. Kappe, *Top. Curr. Chem.*, 2019, **377**, 1–44.
- 24 M. Guidi, H. Seeberger and K. Gilmore, *Chem. Soc. Rev.*, 2020, **49**, 8910–8932.
- 25 B. Pieber and C. O. Kappe, *Green Chem.*, 2012, **15**, 320–324.
- 26 N. G. Anderson, *Org. Process Res. Dev.*, 2012, **16**, 852–869.